

AD-A279 404



PL-TR-93-2216 (I)

**INVESTIGATIONS OF ULTRAVIOLET EMISSIONS
FROM THE IONOSPHERE**

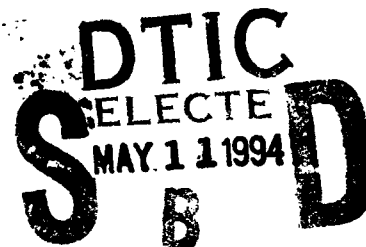
Francis J. LeBlanc

Northwest Research Associates, Inc.
P.O. Box 3027
Bellevue, WA 98005

21 May 1993

Final Report
16 January 1990 - 15 January 1993

Approved for public release; distribution unlimited



PHILLIPS LABORATORY
Directorate of Geophysics
AIR FORCE MATERIEL COMMAND
HANSCOM AIR FORCE BASE, MA 01731-3010


5494-13947

DTIC QUALITY ASSURED 1

94 5 09 038

"This technical report has been reviewed and is approved for publication"


Robert E. Huffman
Contract Manager


David N. Anderson
Branch Chief, GPIM


William K. Vickery
Division Director, GPI

This report has been reviewed by the ESC Public Affairs Office (PA) and is releasable to the National Technical Information Service (NTIS).

Qualified requestors may obtain additional copies from the Defense Technical Information Center (DTIC). All others should apply to the National Technical Information Service (NTIS).

If your address has changed, or if you wish to be removed from the mailing list, or if the addressee is no longer employed by your organization, please notify PL/TSI, 29 Randolph Road, Hanscom AFB, MA 01731-3010. This will assist us in maintaining a current mailing list.

Do not return copies of this report unless contractual obligations or notices on a specific document requires that it be returned.

REPORT DOCUMENTATION PAGE			Form Approved GSA No. 0704-0188	
<small>Public reporting burden for this collection of information is estimated to average 1 hour per response, including the time for reviewing instructions, searching existing data sources, gathering and maintaining the data needed, and completing and reviewing the collection of information. Send comments regarding this burden estimate or any other aspect of this collection of information, including suggestions for reducing this burden, to Washington Headquarters Service, Directorate for Information Operations and Reports, 1215 Jefferson Davis Highway, Suite 1204, Arlington, VA 22202-4302, and to the Office of Management and Budget, Paperwork Reduction Project (0704-0188), Washington, DC 20503.</small>				
1. AGENCY USE ONLY (Leave blank)	2. REPORT DATE 21 May 1993	3. REPORT TYPE AND DATES COVERED Final report: 16 Jan 90 to 15 Jan 93		
4. TITLE AND SUBTITLE Investigations of Ultraviolet Emissions From the Ionosphere		5. FUNDING NUMBERS F19628-90-C-0050 PE5321 TA06 WU AL		
6. AUTHOR(S) Francis J. LeBlanc				
7. PERFORMING ORGANIZATION NAME(S) AND ADDRESS(ES) Northwest Research Associates, Inc. PO Box 3027 Bellevue, WA 98005		8. PERFORMING ORGANIZATION REPORT NUMBER NWRA-CR-93-R100		
9. SPONSORING/MONITORING AGENCY NAME(S) AND ADDRESS(ES) Phillips Laboratory 29 Randolph Road Hanscom AFB, MA 01731-3010 Contract Manager: Robert Huffman/GPIM		10. SPONSORING/MONITORING AGENCY REPORT NUMBER PL-TR-93-2216(I)		
11. SUPPLEMENTARY NOTES				
12a. DISTRIBUTION/AVAILABILITY STATEMENT approved for public release; distribution unlimited		12b. DISTRIBUTION CODE		
<p>13 The work of Contract F19268-C-0050 has improved the accessibility and utilization of databases containing ultraviolet (UV) measurements of the ionosphere obtained from satellite and Space Shuttle experiments. These experiments were the Ultraviolet Backgrounds on the S3-4 satellite, the Auroral Ionospheric Remote Sensor (AIRS) on the PolarBEAR satellite, the Horizon Ultraviolet Program (HUP), and shuttles STS-4 and STS-39.</p> <p>These databases were used to analyze the ionosphere and to validate the Atmospheric Ultraviolet Radiation Integrated Code (AURIC).</p> <p>The S3-4 experiment measured the UV emissions from the ionosphere looking in nadir while in a polar orbit. Data were collected simultaneously from three instruments. The telemetry tapes, processed into VAX compatible tapes, are stored at the Phillips Laboratory/Geophysics Directorate, where they remain active in ionospheric analysis.</p> <p>The AIRS data contain a series of ionospheric images recorded mainly at high latitudes and at selected wavelength. These have been placed on a set of optical disks and are accompanied with software which allows quick looks at the images or the acquiring of a raw image for further processing.</p> <p>The HUP instrument collected horizon profiles from Space Shuttle at selected UV wavelengths. These absolute intensity measurements contribute to the understanding of ionospheric processes and are useful where backgrounds are a consideration. This database has also been placed on an optical disk. These data were also used as comparison checks between AURIC and actual recorded measurements. The initial results were favorable.</p>				
14. SUBJECT TERMS ionospheric emissions, ultraviolet aurora, atmospheric rad-		15. NUMBER OF PAGES 54		
		16. PRICE CODE		
17. SECURITY CLASSIFICATION OF REPORT unclassified	18. SECURITY CLASSIFICATION OF THIS PAGE unclassified	19. SECURITY CLASSIFICATION OF ABSTRACT unclassified	20. LIMITATION OF ABSTRACT SAR	

Table of Contents

	Page
Ultraviolet Backgrounds Satellite (S3-4)	1
Horizon Ultraviolet Program (HUP)	1
Auroral Ionospheric Remote Sensor (AIRS)	2
Model Comparison	2
Appendix 1: S3-4 Database	9
Appendix 2: Reprint of Paper Entitled "NO and O ₂ Ultraviolet Nightglow and Spacecraft Glow From the S3-4 Satellite"	25
Appendix 3: Reprint of Paper Entitled "Horizon UV Program (HUP) Atmospheric Radiance Measurements," Describing HUP Measurements	39
* Appendix 4: HUP Database and Programs	
* Appendix 5: AIRS Database and Programs	
* Appendix 6: Use of AURIC Model	

* Included in Volume II

Accession For	
NTIS GRA&I	<input checked="checked" type="checkbox"/>
DTIC TAB	<input type="checkbox"/>
Unannounced	<input type="checkbox"/>
Justification	
By _____	
Distribution/	
Availability Codes	
Dist	Avail and/or Special
A-1	

List of Figures

	Page
1. Upward and downward horizon intensity scans for the wavelengths indicated in the panel headings, observed from Space Shuttle STS-4 on Day 179, 1982 at 59400.0 UTsec and lat/lon = 24.5/280.0. The 10.7-cm solar index was 123.0. The dotted lines are the AURIC predictions modified by the scale factors in the headings.	4
2. Upward and downward horizon intensity scans for the wavelengths indicated in the panel headings, observed from Space Shuttle STS-4 on Day 179, 1982 at 76918 UTsec and lat/lon = 16.8/233.7. The 10.7-cm solar index was 123.0. The dotted lines are the AURIC predictions modified by the scale factors in the headings.	5
3. Upward and downward horizon intensity scans for the wavelengths indicated in the panel headings, observed from Space Shuttle STS-4 on Day 179, 1982 at 76230 UTsec and lat/lon = 28.4/188.4. The 10.7-cm solar index was 123.0. The dotted lines are the AURIC predictions modified by the scale factors in the headings.	6
4. Upward and downward horizon intensity scans for the wavelengths indicated in the panel headings, observed from Space Shuttle STS-4 on Day 179, 1982 at 60970 UTsec and lat/lon = 7.6/321.0. The 10.7-cm solar index was 123.0. The dotted lines are the AURIC predictions modified by the scale factors in the headings.	7
5. Upward and downward horizon intensity scans for the wavelengths indicated in the panel headings, observed from Space Shuttle STS-4 on Day 179, 1982 at 66955 UTsec and lat/lon = -10/328.0. The 10.7-cm solar index was 123.0. The dotted lines are the AURIC predictions modified by the scale factors in the headings.	8

This report describes the location, accessibility and utilization of the databases created from the measurements collected from the S3-4 satellite experiment, the Auroral Ionospheric Remote Sensor (AIRS) satellite experiment and the Horizon Ultraviolet Program (HUP) flown on Space Shuttles STS-4 and STS-39. Particular emphasis has been placed on comparing the predictions of the Atmospheric Ultraviolet Radiation Integrated Code (AURIC) with observed data.

The work of this contract involved the compilation and utilization of databases for satellite and Space Shuttle experiments conducted by the Phillips Laboratory/Geophysics Directorate/Ionospheric Modeling and Remote Sensing Branch (GPIM). The goal was to structure the results of these ionospheric measurements so that GPIM personnel and others could easily access these files to make ultraviolet background measurements and studies of the dynamics and composition of the auroral oval, the polar cap and the tropical belts. The auroral ovals are formed by the glowing ionosphere encircling each of the magnetic poles and are related to solar activity. The polar caps are not as bright as the ovals but have a number of features, such as sun-aligned arcs, that are the subject of current studies. The tropical belts are ionospheric emissions that circle the earth about 10 degrees poleward of the magnetic equator.

ULTRAVIOLET BACKGROUNDS SATELLITE (S3-4)

The raw telemetry tapes of the Ultraviolet Backgrounds experiment (S3-4) have been processed into vax-compatible tapes and are accessible at the Phillips Laboratory. Appendix 1 lists the files on these tapes for the revolution number (REV), day, format, and photometer filter. The S3-4 experiment made three simultaneous measurements. These were two spectrometer readings and one photometer measurement. The spectrometers scanned in the wavelength ranges 1070 A to 1930 A and 1620 A to 2900 A. The photometer had four bandpass filters that could be selected. These were centered at 1216 A, 1340 A, 1550 A, 1720 A and, also, no filter. The bandpass with no filter was that of the EMR 542G photomultiplier tube, 1070 A to 1930 A. From 3/22/78 to 9/10/78, data were collected from 355 full orbits and 447 partial orbits for a total of 728 hours of read-in time from a nominal altitude of 210 km and pointed in the nadir direction.

This database is being used to catalog the earth's ultraviolet glow and for scientific investigations of the ionosphere and auroral oval. GPIM and other laboratories believe there is still much information to be extracted from these data, which were collected in 1978. An example of the value of this database is the enclosed paper (Appendix 5) published in *Planet. Space Sci.*, Vol. 40, No. 4, pp 481-493, 1992 by R. W. Eastes, R. E. Huffman and F. J. LeBlanc. This paper is a report on the nightglow emissions of atmospheric nitric oxide and molecular oxygen as seen in the ultraviolet from the S3-4 satellite.

HORIZON ULTRAVIOLET PROGRAM (HUP)

As part of the Horizon Ultraviolet Program, experiment 801A was flown on Space Shuttle STS-4. Also, a few hours of HUP data were collected on STS-39 with the instrument modified to collect data at 5 A wavelength resolution rather than 20 A as on STS-4. The HUP

instrument was designed to scan the earth's horizon at selected ultraviolet wavelengths, or to make spectral scans in the wavelength region between 1100 A and 1900 A. These data are stored on one side of an optical disc marked FPD002. A list of these data files can be found in Appendix 2, along with some of the fortran programs used in handling this data. The SETSDISC.DAT file, created from the STS-4 measurements, describes the disc arrangement of the data and lists the directories. The programs SETAVE.FOR, SETSVAL.FOR and GOSUN.FOR average, convert to radiance values, and assign these values to the tangent heights for the STS-4 data. These files were used for comparison with the AURIC predictions. Appendices 2.5 to 2.9 were written to manage the STS-39 data. SPECTRA.FOR extracts spectra from the files created by Boston College from the raw Lockheed tapes. HUPAVE.FOR averages the spectra. SENSALC.PRO converts the counts to Rayleighs. HUPTIM.FOR writes the starting time of each spectra. SCAN40.FOR assigns radiance values for the HUP scan angles.

Because of personnel changes, Mr. LeBlanc became the principal point of contact for the HUP experiment being prepared to fly on Space Shuttle STS-39. He became involved in all phases of the project, including testing, integration, training, and flight operations. He was selected because a replacement was needed and he had performed similar functions in the past. These activities were very intensive from February 1990 until May 1991. Beyond this, the instrument sensitivities, wavelength, and scan-angle positions were redetermined. Results of this effort can be seen in the included paper "Horizon UV Program (HUP) Atmospheric Radiance Measurements" (Appendix 6).

AURORAL IONOSPHERIC REMOTE SENSOR (AIRS)

AIRS was designed to image the ionosphere between the east and west horizons at selected ultraviolet (UV) wavelengths from the PolarBEAR satellite and at times recorded the UV spectra looking in nadir. Data were collected primarily at northern latitudes, over the auroral oval and polar cap. The database is described in Appendix 3, along with the list of tapes containing AIRS spectra, the spectra files recorded on optical disc, and programs used to handle this data. The bulk of the image data have been placed on five double-sided optical disks. The unprocessed images can be accessed by keying in the desired observation times. This facilitates access to the data to such an extent as to make casual perusal feasible.

These databases (S3-4, HUP and AIRS) have been processed to obtain images, spectra, and background radiances of the earth's ionosphere and auroral oval. This was done for in-house studies, presentations, and papers, and also to answer requests from other laboratories. These occurrences have been documented in quarterly reports.

MODEL COMPARISON

The most recent use of these databases has been toward validation and modification of AURIC. AURIC predicts the atmospheric radiance for given look angles, altitudes, latitude and longitudes, 10.7-cm indices, universal times, and wavelengths. Appendix 4 contains information on the use of AURIC and associated programs. These files and programs are found in the

Auricsun workstation. The AURIC code is being used to predict horizon backgrounds for the oxygen 1356 A line (OI) and the Lyman Birge Hopfield (LBH) 1384 A and 1464 A bands. Figures 1 through 5 compare the results of AURIC, version 1.2, with HUP data. These horizon scans were selected to cover a range of solar zenith angles (SZA). The headings also identify the data set, the wavelength, and the scale factor used to make the AURIC model match the HUP data. Agreement with OI is reasonable, but the intensities of the LBH scans will need modification in the next version (AURIC 2.0).

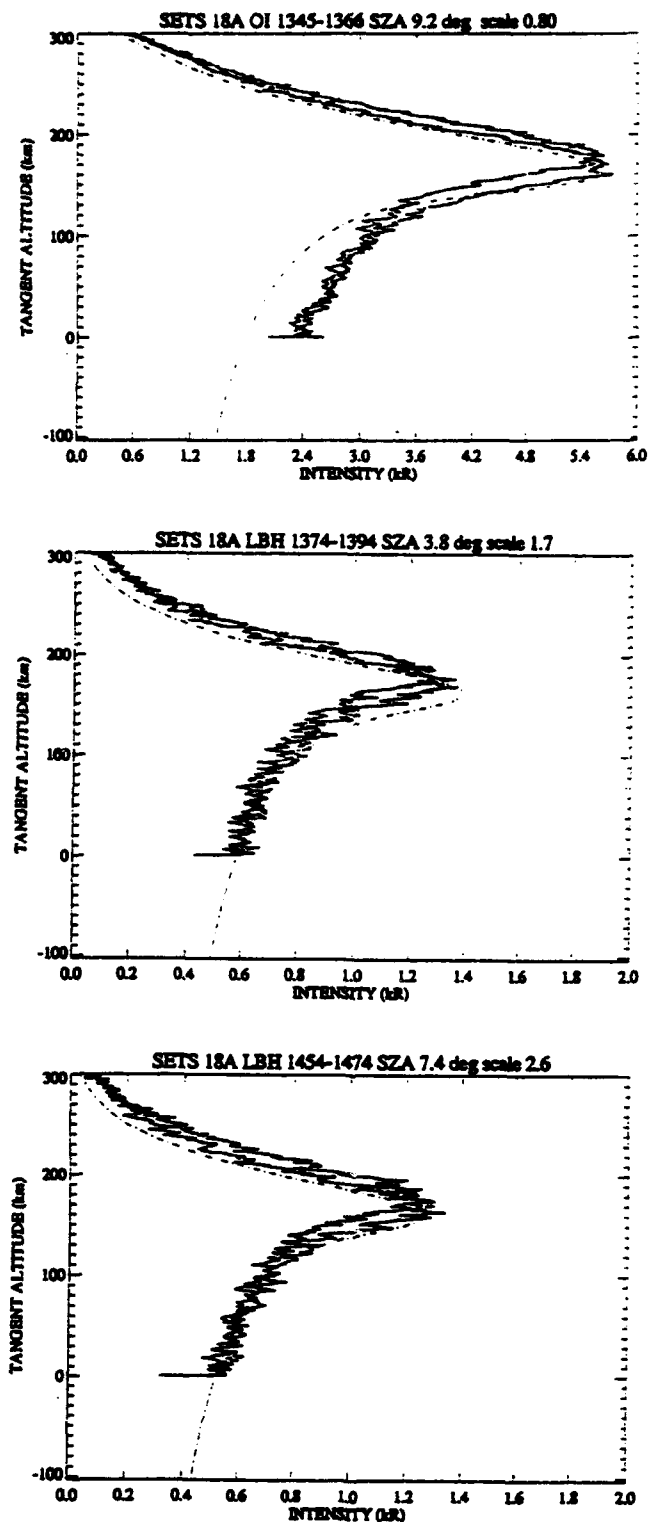


Figure 1. Upward and downward horizon intensity scans for the wavelengths indicated in the panel headings, observed from Space Shuttle STS-4 on Day 179, 1982 at 59400.0 UTsec and lat/lon = 24.5/280.0. The 10.7-cm solar index was 123.0. The dotted lines are the AURIC predictions modified by the scale factors in the headings.

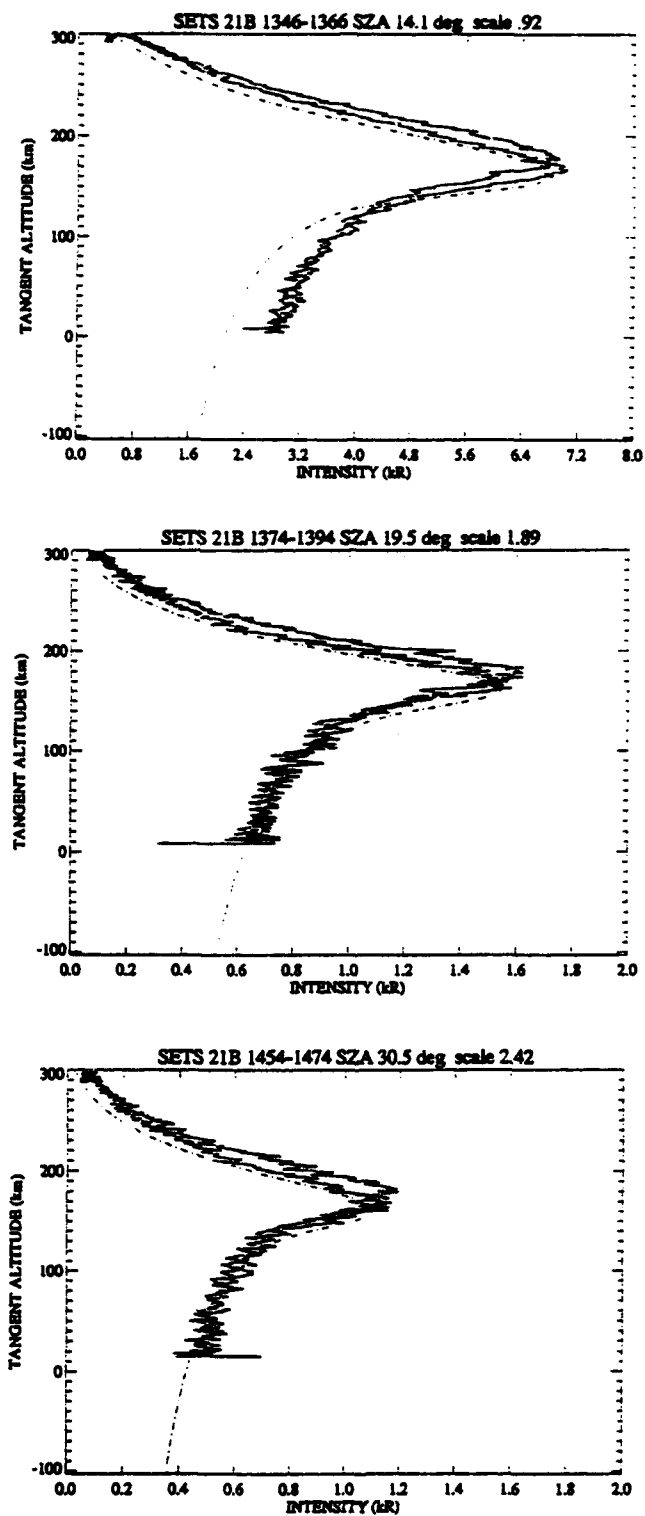


Figure 2. Upward and downward horizon intensity scans for the wavelengths indicated in the panel headings, observed from Space Shuttle STS-4 on Day 179, 1982 at 76918 UTsec and lat/lon = 16.8/233.7. The 10.7-cm solar index was 123.0. The dotted lines are the AURIC predictions modified by the scale factors in the headings.

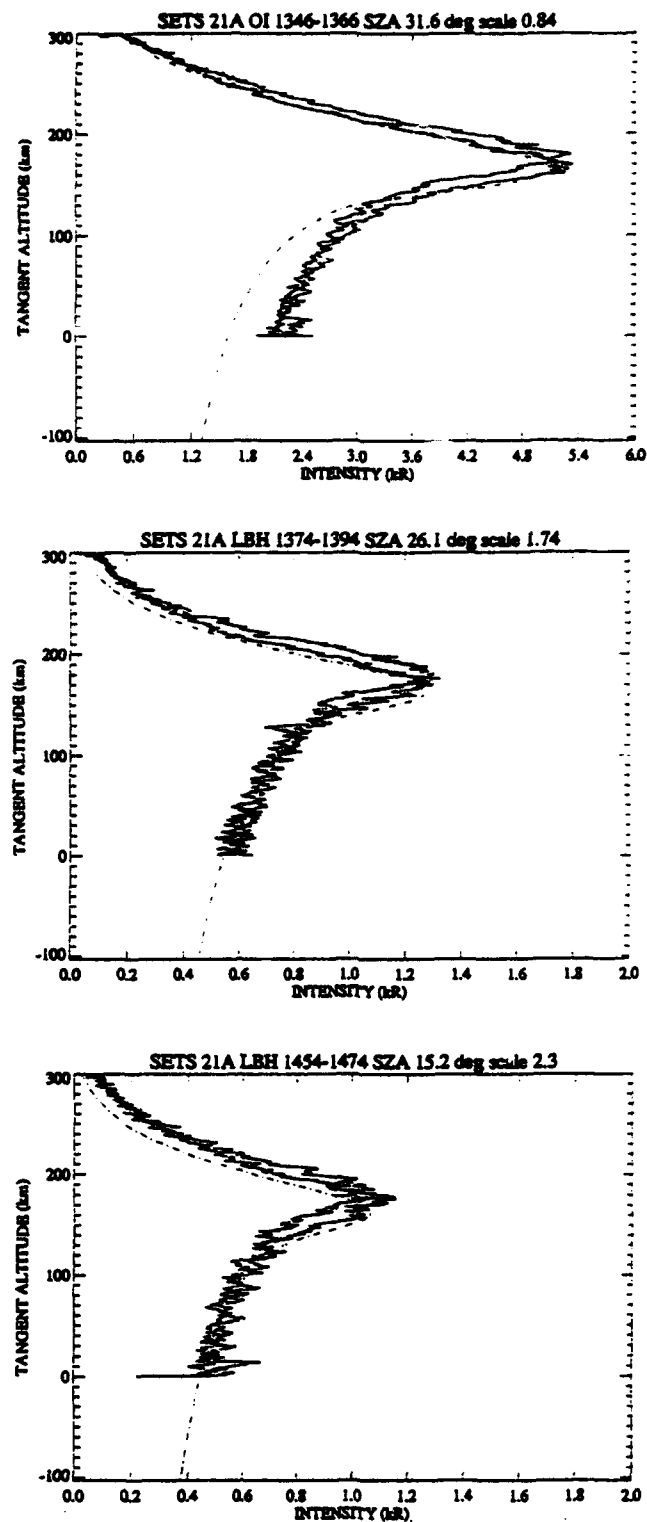


Figure 3. Upward and downward horizon intensity scans for the wavelengths indicated the panel headings, observed from Space Shuttle STS-4 on Day 179, 1982 at 76230 UTsec and lat/lon = 28.4/188.4. The 10.7-cm solar index was 123.0. The dotted lines are the AURIC predictions modified by the scale factors in the headings.

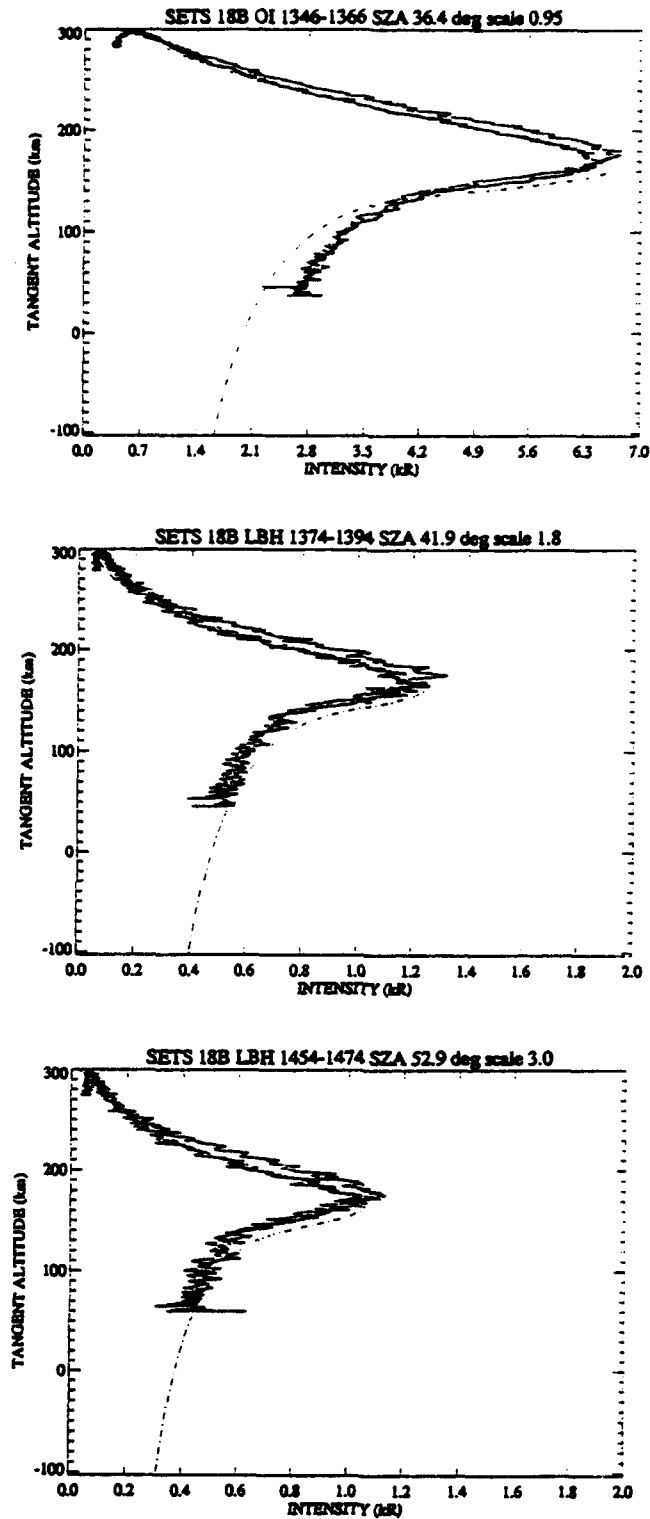


Figure 4. Upward and downward horizon intensity scans for the wavelengths indicated in the panel headings, observed from Space Shuttle STS-4 on Day 179, 1982 at 60970 UTsec and lat/lon = 7.6/321.0. The 10.7-cm solar index was 123.0. The dotted lines are the AURIC predictions modified by the scale factors in the headings.

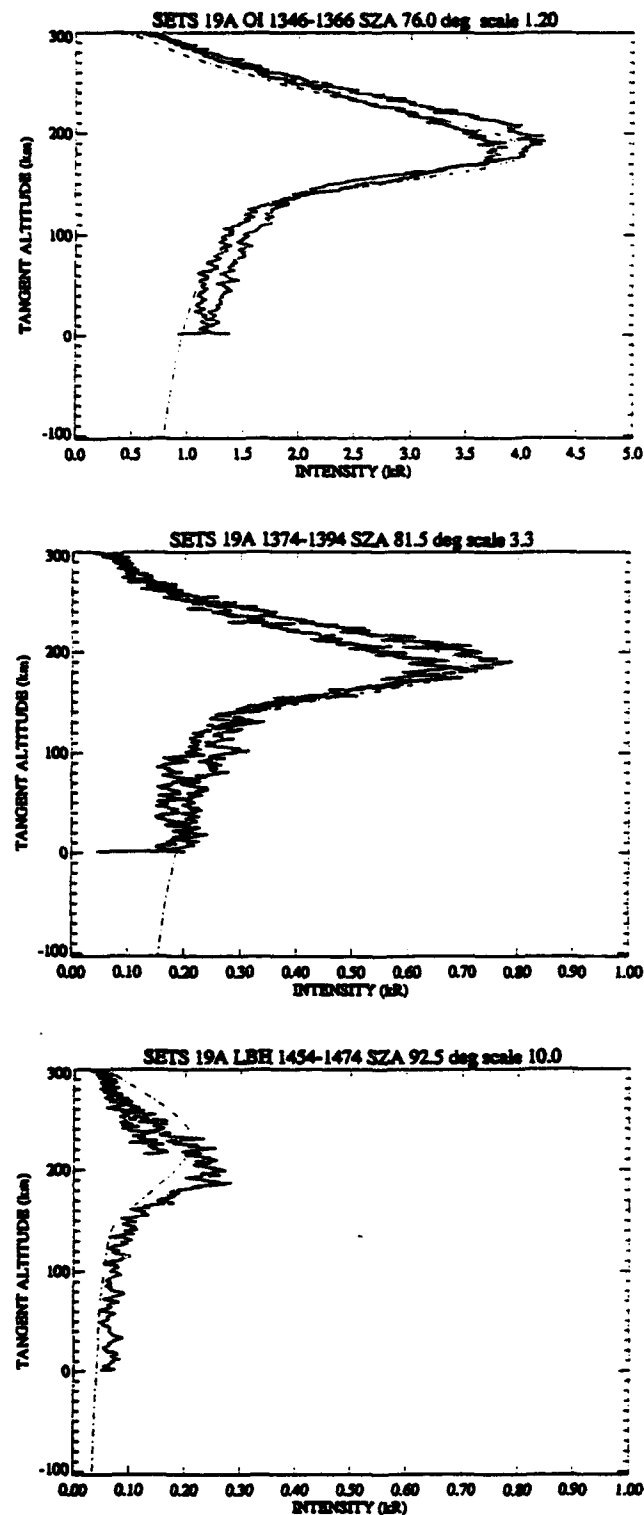


Figure 5. Upward and downward horizon intensity scans for the wavelengths indicated in the panel headings, observed from Space Shuttle STS-4 on Day 179, 1982 at 66955 UTsec and lat/lon = -10/328.0. The 10.7-cm solar index was 123.0. The dotted lines are the AURIC predictions modified by the scale factors in the headings.

APPENDIX 1: S3-4 Database

APPENDIX 1: S3-4 DATABASE

This table lists the raw telemetry tapes (SPECT. TAPE), the pre-processed spectrometer and photometer tapes (SPECT. P.P. TAPE and PHOT. P.P. TAPE) and the corresponding VAX compatible tapes. There are also columns for the orbit revolution number (REV), the month, day, year, telemetry format, and filter number. The number following the slash in tape identification numbers is the position of the file on the tape.

The data from the vehicle are Pulse-Code Modulated (PCM). Each mainframe consists of 120 words, 8 bits per word. The data, however, may be acquired at two data rates (32kbps and 64kbps). In general, the mainframe word locations for the designations are different for the two data rates. The 32kbps data rate is designated as Format A, and the 64kbps data rate is designated as Format C. A masterframe (one readout of each sub-commutated value) is 32 frames in Format A and 64 frames in Format C. The telemetry system may be summarized as follows:

8 bits/word		
120 words/mainframe		
960 bits/mainframe		
<u>Format A</u>		<u>Format C</u>
32K	BITS/SEC	64K
33, 33	FRAMES/SEC	66.67
.03	SEC/FRAME	.015

S3-4

SPECTROMETER AND PHOTOMETER

AGENCY, PRE-PROCESSED AND VAX COMPATIBLE TAPES

AGENCY S4S NT/800 BPI ,D-HD

SPECTROMETER PRE-PROC. S4E NT/1600 BPI ,D-PE

PHOTOMETER PRE-PROC. S4P NT/1600 BPI ,D-PE

VAX COMPATIBLE RM NT/6250 BPI ,D-GE (EXCEPT FOR (RM2885-
RM2901), WHICH ARE NT/1600 BPI

1	S3-4	SPECT.	SPECT.	VAX COMP.	PHOT.	VAX COMP.
REV	MTH DAY YR	TAPE	P.P.TAPE	TAPE	P.P.TAPE	TAPE
94	NO C	1 S4S343/1				
99	3 22 78 A	3 S4S343/2	S4E136/1	RM2761/5	S4P555/1	RM2044/1
164 *	3 26 78 C	3 S4S004/1	PARITY	ERRORS	UNABLE TO	PROCESS
217	3 30 78 C	3 S4S343/5	S4E137/1	RM2762/5	S4P556/1	RM2045/1
221	3 30 78 A	3 S4S342/1	S4E004/16	RM2913/5	S4P527/26	RM3513/6
226 *	3 30 78 A	3 S4S022/1	S4E134/1	RM2895/3	S4P534/1	RM2784/1
230	3 30 78 C	3 S4S138/1	S4E161/1	RM2625/13	S4P557/1	RM2046/1
244	3 31 78 A	3 S4S118/1	S4E101/6	RM2904/2	S4P501/21	RM2784/6
249	4 1 78 C	2 S4S333/1	S4E138/1	RM2759/6	S4P558/1	RM2047/1
254	4 1 78 A	4 S4S342/4	S4E036/11	RM2898/2	S4P570/41	RM2044/14
258	4 1 78 A	3 S4S333/3	S4E005/16	RM2896/1	S4P527/21	RM3513/5
262	4 1 78 A	2 S4S333/6	S4E118/1	RM2885/1	S4P530/41	RM3516/8
266	4 2 78 C	3 S4S342/8	S4E139/1	RM2760/6	S4P559/1	RM2048/1
270	4 2 78 A	3 S4S318/1	S4E001/6	RM2908/3	S4P526/11	RM3512/3
274	4 2 78 A	3 S4S318/4	S4E002/6	RM2895/1	S4P527/11	RM3513/3
277	4 2 78 A	3 S4S322/1	S4E102/6	RM2901/3	S4P525/11	RM3511/3
282	4 3 78 A	1 S4S322/4	S4E140/1	RM2759/7	S4P560/1	RM2049/1
284	4 3 78 C	3 S4S322/5	S4E141/1	RM2760/7	S4P561/1	RM2050/1
287	4 3 78 A	3 S4S328/1	S4E019/11	RM2886/1	S4P530/16	RM3516/4
291	4 3 78 A	3 S4S328/4	S4E020/11	RM2904/3	S4P531/16	RM3507/13
295 *	4 3 78 A	3 S4S027/1	S4E134/6	RM2895/4	S4P562/1	RM2051/1
301	4 4 78 C	2 S4S327/1	S4E142/1	RM2761/6	S4P563/1	RM2052/1
306	4 4 78 A	3 S4S327/3	S4E017/11	RM2901/1	S4P528/16	RM3514/4
308	4 4 78 A	3 S4S327/6	S4E018/11	RM2896/2	S4P529/16	RM3515/4
312	4 4 78 A	3 S4S326/1	S4E015/11	RM2904/4	S4P527/16	RM3513/4
318	4 5 78 C	3 S4S326/4	S4E143/1	RM2762/6	S4P564/1	RM2053/1
322	4 5 78 A	3 S4S326/7	S4E016/11	RM2904/5	S4P525/16	RM3511/4
325	4 5 78 A	3 S4S301/1	S4E074/16	RM2904/6	S4P527/6	RM3513/2
329	4 6 78 A	4 S4S301/4	S4E096/11	RM2667/3	S4P528/6	RM3514/2
335	4 6 78 C	3 S4S301/8	S4E144/1	RM2761/7	S4P555/6	RM2044/2
339	4 6 78 A	3 S4S321/1	S4E007/1	RM2903/1	S4P529/11	RM3515/3
343	4 6 78 A	3 S4S321/4	S4E008/11	RM2897/1	S4P530/11	RM3516/3
347	4 7 78 A	4 S4S321/7	S4E009/11	RM2898/1	S4P531/11	RM3515/10
353	4 7 78 C	3 S4S117/1	S4E145/1	RM2762/7	S4P556/6	RM2045/2
357	4 7 78 A	3 S4S332/1	S4E022/11	RM2887/1	S4P524/21	RM3510/5
360	4 7 78 A	3 S4S324/1	S4E012/11	RM2899/1	S4P523/16	RM3509/4

364	4	8	78	A	2	S4S324/4	S4E117/1	RM2898/4	S4P529/41	RM3515/8
370	4	8	78	C	3	S4S324/6	S4E136/6	RM2759/8	S4P557/6	RM2046/2
373	4	8	78	A	3	S4S332/4	S4E103/6	RM2895/2	S4P525/21	RM3511/5
377	4	8	78	A	3	S4S320/1	S4E006/11	RM2905/1	S4P528/11	RM3514/3
382	4	9	78	A	2	S4S320/5	S4E137/6	RM2760/8	S4P558/6	RM2047/2
388	4	9	78	C	3	S4S297/1	S4E138/6	RM2761/8	S4P559/6	RM2048/2
390	4	9	78	A	3	S4S118/4	S4E003/16	RM2906/1	S4P501/16	RM2784/5
393	4	9	78	A	3	S4S320/7	S4E121/11	RM2899/4	S4P526/26	RM3512/6
398	4	10	78	A	3	S4S325/1	S4E013/11	RM2911/5	S4P524/16	RM3510/4
405	4	10	78	C	3	S4S325/4	S4E139/6	RM2762/8	S4P560/6	RM2049/2
408	4	10	78	A	3	S4S332/7	S4E023/11	RM2897/2	S4P526/21	RM3512/5
412	4	11	78	A	3	S4S325/7	S4E014/11	RM2904/7	S4P526/16	RM3512/4
417	4	11	78	A	3	S4S323/1	S4E010/11	RM2903/2	S4P522/16	RM3508/4
422	4	11	78	C	3	S4S297/4	S4E140/6	RM2759/9	UNABLE TO	PROCESS
425 *	4	11	78	A	3	S4S029/1	S4E133/1	RM2901/4	S4P532/1	RM3512/12
429	4	12	78	A	2	S4S297/7	S4E115/1	RM2896/4	S4P527/46	RM3514/11
433	4	12	78	A	3	S4S298/1	S4E141/6	RM2760/9	S4P522/6	RM3508/2
439	4	12	78	C	3	S4S298/4	S4E142/6	RM2761/9	S4P562/6	RM2051/2
441	4	12	78	A	3	S4S298/7	S4E091/11	RM2901/2	S4P523/6	RM3509/2
445	4	13	78	A	3	S4S300/1	S4E093/11	RM2897/3	S4P525/6	RM3511/2
449 *	4	13	78	A	3	S4S093/1	S4E143/6	RM2762/9	PARITY	ERRORS
1		S3-4				SPECT.	SPECT.	VAX COMP.	PHOT.	VAX COMP.
						TAPE	P.P.TAPE	TAPE	P.P.TAPE	TAPE
REV	MTN	DAY	YR	FT/F		-----	-----	-----	-----	-----
453	4	13	78	A	3	S4S300/4	S4E094/11	RM2898/3	S4P526/6	RM3512/2
457	4	13	78	C	3	S4S300/7	S4E144/6	RM2621/1	S4P564/6	RM2053/2
460 *	4	14	78	A	4	S4S072/1	S4E145/6	RM2622/1	PARITY	ERRORS
464	4	14	78	A	4	S4S337/1	S4E046/11	RM2917/8	S4P522/21	RM3508/5
474	4	14	78	C	3	S4S299/1	S4E136/11	RM2623/1	S4P561/6	RM2050/2
477	4	15	78	A	2	S4S299/4	S4E116/1	RM2897/4	S4P528/51	RM3511/11
482	4	15	78	A	4	S4S302/1	S4E097/11	RM2899/3	S4P529/6	RM3515/2
486	4	15	78	A	3	S4S302/5	S4E098/11	RM2889/1	S4P530/6	RM3516/2
491	4	15	78	C	3	S4S302/8	S4E137/11	RM2624/1	S4P555/11	RM2044/3
495	4	16	78	A	2	S4S313/1	S4E138/11	RM2625/1	S4P556/11	RM2045/3
498	4	16	78	A	4	S4S299/6	S4E092/11	RM2896/3	S4P524/6	RM3510/2
502	4	16	78	A	3	S4S313/3	S4E086/11	RM2904/8	S4P524/11	RM3510/3
508	4	16	78	C	4	S4S331/1	S4E139/11	RM2621/2	S4P557/11	RM2046/3
512	4	17	78	A	2	S4S313/6	S4E140/11	RM2622/2	S4P558/11	RM2047/3
518	4	17	78	A	3	S4S310/1	S4E109/11	RM2904/9	S4P523/11	RM3509/3
522	4	17	78	A	1	S4S310/4	S4E141/11	RM2623/2	S4P559/11	RM2048/3
523	4	17	78	A	1	S4S310/5	S4E142/11	RM2625/2	S4P560/11	RM2049/3
524	NO	B+L		A	1	S4S314/1				
525	4	18	78	A	1	S4S314/2	S4E143/11	RM2624/2	S4P561/11	RM2050/3
526	4	18	78	A	1	S4S314/3	S4E144/11	RM2621/3	S4P562/11	RM2051/3
527	4	18	78	A	1	S4S315/1	S4E145/11	RM2622/3	S4P564/11	RM2053/3
528	4	18	78	A	1	S4S315/2	S4E136/16	RM2623/3	S4P563/6	RM2052/2
529	4	18	78	A	1	S4S315/3	S4E137/16	RM2624/3	S4P563/11	RM2052/3
530	4	18	78	A	1	S4S317/1	S4E138/16	RM2625/3	S4P555/21	RM2044/5
531	4	18	78	A	1	S4S317/2	S4E139/16	RM2626/1	S4P556/21	RM2045/5
533	4	18	78	A	1	S4S331/5	S4E140/16	RM2627/1	S4P557/21	RM2046/5
534	4	18	78	A	1	S4S317/3	S4E136/21	RM2623/4	S4P558/21	RM2047/5
535	4	18	78	A	1	S4S331/6	S4E137/21	RM2624/4	S4P559/21	RM2048/5
536	4	18	78	A	1	S4S309/1	S4E138/21	RM2625/4	S4P560/21	RM2049/5
537	4	18	78	A	1	S4S309/2	S4E139/21	RM2626/2	S4P561/21	RM2050/5
538	4	18	78	A	1	S4S309/3	S4E140/21	RM2627/2	S4P562/21	RM2051/5
539	4	18	78	A	1	S4S308/1	S4E141/16	RM2628/1	S4P563/21	RM2052/5
540	4	18	78	A	1	S4S308/2	S4E142/16	RM2629/1	S4P564/21	RM2053/5
541	4	19	78	A	1	S4S308/3	S4E143/16	RM2630/1	S4P555/26	RM2044/6
542	4	19	78	A	1	S4S316/1	S4E144/16	RM2621/4	S4P556/26	RM2045/6
543	4	19	78	A	1	S4S316/2	S4E145/16	RM2622/4	S4P557/26	RM2046/6

545	4	19	78	A	1	S4S316/3	S4E142/21	RM2629/2	S4P558/26	RM2047/6
547	4	19	78	A	1	S4S312/1	S4E143/21	RM2630/2	S4P559/26	RM2048/6
549	4	19	78	A	1	S4S312/2	S4E145/21	RM2622/5	S4P560/26	RM2049/6
550	4	19	78	A	1	S4S312/3	S4E144/21	RM2621/5	S4P561/26	RM2050/6
551	4	19	78	A	1	S4S340/1	S4E141/21	RM2628/2	S4P562/26	RM2051/6
552	4	19	78	A	1	S4S307/1	S4E136/26	RM2623/5	S4P563/26	RM2052/6
553	4	19	78	A	1	S4S307/2	S4E137/26	RM2624/5	S4P564/26	RM2053/6
554	4	19	78	A	1	S4S307/3	S4E138/26	RM2625/5	S4P555/31	RM2044/7
555	4	19	78	A	1	S4S304/1	S4E139/26	RM2626/3	S4P556/31	RM2045/7
556	4	19	78	A	1	S4S304/2	S4E140/26	RM2627/3	S4P557/31	RM2046/7
557	4	19	78	A	1	S4S304/3	ERRONEOUS	TIMES	S4P558/31	RM2047/7
558	4	20	78	A	1	S4S305/1	S4E147/1	RM2624/6	S4P559/31	RM2048/7
559	4	20	78	A	1	S4S305/2	S4E148/1	RM2625/6	S4P560/31	RM2049/7
560	4	20	78	A	1	S4S305/3	S4E149/1	RM2626/4	S4P561/31	RM2050/7
561	4	20	78	A	1	S4S311/1	S4E150/1	RM2627/4	S4P562/31	RM2051/7
563	4	20	78	A	1	S4S311/2	S4E147/6	RM2629/4	S4P563/31	RM2052/7
582	4	21	78	A	1	S4S311/3	S4E148/6	RM2630/4	S4P564/31	RM2053/7
583	4	21	78	A	1	S4S306/1	S4E149/6	RM2621/7	S4P555/36	RM2044/8
584	4	21	78	A	1	S4S306/2	S4E150/6	RM2622/7	S4P556/36	RM2045/8
585	4	21	78	A	1	S4S306/3	S4E141/26	RM2628/12	S4P557/36	RM2046/8
586	4	21	78	A	3	S4S303/1	S4E099/11	RM2904/10	S4P531/6	RM3514/10
1		S3-4				SPECT.	SPECT.	VAX COMP.	PHOT.	VAX COMP.
						TAPE	P.P. TAPE	TAPE	P.P. TAPE	TAPE
REV	MTN	DAY	YR	FT/F		-----	-----	-----	-----	-----
591	4	22	78	C	3	S4S303/4	S4E142/26	RM2629/3	S4P558/36	RM2047/8
596	4	22	78	A	3	S4S303/7	S4E100/11	RM2900/3	S4P522/11	RM3508/3
601	4	22	78	A	3	S4S126/1	S4E104/6	RM2886/2	S4P503/31	RM2510/7
604	4	22	78	A	3	S4S126/4	S4E105/6	RM2887/2	S4P503/36	RM2556/8
608	4	23	78	C	3	S4S117/4	S4E143/26	RM2630/3	S4P559/36	RM2048/8
612	4	23	78	A	3	S4S126/7	S4E057/11	RM2930/1	S4P503/41	RM2556/9
616	4	23	78	A	3	S4S337/5	S4E029/11	RM2917/2	S4P523/26	RM3509/6
620	4	23	78	A	3	S4S127/1	S4E058/11	RM2889/2	S4P503/46	RM2510/10
625	4	24	78	C	3	S4S117/7	S4E144/26	RM2621/6	S4P560/36	RM2049/8
631	4	24	78	A	3	S4S127/4	S4E059/11	RM2891/5	S4P504/1	RM2511/1
634	4	24	78	A	3	S4S127/7	S4E060/11	RM2931/1	S4P504/6	RM2511/2
638	4	25	78	A	4	S4S123/1	S4E052/11	RM2915/8	S4P502/46	RM2509/11
643	4	25	78	C	3	S4S121/1	S4E135/1	RM2892/1	S4P555/16	RM2044/4
648	4	25	78	A	3	S4S123/5	S4E053/11	RM2927/1	S4P503/1	RM2510/1
652	4	25	78	A	3	S4S123/8	S4E054/11	RM2928/1	S4P503/6	RM2510/2
656	4	26	78	A	3	S4S124/1	S4E145/26	RM2622/6	S4P556/16	RM2045/4
660	4	26	78	C	3	S4S121/4	S4E162/1	RM2626/9	S4P557/16	RM2046/4
666	4	26	78	A	3	S4S124/4	S4E111/1	RM2667/4	S4P503/11	RM2510/3
669	4	26	78	A	3	S4S124/7	S4E055/11	RM2929/1	S4P503/16	RM2510/4
673	4	27	78	A	2	S4S120/1	S4E112/1	RM2668/4	S4P526/46	RM3512/9
677	4	27	78	C	3	S4S121/7	S4E163/1	RM2627/9	S4P558/16	RM2047/4
680	4	27	78	A	3	S4S120/3	S4E146/1	RM2623/6	S4P502/36	RM2509/8
683	4	27	78	A	3	S4S120/6	S4E106/6	RM2890/1	S4P502/41	RM2509/9
686	4	27	78	A	4	S4S125/1	S4E047/11	RM2888/1	S4P503/21	RM2510/5
691	4	28	78	A	1	S4S125/5	S4E164/1	RM2628/8	S4P559/16	RM2048/4
694	4	28	78	C	2	S4S122/1	S4E146/6	RM2628/3	S4P560/16	RM2049/4
697	4	28	78			NO S4S	TAPE			
701	4	28	78	A	3	S4S125/6	S4E010/16	RM2910/5	S4P503/26	RM2510/6
706	4	29	78	A	3	S4S119/1	S4E049/11	RM2918/8	S4P502/26	RM2509/6
710	4	29	78	A	1	S4S119/4	S4E147/11	RM2623/7	S4P561/16	RM2050/4
712	4	29	78	C	3	S4S122/3	S4E148/11	RM2624/7	S4P562/16	RM2051/4
715	4	29	78	A	3	S4S119/5	S4E050/11	RM2907/1	S4P502/31	RM2509/7
718	4	29	78	A	3	S4S112/1	S4E048/11	RM2905/2	S4P502/6	RM2509/2
721	4	30	78	A	2	S4S138/4	S4E113/1	RM2906/2	S4P527/41	RM3516/10
724	4	30	78	A	2	S4S138/6	S4E114/1	RM2907/2	S4P528/46	RM3514/9
729	4	30	78	C	3	S4S135/1	S4E149/11	RM2625/7	S4P566/41	RM2047/13

732	4	30	78	A	3	S4S135/4	S4E107/6	RM2905/3	S4P504/46	RM2511/10
735	4	30	78	A	3	S4S135/7	S4E150/1	RM2626/5	S4P564/16	RM2053/4
740	5	1	78	A	3	S4S337/8	S4E030/11	RM2891/1	S4P524/26	RM3510/6
746	5	1	78	C	3	S4S128/1	S4E161/26	RM2980/3	S4P561/36	RM2050/8
748	5	1	78	A	3	S4S335/1	S4E045/11	RM2915/7	S4P530/21	RM3516/5
752	5	2	78	A	3	S4S136/1	S4E110/11	RM2668/6	S4P505/1	RM2512/1
759	5	2	78	A	3	S4S136/4	S4E062/11	RM2928/4	S4P505/6	RM2512/2
763	5	2	78	C	3	S4S136/7	S4E157/6	RM2626/10	S4P562/36	RM2051/8
765	5	2	78	A	3	S4S137/1	S4E063/11	RM2885/3	S4P505/11	RM2512/3
769	5	3	78	A	3	S4S128/4	S4E005/11	RM2886/3	S4P504/11	RM2511/3
774	5	3	78	A	3	S4S137/4	S4E158/6	RM2627/10	S4P529/26	RM3515/6
781	5	3	78	C	3	S4S128/7	S4E159/6	RM2628/9	S4P563/36	RM2052/8
784	5	4	78	A	3	S4S112/4	S4E064/11	RM2890/2	S4P502/11	RM2509/3
788	5	4	78	A	3	S4S137/7	S4E108/6	RM2906/3	S4P505/16	RM2512/4
794	5	4	78	A	3	S4S134/1	S4E065/11	RM2907/3	S4P504/36	RM2511/8
798	5	4	78	C	3	S4S335/4	S4E160/6	RM2629/10	S4P564/36	RM2053/8
801	5	5	78	A	3	S4S134/4	S4E066/11	RM2927/8	S4P504/41	RM2511/9
807	5	5	78	A	3	S4S134/7	S4E122/11	RM2760/3	S4P528/26	RM3514/6
811	5	5	78			NO S4S	TAPE			
815	5	5	78	C	3	S4S130/1	S4E161/6	RM2630/9	S4P555/41	RM2044/9
821	NO	B+L	A	4		S4S130/4				
1	S3-4					SPECT. TAPE	SPECT. P.P. TAPE	VAX COMP. TAPE	PHOT. P.P. TAPE	VAX COMP. TAPE
REV	MTN	DAY	YR	FT/F						
852	5	8	78	A	3	S4S130/5	S4E069/11	RM2905/7	S4P504/16	RM2511/4
856	5	8	78	A	3	S4S133/1	S4E046/1	RM2906/9	S4P504/26	RM2511/6
860	5	8	78			NO S4S	TAPE			
865	5	8	78	C	3	S4S133/4	S4E162/6	RM2626/11	S4P556/41	RM2045/9
868	5	9	78	A	3	S4S133/7	S4E070/11	RM2889/3	S4P504/31	RM2511/7
872	5	9	78	A	3	S4S335/7	S4E028/11	RM2885/4	S4P531/21	RM3516/9
877	5	9	78	A	3	S4S154/1	S4E079/1	RM2886/4	S4P507/11	RM2514/3
882	5	10	78	C	4	S4S338/1	S4E163/6	RM2627/11	S4P557/41	RM2046/9
886	5	10	78	A	3	S4S131/1	S4E045/1	RM2915/4	S4P504/21	RM2511/5
892	5	10	78	A	2	S4S131/4	S4E120/1	RM2669/4	S4P522/51	RM3508/8
894	5	10	78	A	1	S4S131/6	S4E164/6	RM2628/10	S4P558/41	RM2047/9
895	5	10	78	A	1	S4S131/7	S4E165/6	RM2629/11	S4P559/41	RM2048/9
896	NO	B+L	A	1		S4S132/1				
897	5	10	78	A	1	S4S132/2	S4E156/11	RM2626/13	S4P560/41	RM2049/9
898	5	11	78	A	1	S4S132/3	S4E157/11	RM2626/12	S4P561/41	RM2050/9
899	5	11	78	A	1	S4S154/4	S4E158/11	RM2627/12	S4P562/41	RM2051/9
900	5	11	78	A	1	S4S132/4	S4E159/11	RM2628/11	S4P563/41	RM2052/9
904	5	11	78	A	1	S4S155/1	S4E160/11	RM2629/12	S4P564/41	RM2053/9
907	5	11	78	A	1	S4S151/1	S4E161/11	RM2627/13	S4P555/46	RM2044/10
909	5	11	78	A	1	S4S129/1	S4E162/11	RM2971/1	S4P556/46	RM2045/10
910	5	11	78	A	1	S4S159/1	S4E163/11	RM2972/1	S4P557/46	RM2046/10
911	5	11	78	A	1	S4S151/2	S4E164/11	RM2973/11	S4P558/46	RM2047/10
912	5	11	78	A	1	S4S129/2	S4E165/11	RM2974/1	S4P559/46	RM2048/10
913	5	11	78	A	1	S4S129/3	S4E156/16	RM2975/1	S4P560/46	RM2049/10
914	5	11	78	A	1	S4S129/4	S4E157/16	RM2976/1	S4P561/46	RM2050/10
915	5	12	78	A	1	S4S151/3	S4E158/16	RM2977/1	S4P562/46	RM2051/10
916	5	12	78	A	1	S4S151/4	S4E159/16	RM2978/1	S4P563/46	RM2052/10
932	5	13	78	A	1	S4S139/1	S4E160/16	RM2979/1	S4P564/46	RM2053/10
992	5	16	78	A	1	S4S139/2	S4E161/16	RM2980/1	S4P555/51	RM2044/11
993	5	16	78	A	3	S4S139/3	S4E123/11	RM2761/3	S4P526/31	RM3512/7
996	5	17	78	C	4	S4S139/6	S4E162/16	RM2971/2	S4P556/51	RM2045/11
1000	5	17	78	A	2	S4S144/1	S4E121/1	RM2907/4	S4P523/56	RM3507/11
1005	5	17	78	A	3	S4S144/3	S4E109/6	RM2670/4	S4P530/31	RM3516/7
1009	5	17	78	A	3	S4S144/6	S4E118/11	RM2888/2	S4P501/36	RM2784/9
1013	5	18	78	C	4	S4S155/2	S4E163/16	RM2972/2	S4P557/51	RM2046/11
1018	5	18	78	A	3	S4S148/1	S4E068/1	RM2928/2	S4P506/21	RM2513/5

1022	5	18	78	A	3	S4S148/4	S4E069/1	RM2929/2	S4P506/26	RM2513/6
1025	5	18	78	A	3	S4S148/7	S4E070/1	RM2889/4	S4P506/31	RM2513/7
1030	5	19	78	C	2	S4S142/1	S4E164/16	RM2973/1	S4P558/51	RM2047/11
1034	5	19	78	A	3	S4S142/3	S4E071/11	RM2888/3	S4P505/36	RM2512/8
1038	5	19	78	A	3	S4S142/6	S4E113/11	RM2663/7	S4P505/41	RM2512/9
1041	5	19	78	A	3	S4S143/1	S4E110/6	RM2663/5	S4P505/46	RM2512/10
1047	5	20	78	C	3	S4S143/4	S4E165/16	RM2974/2	S4P559/51	RM2048/11
1053	5	20	78	A	3	S4S143/7	S4E101/11	RM2664/6	S4P501/31	RM2784/8
1056	5	20	78	A	3	S4S141/1	S4E102/11	RM2665/6	S4P505/26	RM2512/6
1060	5	21	78	A	4	S4S141/4	S4E103/11	RM2666/6	S4P505/31	RM2512/7
1065	5	21	78	C	3	S4S162/1	S4E156/21	RM2975/2	S4P560/51	RM2049/11
1070	5	21	78	A	3	S4S141/8	S4E001/11	RM2905/5	S4P501/26	RM2784/7
1073	5	21	78	A	3	S4S162/4	S4E157/21	RM2976/2	S4P508/21	RM2515/5
1077	5	22	78	A	3	S4S145/1	S4E002/11	RM2913/4	S4P506/1	RM2513/1
1082	5	22	78	C	3	S4S145/4	S4E158/21	RM2977/2	S4P561/51	RM2050/11
1087	5	22	78	A	3	S4S162/7	S4E159/21	RM2978/2	S4P562/51	RM2051/11
1090	5	22	78	A	3	S4S145/7	S4E003/11	RM2908/5	S4P506/6	RM2513/2
1094	5	23	78	A	3	S4S140/1	S4E125/1	RM2889/5	S4P531/26	RM3510/13
1099	5	23	78	C	3	S4S157/1	S4E160/21	RM2979/2	S4P563/51	RM2052/11
1103	5	23	78	A	3	S4S140/4	S4E126/11	RM2759/4	S4P529/31	RM3515/7
1106	5	23	78	A	3	S4S140/7	S4E004/11	RM2909/5	S4P505/21	RM2512/5
1	S3-4					SPECT.	SPECT.	VAX COMP.	PHOT.	VAX COMP.
						TAPE.	P.P. TAPE	TAPE	P.P. TAPE	TAPE
REV	MTH	DAY	YR	FT/F	-----	-----	-----	-----	-----	-----
1110	5	24	78	A	3	S4S147/1	S4E128/11	RM2760/4	S4P522/26	RM3508/6
1117	5	24	78	C	3	S4S158/1	S4E161/21	RM2980/2	S4P564/51	RM2053/11
1121	5	24	78	A	3	S4S147/4	S4E066/1	RM2903/3	S4P506/16	RM2513/4
1124	5	24	78	A	4	S4S290/1	S4E104/11	RM2906/5	S4P531/31	RM3508/13
1129	5	25	78	A	3	S4S147/7	S4E067/1	RM2903/4	S4P501/46	RM2784/11
1134	5	25	78	C	3	S4S146/1	S4E162/21	RM2971/3	S4P555/56	RM2044/12
1136	5	25	78	A	3	S4S340/2	S4E033/11	RM2907/5	S4P565/46	RM2045/14
1139	5	25	78	A	3	S4S146/4	S4E105/11	RM2905/6	S4P506/11	RM2513/3
1143	5	26	78			NO S4S	TAPE			
1148	5	26	78	A	2	S4S112/7	S4E119/1	RM2906/6	S4P531/41	RM3512/13
1151	5	26	78	C	3	S4S157/4	S4E163/21	RM2972/3	S4P556/56	RM2045/12
1154	5	26	78	A	3	S4S146/7	S4E129/11	RM2761/4	S4P501/41	RM2784/10
1158	5	27	78	A	3	S4S157/7	S4E081/1	RM2928/7	S4P507/36	RM2514/8
1164	5	27	78	A	3	S4S163/1	S4E164/21	RM2973/2	S4P508/26	RM2515/6
1168	5	27	78	C	3	S4S158/4	S4E165/21	RM2974/3	S4P557/56	RM2046/12
1171	5	27	78	A	3	S4S158/7	S4E082/1	RM2887/3	S4P507/41	RM2514/9
1175	5	28	78	A	3	S4S152/1	S4E074/1	RM2885/5	S4P506/36	RM2513/8
1180	5	28	78	A	3	S4S152/4	S4E075/1	RM2929/3	S4P506/41	RM2513/9
1185	5	28	78	C	3	S4S152/7	S4E156/26	RM2975/3	S4P558/56	RM2047/12
1188	5	28	78	A	3	S4S153/1	S4E076/1	RM2907/6	S4P506/46	RM2513/10
1192	5	29	78	A	3	S4S153/4	S4E157/26	RM2976/3	S4P507/1	RM2514/1
1196	5	29	78	A	3	S4S153/7	S4E078/1	RM2906/7	S4P507/6	RM2514/2
1200	5	29	78	A	3	S4S163/4	S4E090/1	RM2907/7	S4P508/31	RM2515/7
1203	5	29	78	C	3	S4S163/7	S4E158/26	RM2977/3	S4P559/56	RM2048/12
1207	5	30	78	A	3	S4S159/2	S4E083/1	RM2929/8	S4P507/46	RM2514/10
1211	5	30	78	A	2	S4S156/1	S4E123/1	RM2669/7	S4P525/51	RM3508/11
1216	5	30	78	A	3	S4S156/3	S4E080/1	RM2903/5	S4P507/16	RM2514/4
1220	5	30	78	C	3	S4S156/6	S4E159/26	RM2978/3	S4P560/56	RM2049/12
1224	5	31	78	A	2	S4S161/1	S4E124/1	RM2903/6	S4P526/51	RM3509/11
1229	5	31	78	A	3	S4S161/3	S4E086/1	RM2907/8	S4P508/11	RM2515/3
1233	5	31	78	A	3	S4S161/6	S4E087/1	RM2906/8	S4P508/16	RM2515/4
1237	5	31	78	C	3	S4S340/5	S4E160/26	RM2979/3	S4P561/56	RM2050/12
1245	6	1	78	A	3	S4S159/5	S4E084/1	RM2930/7	S4P508/1	RM2515/1
1264	6	2	78	A	3	S4S149/1	S4E071/1	RM2931/2	S4P507/21	RM2514/5
1267	6	2	78	A	3	S4S149/4	S4E072/1	RM2932/2	S4P507/26	RM2514/6
1271	6	3	78	C	4	S4S122/6	S4E176/1	RM2786/1	S4P537/31	RM3228/7

1276	6	3	78	A	3	S4S149/7	S4E073/1	RM2927/3	S4P507/31	RM2514/7
1281	6	3	78	A	3	S4S160/1	S4E085/1	RM2931/6	S4P508/6	RM2515/2
1285	6	3	78	A	1	S4S336/4	S4E177/1	RM2787/1	S4P538/31	BAD DATA
1286	6	3	78	A	1	S4S338/5	S4E178/1	RM2788/1	S4P539/31	RM3230/6
1287	6	3	78	A	1	S4S167/1	S4E179/1	RM2789/1	S4P540/31	RM3231/7
1288	6	4	78	A	1	S4S160/4	S4E180/1	RM2790/1	S4P541/31	RM3232/7
1289	6	4	78	A	1	S4S160/5	S4E181/1	RM2791/1	S4P542/31	RM3233/7
1290	6	4	78	A	1	S4S160/6	S4E182/1	RM2792/1	S4P543/31	RM3234/7
1292	6	4	78	A	1	S4S160/7	S4E183/1	RM2938/1	S4P544/31	RM3235/7
1293	6	4	78	A	1	S4S150/1	S4E184/1	RM2939/1	S4P535/36	RM3226/8
1294	6	4	78	A	1	S4S150/2	S4E185/1	RM2940/1	S4P536/36	RM3227/8
1296	6	4	78	A	1	S4S166/1	S4E176/6	RM2786/2	S4P537/36	RM3228/8
1297	6	4	78	A	1	S4S166/2	S4E177/6	RM2787/2	S4P538/36	RM3229/7
1298	6	4	78	A	1	S4S166/3	S4E178/6	RM2788/2	S4P539/36	RM3230/7
1299	6	4	78	A	1	S4S166/4	S4E179/6	RM2789/2	S4P540/36	RM3231/8
1300	6	4	78	A	1	S4S166/5	S4E180/6	RM2790/2	S4P541/36	RM3232/8
1301	6	4	78	A	1	S4S166/6	S4E181/6	RM2791/3	S4P542/36	RM3233/8
1302	6	4	78	A	1	S4S166/7	S4E135/6	RM2893/1	S4P543/36	RM3234/8
1303	6	4	78	A	1	S4S166/8	S4E182/6	RM2792/3	S4P544/36	RM3235/8
1304	6	5	78	A	1	S4S164/1	S4E183/6	RM2938/3	S4P535/41	RM3226/9
1305	6	5	78	A	1	S4S164/2	S4E184/6	RM2939/3	S4P536/41	RM3227/9
1			S3-4			SPECT.	SPECT.	VAX COMP.	PHOT.	VAX COMP.
						TAPE	P.P. TAPE	TAPE	P.P. TAPE	TAPE
REV	MTN	DAY	YR	FT/F		-----	-----	-----	-----	-----
1306	6	5	78	A	1	S4S164/3	S4E185/6	RM2940/3	S4P537/41	RM3228/9
1307	6	5	78	A	1	S4S164/4	S4E176/11	RM2786/3	S4P538/41	RM3229/8
1308	6	5	78			NO S4S	TAPE			
1309	NO	B+L	A	1		S4S167/2				
1310	6	5	78	A	1	S4S167/3	S4E135/11	RM2892/2	S4P539/41	RM3230/8
1312	6	5	78	A	1	S4S164/5	S4E177/11	RM2787/3	S4P540/41	RM3231/9
1313	6	5	78	A	1	S4S164/6	S4E178/11	RM2788/3	S4P541/41	RM3232/9
1314	6	5	78	A	1	S4S164/7	S4E179/11	RM2789/3	S4P542/41	RM3233/9
1315	6	5	78	A	1	S4S164/8	S4E180/11	RM2790/3	S4P543/41	RM3234/9
1316	6	5	78	A	1	S4S165/1	S4E181/11	RM2791/2	S4P544/41	RM3235/9
1317	6	5	78	A	1	S4S165/2	S4E182/11	RM2792/2	S4P535/46	RM3226/10
1318	6	5	78	A	1	S4S165/3	S4E183/11	RM2938/2	S4P536/46	RM3227/10
1319	6	5	78	A	1	S4S165/4	S4E184/11	RM2939/2	S4P537/46	RM3228/10
1320	6	6	78	A	1	S4S165/5	S4E185/11	RM2940/2	S4P538/46	RM3229/9
1321	6	6	78	A	1	S4S165/6	S4E176/16	RM2786/4	S4P539/46	RM3230/9
1322	6	6	78	A	1	S4S165/7	S4E177/16	RM2787/4	S4P540/46	RM3231/10
1323	6	6	78	A	1	S4S165/8	S4E178/16	RM2788/4	S4P541/46	RM3232/10
1324	6	6	78	A	1	S4S150/3	S4E179/16	RM2789/4	S4P542/46	RM3233/10
1325	6	6	78	A	1	S4S150/4	S4E180/16	RM2790/4	S4P543/46	RM3234/10
1326	6	6	78	A	1	S4S167/4	S4E181/16	RM2791/4	S4P544/46	RM3235/10
1329	6	6	78	A	1	S4S150/5	S4E182/16	RM2792/4	S4P545/1	RM2075/1
1330	6	6	78	A	1	S4S172/1	S4E183/16	RM2938/4	S4P546/1	RM2076/1
1331	6	6	78	A	1	S4S172/2	S4E184/16	RM2939/4	S4P547/1	RM2077/1
1332	6	6	78	A	1	S4S150/6	S4E185/16	RM2940/4	S4P548/1	RM2078/1
1333	6	6	78	A	1	S4S150/7	S4E176/21	RM2786/5	S4P549/1	RM2079/1
1334	6	6	78	A	3	S4S338/6	S4E119/11	RM2668/7	S4P525/26	RM3511/6
1337	6	7	78	C	3	S4S172/3	S4E177/21	RM2787/5	S4P550/1	RM3898/1
1342	6	7	78	A	3	S4S171/1	S4E097/1	RM2928/8	S4P509/16	RM2555/4
1347	6	7	78	A	3	S4S171/4	S4E098/1	RM2663/1	S4P509/21	RM2555/5
1350	6	7	78	A	3	S4S171/7	S4E099/1	RM2664/1	S4P509/26	RM2555/6
1355	6	8	78	C	3	S4S173/1	S4E178/21	RM2788/5	S4P551/1	RM3899/1
1359	6	8	78	A	3	S4S173/4	S4E100/1	RM2665/1	S4P509/31	RM2555/7
1363	6	8	78	A	3	S4S173/7	S4E001/2	RM2908/1	S4P509/36	RM2555/8
1366	6	8	78	A	3	S4S168/1	S4E091/1	RM2930/8	S4P508/36	RM2515/8
1371	6	9	78	C	2	S4S168/4	S4E179/21	RM2789/5	S4P552/1	RM3900/1
1375	6	9	78	A	3	S4S168/6	S4E130/11	RM2762/4	S4P530/26	RM3516/6

1379	6	9	78	A	3	S4S169/1	S4E092/1	RM2902/1	S4P508/41	RM2515/9
1383	6	9	78	A	3	S4S169/4	S4E093/1	RM2902/2	S4P508/46	RM2515/10
1388	6	10	78	C	2	S4S169/7	S4E180/21	RM2790/5	S4P553/1	RM3901/1
1394	6	10	78	A	3	S4S170/1	S4E094/1	RM2902/3	S4P509/1	RM2555/1
1397	6	10	78	A	3	S4S170/4	S4E095/1	RM2902/4	S4P509/6	RM2555/2
1401	6	11	78	A	3	S4S170/7	S4E096/1	RM2902/5	S4P509/11	RM2555/3
1405	6	11	78	C	2	S4S188/1	S4E181/21	RM2791/5	S4P554/1	RM3902/1
1410	6	11	78	A	3	S4S181/1	S4E010/6	RM2902/6	S4P510/31	RM2556/7
1414	6	11	78	A	3	S4S181/4	S4E011/6	RM2913/3	S4P510/36	RM2510/8
1418	6	12	78	A	3	S4S181/7	S4E012/6	RM2903/7	S4P510/41	RM2509/10
1423	6	12	78	C	3	S4S182/1	S4E182/21	RM2792/5	S4P545/6	RM2075/2
1428	6	12	78	A	3	S4S182/4	S4E042/11	RM2918/7	S4P510/46	RM2556/10
1431	6	12	78	A	3	S4S182/7	S4E043/11	RM2919/8	S4P511/1	RM3067/1
1435	6	13	78	A	2	S4S179/1	S4E128/1	RM2664/8	S4P531/46	RM3509/13
1440	6	13	78	C	3	S4S179/3	S4E183/21	RM2938/5	S4P546/6	RM2076/2
1444	6	13	78	A	3	S4S179/6	S4E007/6	RM2913/6	S4P510/16	RM2556/4
1447	6	13	78	A	3	S4S180/1	S4E008/6	RM2914/3	S4P510/21	RM2556/5
1451	6	14	78			NO S4S	TAPE			
1457	6	14	78	C	3	S4S180/4	S4E184/21	RM2939/5	S4P547/6	RM2077/2
1461	6	14	78	A	3	S4S180/6	S4E009/6	RM2912/3	S4P510/26	RM2556/6
1470	6	15	78	A	2	S4S178/1	S4E127/1	RM2663/8	S4P527/56	RM3509/12
1		S3-4				SPECT.	SPECT.	VAX COMP.	PHOT.	VAX COMP.
						TAPE	P.P. TAPE	TAPE	P.P. TAPE	TAPE
REV	MTH	DAY	YR	FT/F	-----	-----	-----	-----	-----	-----
1475	6	15	78	C	3	S4S201/4	S4E185/21	RM2940/5	S4P548/6	RM2078/2
1589	6	22	78	C	3	S4S201/7	S4E176/26	RM2786/6	S4P549/6	RM2079/2
1593	6	22	78	A	3	S4S189/1	S4E126/1	RM2670/7	S4P529/46	RM3067/8
1598	6	23	78	A	2	S4S189/4	S4E112/6	RM2665/5	S4P529/51	RM3512/11
1602	6	23	78	A	3	S4S177/4	S4E006/6	RM2912/6	S4P510/11	RM2556/3
1607	6	23	78	C	3	S4S188/3	S4E177/26	RM2787/6	S4P550/6	RM3898/2
1610	6	23	78	A	3	S4S189/6	S4E006/16	RM2903/8	S4P511/41	RM3067/9
1614	6	24	78	A	3	S4S175/1	S4E181/26	RM2791/6	S4P551/6	RM3899/2
1618	6	24	78	A	3	S4S175/4	S4E003/1	RM2910/1	S4P509/46	RM2555/10
1624	6	24	78	C	3	S4S184/2	S4E178/26	RM2788/6	S4P552/6	RM3900/2
1626	6	24	78	A	3	S4S184/5	S4E040/11	RM2917/3	S4P511/11	RM3067/3
1630	6	25	78	A	3	S4S183/1	S4E068/6	RM2930/4	S4P511/6	RM3067/2
1635	6	25	78	A	2	S4S183/4	S4E129/1	RM2665/8	S4P522/56	RM3512/10
1638	6	25	78	A	2	S4S183/6	S4E130/1	RM2666/8	S4P523/56	RM3507/12
1669	6	27	78	A	3	S4S175/7	S4E004/1	RM2911/1	S4P510/1	RM2556/1
1673	6	27	78	C	3	S4S185/1	S4E179/26	RM2789/6	S4P553/6	RM3901/2
1676	6	27	78	A	3	S4S188/6	S4E041/11	RM2917/7	S4P511/16	RM3067/4
1681	6	28	78	A	2	S4S185/7	S4E111/6	RM2664/5	S4P525/56	RM3508/12
1686	6	28	78	A	3	S4S187/1	S4E073/6	RM2931/4	S4P511/31	RM3067/7
1689	6	28	78	A	2	S4S330/2	S4E002/16	RM2912/5	S4P531/51	RM3515/11
1691	6	28	78	C	3	S4S187/4	S4E068/16	RM2667/9	S4P546/11	RM2076/3
1694	6	29	78	A	3	S4S187/7	S4E131/1	RM2667/8	S4P524/31	RM3510/7
1698	6	29	78	A	2	S4S114/4	S4E120/11	RM2891/3	S4P527/51	RM3510/11
1703	6	29	78	A	3	S4S186/1	S4E039/11	RM2916/3	S4P511/21	RM3067/5
1708	6	29	78	C	3	S4S186/4	S4E180/26	RM2790/6	S4P554/6	RM3902/2
1713	6	30	78	A	3	S4S186/7	S4E072/6	RM2930/5	S4P511/26	RM3067/6
1718	6	30	78	A	3	S4S195/1	S4E087/6	RM2931/7	S4P512/31	RM3068/7
1723	6	30	78	A	3	S4S195/4	S4E182/26	RM2792/6	S4P512/36	RM3068/8
1725	6	30	78	C	3	S4S174/1	S4E183/26	RM2938/6	S4P545/11	RM2075/3
1728	7	1	78	A	2	S4S174/4	S4E001/16	RM2914/5	S4P530/51	RM3510/12
1732	7	1	78	A	4	S4S174/6	S4E002/1	RM2909/1	S4P509/41	RM2555/9
1737	7	1	78	A	3	S4S176/1	S4E005/1	RM2912/1	S4P510/6	RM2556/2
1739	7	1	78	A	1	S4S176/4	S4E184/26	RM2939/6	S4P547/11	RM2077/3
1740	7	1	78	A	1	S4S195/7	S4E147/16	RM2972/4	S4P548/11	RM2078/3
1741	7	1	78	A	1	S4S200/1	S4E148/16	RM2973/3	S4P549/11	RM2079/3
1742	7	2	78	A	1	S4S200/2	S4E149/16	RM2974/4	S4P550/11	BAD TIMES

1743	7	2	78	A	1	S4S200/3	S4E150/16	RM2975/4	S4P551/11	RM3899/3
1744	7	2	78	A	1	S4S200/4	S4E146/16	RM2971/4	S4P552/11	RM3900/3
1745	7	2	78	A	1	S4S200/5	S4E147/21	RM2977/4	S4P553/11	RM3901/3
1746	7	2	78	A	1	S4S200/6	S4E148/21	RM2978/4	S4P554/11	RM3902/3
1747	7	2	78	A	1	S4S196/1	S4E149/21	RM2979/4	UNABLE TO	PROCESS
1748	7	2	78			NO S4S	TAPE			
1749	NO	B+L	A	1		S4S290/5				
1751	7	2	78	A	1	NO S4S	TAPE			
1752	7	2	78	A	1	S4S196/3	S4E162/26	RM2971/7	S4P546/16	BAD TIMES
1753	7	2	78	A	1	S4S196/4	S4E163/26	RM2972/7	S4P547/16	RM2076/4
1754	NO	B+L	A	1						
1755	7	2	78	A	1	S4S196/5	S4E164/26	RM2973/6	S4P548/16	BAD TIMES
1756	7	2	78	A	1	S4S202/1	S4E174/31	RM2972/13	S4P549/16	RM2078/4
1757	7	2	78	A	1	S4S202/2	S4E166/36	RM2974/13	S4P545/16	RM3898/3
1758	7	3	78	A	1	S4S202/3	S4E170/36	RM2975/13	S4P550/16	RM2079/4
1759	7	3	78	A	1	S4S202/4	S4E171/36	RM2976/13	S4P551/16	RM3899/4
1760	7	3	78	A	1	S4S202/5	S4E172/36	RM2977/13	S4P552/16	RM3900/4
1761	7	3	78	A	1	S4S202/6	S4E173/36	RM2978/13	S4P553/16	RM3901/4
1762	7	3	78	A	1	S4S203/1	S4E175/1	RM2975/6	S4P554/16	RM3902/4
1763	7	3	78	A	1	S4S203/2	S4E169/1	RM2979/5	S4P545/21	RM3898/4
1764	7	3	78	A	1	S4S203/3	S4E170/1	RM2980/5	S4P546/21	RM2075/5
1	S3-4					SPECT.	SPECT.	VAX COMP.	PHOT.	VAX COMP.
						TAPE	P.P. TAPE	TAPE	P.P. TAPE	TAPE
REV	MTH	DAY	YR	FT/F		-----	-----	-----	-----	-----
1765	7	3	78			NO S4S	TAPE			
1766	NO	B+L	A	4		S4S203/4				
1767	7	3	78	A	1	S4S203/5	S4E171/1	RM2971/6	S4P547/21	RM2076/5
1768	7	3	78	A	1	S4S203/6	S4E172/1	RM2972/6	S4P548/21	RM2077/4
1769	7	3	78	A	1	S4S197/1	S4E173/1	RM2973/5	S4P549/21	RM2078/5
1770	7	3	78	A	1	S4S197/2	S4E174/1	RM2974/6	S4P550/21	RM2079/5
1771	7	3	78	A	1	S4S197/3	S4E146/21	RM2976/4	S4P551/21	RM3899/5
1772	7	3	78	A	1	S4S197/4	S4E150/21	RM2980/4	S4P552/21	RM3900/5
1773	7	3	78	A	1	S4S197/5	S4E166/6	RM2976/5	S4P553/21	RM3901/5
1774	7	3	78	A	1	S4S197/6	S4E135/16	RM2893/2	S4P554/21	RM3902/5
1775	7	4	78	A	1	S4S204/1	S4E167/6	RM2977/5	S4P545/26	RM2075/6
1776	7	4	78	A	1	S4S204/2	S4E168/6	RM2978/5	S4P546/26	RM2076/6
1777	7	4	78	A	1	S4S204/3	S4E169/6	RM2974/7	S4P547/26	RM2077/5
1779	7	4	78	A	1	S4S204/4	S4E170/6	RM2975/7	S4P548/26	RM2078/6
1780	7	4	78	A	1	S4S204/5	S4E146/26	RM2971/5	S4P549/26	RM2079/6
1781	7	4	78			NO S4S	TAPE			
1783	7	4	78	A	1	S4S199/1	S4E147/26	RM2972/5	S4P567/41	RM2048/13
1784	7	4	78	A	1	S4S199/2	S4E135/21	RM2892/3	S4P551/26	RM3898/5
1785	7	4	78	A	1	S4S199/3	S4E135/36	RM2893/4	S4P552/26	RM3900/6
1786	7	4	78	A	1	S4S199/4	S4E148/26	RM2973/4	S4P553/26	RM3901/6
1787	7	4	78	A	1	S4S199/5	S4E149/26	RM2974/5	S4P554/26	RM3902/6
1788	NO	B+L	A	2		S4S199/6				
1791	7	5	78	C	3	S4S198/1	S4E150/26	RM2975/5	S4P545/31	RM2075/7
1797	7	5	78	A	3	S4S198/4	S4E135/41	RM2892/5	S4P512/41	RM3068/9
1801	7	5	78	A	2	S4S198/7	S4E117/6	RM2669/5	S4P525/36	RM3511/10
1804	7	5	78	A	3	S4S190/1	S4E132/6	RM2759/3	S4P511/46	RM3067/10
1808	7	6	78	C	3	S4S251/1	S4E171/6	RM2976/6	S4P546/31	RM2076/7
1813	7	6	78	A	3	S4S190/4	S4E081/6	RM2666/1	S4P512/1	RM3068/1
1817	7	6	78	A	3	S4S329/1	S4E021/11	RM2918/3	S4P523/21	RM3509/5
1821	7	6	78	A	3	S4S114/6	S4E125/6	RM2760/1	S4P525/31	RM3511/7
1826	7	7	78	C	3	S4S329/4	S4E172/6	RM2977/6	S4P547/31	RM2077/6
1830	7	7	78	A	2	S4S329/7	S4E114/6	RM2666/5	S4P522/36	RM3508/10
1834	7	7	78	A	3	S4S192/1	S4E083/6	RM2668/1	S4P512/11	RM3068/3
1837	7	7	78	A	3	S4S192/4	S4E084/6	RM2669/1	S4P512/16	RM3068/4
1841	7	8	78	A	2	S4S192/7	S4E115/6	RM2667/5	S4P523/36	RM3509/10
1843	7	8	78	C	3	S4S194/1	S4E135/26	RM2893/3	S4P548/31	RM2078/7

1848	7	8	78	A	2	S4S194/4	S4E116/6	RM2668/5	S4P524/36	RM3510/10
1851	7	8	78	A	3	S4S194/6	S4E044/11	RM2915/6	S4P512/26	RM3068/6
1855	7	8	78	A	4	S4S193/1	S4E131/6	RM2762/2	S4P522/31	RM3508/7
1860	7	9	78	C	2	S4S193/5	S4E173/6	RM2978/6	S4P549/31	RM2079/7
1864	7	9	78	A	3	S4S193/7	S4E085/6	RM2670/1	S4P512/21	RM3068/5
1867	7	9	78	A	3	S4S191/1	S4E125/11	RM2762/3	S4P523/31	RM3509/7
1871	7	9	78	A	4	S4S191/4	S4E174/6	RM2979/6	S4P550/31	RM3898/6
1877	7	10	78	C	3	S4S191/8	S4E175/6	RM2980/6	S4P551/31	RM3899/6
1882	7	10	78	A	3	S4S334/3	S4E025/11	RM2915/2	S4P528/21	RM3514/5
1886	7	10	78	A	3	S4S334/6	S4E026/11	RM2916/2	S4P529/21	RM3515/5
1890	7	11	78	A	3	S4S222/1	NOT ABLE	TO READ		
1894	7	11	78	C	3	S4S251/4	S4E167/11	RM2972/8	S4P552/31	RM3900/7
1902	7	11	78	C	3	S4S222/4	NOT ABLE	TO READ		
1907	7	12	78	A	3	S4S222/7	NOT ABLE	TO READ		
1912	7	12	78	C	3	S4S225/1	S4E170/11	RM2975/8	S4P553/31	RM3901/7
1915	7	12	78	A	3	S4S225/4	S4E009/16	RM2909/6	S4P516/11	RM3072/3
1919	7	12	78	A	3	S4S225/7	S4E036/6	RM2916/1	S4P526/36	RM3072/4
1923	7	13	78	A	2	S4S234/1	S4E120/6	RM2663/6	S4P528/31	RM3514/7
1929	7	13	78	C	3	S4S234/3	S4E135/31	RM2892/4	S4P554/31	RM3902/7
1932	7	13	78	A	3	S4S234/6	S4E048/6	RM2918/5	S4P517/16	RM3073/4
1946	7	14	78	C	3	S4S226/1	S4E171/11	RM2976/7	S4P545/36	RM2075/8
1	S3-4					SPECT.	SPECT.	VAX COMP.	PHOT.	VAX COMP.
						TAPE	P.P.TAPE	TAPE	P.P.TAPE	TAPE
REV	MTH	DAY	YR	FT/F						
1948	7	14	78	A	3	S4S226/4	S4E037/6	RM2891/4	S4P516/21	RM3072/5
1951	7	14	78	A	3	S4S226/7	S4E038/6	RM2917/1	S4P516/26	RM3072/6
1955	7	15	78	A	3	S4S227/1	S4E039/6	RM2918/1	S4P516/31	RM3072/7
1959	7	15	78	A	3	S4S251/7	S4E065/6	RM2932/5	S4P518/46	RM3074/10
1964	7	15	78	C	3	S4S227/4	S4E172/11	RM2977/7	S4P546/36	RM2076/8
1968	7	15	78			NO S4S	TAPE			
1971	7	16	78	A	3	S4S227/7	S4E040/6	RM2919/1	S4P516/36	RM3072/8
1981	7	16	78	C	2	S4S230/1	S4E173/11	RM2978/7	BAD TIMES	(UTP)
1983	7	16	78	A	2	S4S230/3	S4E119/6	RM2670/5	S4P527/31	RM3513/7
1987	7	17	78	A	3	S4S230/5	S4E046/6	RM2916/5	S4P568/41	BAD DATA
1995	7	17	78	A	3	S4S224/1	S4E033/6	RM2913/8	S4P516/1	RM3072/1
1998	7	17	78	C	3	S4S224/4	S4E174/11	RM2979/7	S4P548/36	RM2078/8
2001	7	17	78	A	3	S4S224/7	S4E034/6	RM2915/1	S4P516/6	RM3072/2
2006	7	18	78	A	3	S4S228/1	S4E041/6	RM2916/4	S4P516/41	RM3072/9
2011	7	18	78	A	3	S4S228/4	S4E042/6	RM2917/4	S4P516/46	RM3072/10
2015	7	18	78	C	3	S4S228/7	S4E175/11	RM2980/7	S4P549/36	RM2079/8
2018	7	19	78	A	4	S4S223/1	S4E030/6	RM2910/8	S4P515/36	RM3071/8
2023	7	19	78	A	3	S4S223/5	S4E031/16	RM2911/8	S4P515/41	RM3071/9
2029	7	19	78	A	3	S4S223/8	S4E032/6	RM2912/8	S4P515/46	RM3071/10
2033	7	19	78	C	2	S4S229/1	S4E168/11	RM2973/7	S4P550/36	RM3898/7
2036	7	20	78	A	3	S4S229/3	S4E043/6	RM2918/4	S4P517/1	RM3073/1
2041	7	20	78	A	3	S4S229/6	S4E044/6	RM2919/4	S4P517/6	RM3073/2
2044	7	20	78			NO S4S	TAPE			
2050	7	20	78	C	3	S4S231/1	S4E169/11	RM2974/8	S4P551/36	RM3899/7
2052	7	21	78	A	3	S4S231/4	S4E047/6	RM2917/5	S4P517/11	RM3073/3
2057	7	21	78	A	3	S4S239/1	S4E049/6	RM2919/5	S4P517/21	RM3073/5
2064	7	21	78	A	1	S4S239/4	S4E166/11	RM2971/8	S4P552/36	RM3900/8
2065	7	21	78	A	1	S4S239/5	S4E167/16	RM2972/9	S4P553/36	RM3901/8
2066	7	21	78	A	1	S4S233/1	S4E168/16	RM2973/8	S4P554/36	RM3902/8
2067	7	22	78	A	1	S4S233/2	S4E169/16	RM2974/9	S4P547/36	RM2077/7
2068	7	22	78	A	1	S4S233/3	S4E170/16	RM2975/9	S4P545/41	RM2075/9
2069	7	22	78	A	1	S4S253/1	S4E171/16	RM2976/8	S4P546/41	RM2076/9
2071	7	22	78	A	1	S4S253/2	S4E172/16	RM2977/8	S4P547/41	RM2077/8
2073	7	22	78	A	1	S4S253/3	S4E174/16	RM2979/8	S4P548/41	RM2078/9
2083	7	22	78	A	1	S4S240/1	S4E175/16	RM2980/8	S4P549/41	RM2079/9
2085	7	23	78	A	1	S4S240/2	S4E166/16	RM2971/9	S4P550/41	RM3898/8

2087	7	23	78	A	1	S4S240/3	S4E167/21	RM2972/10	S4P551/41	RM3899/8
2089	7	23	78	A	1	S4S232/1	S4E168/21	RM2973/9	S4P552/41	RM3900/9
2091	7	23	78	A	1	S4S232/2	S4E169/21	RM2974/10	S4P553/41	RM3901/9
2092	7	23	78	A	1	S4S232/3	S4E173/16	RM2978/8	S4P554/41	RM3902/9
2093	7	23	78	A	1	S4S236/1	S4E175/21	RM2980/10	S4P545/46	RM2075/10
2094	7	23	78	A	1	S4S236/2	S4E170/21	RM2975/10	S4P546/46	RM2076/12
2095	7	23	78	A	1	S4S236/3	S4E171/21	RM2976/9	S4P547/46	RM2077/9
2096	7	23	78	A	1	S4S237/1	S4E172/21	RM2977/9	S4P548/46	RM2078/10
2097	7	23	78	A	1	S4S237/2	S4E173/21	RM2978/9	S4P549/46	RM2079/10
2098	7	23	78	A	1	S4S237/3	S4E174/21	RM2979/9	S4P550/46	RM3898/9
2099	7	23	78	A	1	S4S253/1	S4E175/26	RM2980/11	S4P551/46	RM3899/9
2100	7	24	78	A	1	S4S253/2	S4E166/21	RM2971/10	S4P552/46	RM3900/10
2101	7	24	78	A	1	S4S253/3	S4E167/26	RM2972/11	S4P553/46	RM3901/10
2102	7	24	78	A	1	S4S235/1	S4E168/26	RM2973/10	S4P554/46	RM3902/10
2103	7	24	78	A	1	S4S235/2	S4E169/26	RM2974/11	S4P545/51	RM2075/11
2104	7	24	78	A	1	S4S235/3	S4E166/26	RM2971/11	S4P546/51	RM2076/10
2105	7	24	78	A	1	S4S238/1	S4E167/31	RM2972/12	S4P547/51	RM2077/10
2108	7	24	78	A	1	S4S238/2	S4E168/31	RM2971/13	S4P548/51	RM2078/11
2109	7	24	78	A	1	S4S238/3	S4E169/31	RM2974/12	S4P549/51	RM2079/11
2110	7	24	78	A	1	S4S115/1	S4E170/26	RM2975/11	S4P550/51	RM3898/10
2111	7	24	78	A	1	S4S249/1	S4E171/26	RM2976/10	S4P551/51	RM3899/10
1	S3-4					SPECT.	SPECT.	VAX COMP.	PHOT.	VAX COMP.
						TAPE	P.P.TAPE	TAPE	P.P.TAPE	TAPE
REV	MTH	DAY	YR	FT/F						
2112	7	24	78	A	1	S4S249/2	S4E172/26	RM2977/10	S4P552/51	RM3900/11
2113	7	24	78	A	2	S4S249/3	S4E123/6	RM2670/8	S4P531/36	RM3511/13
2116	7	25	78	A	3	S4S252/1	S4E066/6	RM2927/6	S4P519/1	RM3075/1
2121	7	25	78	C	3	S4S113/1	S4E173/26	RM2978/10	S4P553/51	RM3901/11
2127	7	25	78	A	3	S4S252/4	S4E067/6	BAD DATA	S4P519/6	RM3075/2
2131	7	25	78	A	3	S4S252/7	S4E086/6	RM2886/5	S4P519/11	RM3075/3
2137	7	26	78	C	2	S4S248/1	S4E174/26	RM2979/10	S4P554/51	RM3902/11
2139	NO	B+L		C	1	S4S248/3				
2142	7	26	78	A	3	S4S248/4	S4E063/6	RM2887/4	S4P518/41	RM3074/9
2146	7	26	78	A	2	S4S248/7	S4E122/6	RM2900/4	S4P530/36	RM3514/10
2150	7	27	78			NO S4S	TAPE			
2154	7	27	78	C	3	S4S245/1	S4E175/31	RM2979/11	S4P545/56	RM2075/12
2159	7	27	78	A	3	S4S245/4	S4E059/6	RM2900/2	S4P518/21	RM3074/5
2163	7	27	78	A	3	S4S245/7	S4E060/6	RM2916/8	S4P518/26	RM3074/6
2170	7	28	78	C	3	S4S250/1	S4E166/31	RM2971/12	S4P546/56	RM2076/11
2177	7	28	78	A	3	S4S115/2	S4E101/1	RM2888/4	S4P502/21	RM2509/5
2181	7	29	78	A	3	S4S241/1	S4E167/36	RM2976/12	S4P547/56	RM2077/11
2186	7	29	78	C	3	S4S250/4	S4E168/36	RM2977/12	S4P548/56	RM2078/12
2191	7	29	78	A	3	S4S290/6	S4E069/6	RM2932/6	S4P520/36	RM3076/8
2194	7	29	78	A	3	S4S250/7	S4E064/6	RM2931/3	S4P569/41	RM2050/13
2198	7	30	78	A	2	S4S246/1	S4E169/36	RM2979/12	S4P549/56	RM2079/12
2202	7	30	78	C	3	S4S246/3	S4E170/31	RM2975/12	S4P550/56	RM3898/11
2207	7	30	78	A	3	S4S246/6	S4E171/31	RM2976/11	S4P518/31	RM3074/7
2211	7	30	78	A	3	S4S241/4	S4E050/6	RM2916/6	S4P517/26	RM3073/6
2215	7	31	78	A	2	S4S247/1	S4E121/6	RM2669/8	S4P529/36	RM3516/11
2219	7	31	78	C	3	S4S247/3	S4E172/31	RM2977/11	S4P551/56	RM3899/11
2223	7	31	78	A	3	S4S247/6	S4E062/6	RM2932/4	S4P518/36	RM3074/8
2227	7	31	78	A	3	S4S241/7	S4E173/31	RM2978/12	S4P517/31	RM3073/7
2231	8	1	78	A	3	S4S244/1	S4E057/6	RM2919/7	S4P518/11	RM3074/3
2236	8	1	78	C	3	S4S244/4	S4E185/26	RM2940/6	S4P552/56	RM3900/12
2239	8	1	78	A	3	S4S244/7	S4E058/6	RM2915/5	S4P518/16	RM3074/4
2242	8	1	78	A	3	S4S243/1	S4E054/6	RM2916/7	S4P517/46	RM3073/10
2246	8	2	78	A	3	S4S243/4	S4E055/6	RM2917/6	S4P518/1	RM3074/1
2254	8	2	78	C	3	S4S293/1	S4E176/31	RM2786/7	S4P536/1	RM3227/1
2256	8	2	78	A	3	S4S293/4	S4E070/6	RM2927/7	S4P521/21	RM3507/5
2259	8	2	78	A	3	S4S243/7	S4E177/31	RM2787/7	S4P518/6	RM3074/2

2263	8	3	78	A	3	S4S242/1	S4E052/6	RM2918/6	S4P517/36	RM3073/8
2268	8	3	78	C	2	S4S113/4	S4E178/31	RM2788/7	S4P565/36	RM2052/13
2273	8	3	78	A	3	S4S242/4	S4E053/6	RM2919/6	S4P517/41	RM3073/8
2277	8	3	78	A	3	S4S293/7	S4E071/6	RM2929/5	S4P521/26	RM3507/6
2285	8	4	78	A	3	S4S291/1	S4E072/11	RM2930/6	S4P520/41	RM3076/9
2289	8	4	78	A	3	S4S339/1	S4E032/11	RM2918/2	S4P528/1	RM3514/1
2292	8	4	78			NO S4S	TAPE			
2296	8	5	78	A	2	S4S291/4	S4E111/11	RM2669/6	S4P524/41	RM3510/8
2303	8	5	78	A	3	S4S291/6	S4E073/11	RM2932/8	S4P521/1	RM3507/1
2308	8	5	78	A	3	S4S286/1	S4E074/11	RM2928/5	S4P520/21	RM3067/5
2312	8	6	78	A	3	S4S295/1	S4E068/11	RM2929/6	S4P521/41	RM3507/8
2316	8	6	78	C	2	S4S295/4	S4E179/31	RM2789/7	S4P537/1	RM3228/1
2317	NO	B+L	C	1		S4S295/6				
2321	8	6	78	A	3	S4S295/7	S4E087/11	RM2666/3	S4P521/46	RM3507/9
2324	8	6	78	A	3	S4S294/1	S4E084/11	BAD DATA	S4P521/31	RM3507/7
2328	8	7	78	A	3	S4S294/4	S4E085/11	RM2665/3	S4P521/36	RM3507/10
2332	8	7	78	C	3	S4S294/7	S4E180/31	RM2790/7	S4P538/1	RM3229/1
2338	8	7	78	A	3	S4S292/1	S4E075/11	RM2931/5	S4P521/6	RM3507/2
2342	8	7	78	A	3	S4S292/4	S4E076/11	RM2928/6	S4P521/11	RM3507/3
2348	8	8	78	C	3	S4S339/4	S4E181/31	RM2791/7	S4P539/1	RM3230/1
2353	8	8	78	A	3	S4S292/7	S4E182/31	RM2792/7	S4P521/16	RM3507/4
1		S3-4				SPECT.	SPECT.	VAX COMP.	PHOT.	VAX COMP.
						TAPE	P.P.TAPE	TAPE	P.P.TAPE	TAPE
REV	MTN	DAY	YR	FT/F						
2356	8	8	78	A	3	S4S296/1	S4E183/31	RM2938/7	S4P522/1	RM3508/1
2360	8	9	78	A	3	S4S296/4	S4E184/31	RM2939/7	S4P523/1	RM3509/1
2365	8	9	78	C	2	S4S296/7	S4E185/31	RM2940/7	S4P540/1	RM3231/1
2367	NO	B+L	C	1		S4S296/9				
2370	8	9	78	A	3	S4S286/4	S4E176/36	RM2786/8	S4P520/26	RM3076/6
2374	8	9	78	A	3	S4S286/7	S4E079/6	RM2929/7	S4P529/31	NO SCANS
2379	8	10	78	A	2	S4S279/1	S4E177/36	RM2787/8	S4P541/1	RM3232/1
2381	8	10	78	C	2	S4S279/3	S4E178/36	RM2788/8	S4P542/1	RM3233/1
2382	NO	B+L	C	1		S4S279/5				
2386	8	10	78	A	3	S4S279/6	S4E132/1	RM2668/8	S4P520/6	RM3076/2
2389	8	10	78	A	3	S4S280/1	S4E081/11	RM2670/2	S4P520/11	RM3076/3
2393	8	11	78	A	3	S4S280/4	S4E179/36	RM2789/8	S4P520/16	RM3076/4
2397	8	11	78	C	3	S4S280/7	S4E180/36	RM2790/8	S4P543/1	RM3234/1
2405	8	11	78	A	1	S4S281/1	S4E186/1	RM2791/8	S4P544/1	RM3235/1
2406	8	11	78	A	1	S4S281/2	S4E187/1	RM2792/8	S4P535/1	RM3226/1
2407	8	11	78	A	1	S4S281/3	S4E188/1	RM2938/8	S4P536/6	RM3227/2
2408	8	12	78	A	1	S4S276/1	S4E189/1	RM2939/8	S4P537/6	RM3228/2
2409	8	12	78	A	1	S4S276/2	S4E190/1	RM2940/8	S4P538/6	RM3229/2
2410	8	12	78	A	1	S4S276/3	S4E191/1	RM2786/9	S4P539/6	RM3230/2
2411	8	12	78	A	1	S4S288/1	S4E192/1	RM2787/9	S4P540/6	RM3231/2
2412	8	12	78			NO S4S	TAPE			
2413	NO	B+L	A	1		S4S288/2				
2414	8	12	78	A	1	S4S288/3	S4E193/1	RM2788/9	S4P541/6	RM3232/2
2416	8	12	78			NO S4S	TAPE			
2417	NO	B+L	A	1		S4S283/1				
2418	8	12	78	A	2	S4S283/2	S4E194/1	RM2789/9	S4P542/6	RM3233/2
2419	8	12	78	A	1	S4S283/4	S4E195/1	RM2790/9	S4P543/6	RM3234/2
2420	8	12	78	A	1	S4S282/1	S4E186/6	RM2791/9	S4P544/6	RM3235/2
2421	8	12	78	A	1	S4S282/2	S4E187/6	RM2792/9	S4P535/6	RM3226/2
2422	8	12	78	A	1	S4S282/3	S4E188/6	RM2938/9	S4P535/11	RM3226/3
2423	8	12	78	A	1	S4S259/1	S4E189/6	RM2939/9	S4P536/11	RM3227/3
2424	8	12	78	A	1	S4S277/1	S4E190/6	RM2940/9	S4P537/11	RM3228/3
2425	8	13	78	A	1	S4S277/2	S4E191/6	RM2786/10	S4P538/11	RM3229/3
2426	8	13	78	A	1	S4S277/3	S4E192/6	RM2787/10	S4P539/11	RM3230/3
2427	8	13	78	A	1	S4S277/4	S4E193/6	RM2788/10	S4P540/11	RM3231/3
2428	8	13	78	A	1	S4S284/1	S4E194/6	RM2789/10	S4P541/11	RM3232/3

2430	8	13	78	A	1	S4S284/2	S4E195/6	RM2790/10	S4P542/11	RM3233/3
2432	8	13	78	A	1	S4S284/3	S4E186/11	RM2791/10	S4P543/11	RM3234/3
2433	8	13	78	A	1	S4S287/1	S4E187/11	RM2792/10	S4P544/11	RM3235/3
2435	8	13	78	A	1	S4S287/2	S4E188/11	RM2938/10	S4P535/16	RM3226/4
2436	8	13	78	A	1	S4S287/3	S4E189/11	RM2939/10	S4P536/16	RM3227/4
2437	8	13	78	A	1	S4S285/1	S4E190/11	RM2940/10	S4P537/16	RM3228/4
2438	8	13	78	A	1	S4S285/2	S4E191/11	RM2786/11	S4P538/16	RM3229/4
2439	8	13	78	A	1	S4S285/3	S4E192/11	RM2787/11	S4P539/16	RM3230/4
2440	8	13	78	A	1	S4S278/1	S4E193/11	RM2788/11	S4P540/16	RM3231/4
2441	8	14	78	A	1	S4S278/2	S4E194/11	RM2789/11	S4P541/16	RM3232/4
2442	8	14	78	A	1	S4S278/3	S4E195/11	RM2790/11	S4P542/16	RM3233/4
2443	8	14	78	A	1	S4S289/1	S4E186/16	RM2791/11	S4P543/16	RM3234/4
2444	8	14	78	A	1	S4S289/2	S4E187/16	RM2792/11	S4P544/16	RM3235/4
2445	8	14	78	A	1	S4S289/3	S4E188/16	RM2938/11	S4P535/21	RM3226/5
2449	8	14	78	A	1	S4S219/1	S4E129/6	RM2760/2	S4P536/21	RM3227/5
2451	8	14	78	A	1	S4S219/3	S4E189/16	RM2939/11	S4P537/21	RM3228/5
2452	8	14	78	A	1	S4S219/4	S4E190/16	RM2940/11	S4P538/21	RM3229/5
2453	8	14	78	A	4	S4S212/1	S4E191/16	RM2786/12	S4P539/21	BAD DATA
2458	8	15	78	C	3	S4S212/5	S4E192/16	RM2787/12	S4P540/21	RM3231/5
2461	8	15	78	A	3	S4S206/1	S4E093/6	RM2931/8	S4P513/11	RM3069/3
2466	8	15	78	A	3	S4S206/4	S4E094/6	RM2663/2	S4P513/16	RM3069/4
1		S3-4				SPECT.	SPECT.	VAX COMP.	PHOT.	VAX COM.
						TAPE	P.P. TAPE	TAPE	P.P. TAPE	TAPE
REV	MTN	DAY	YR	FT/F						
2470	8	15	78	A	3	S4S115/5	S4E106/11	RM2887/5	S4P501/11	RM2784/4
2475	8	16	78	C	2	S4S206/7	S4E193/16	RM2788/12	S4P541/21	RM3232/5
2479	8	16	78	A	3	S4S220/1	S4E026/6	RM2913/7	S4P515/16	RM3071/4
2483	8	16	78	A	3	S4S220/4	S4E011/16	RM2911/6	S4P515/21	RM3071/5
2487	8	16	78	A	3	S4S220/7	S4E028/6	RM2908/8	S4P515/26	RM3071/6
2492	8	17	78	C	2	S4S207/1	S4E194/16	RM2789/12	S4P542/21	RM3233/5
2495	8	17	78	A	3	S4S207/3	S4E095/6	RM2664/2	S4P513/21	RM3069/5
2499	8	17	78	A	3	S4S207/6	S4E096/6	RM2665/2	S4P513/26	RM3069/6
2502	8	17	78	A	3	S4S221/1	S4E029/6	RM2909/8	S4P515/31	RM3071/7
2506	8	18	78	A	2	S4S221/4	S4E130/6	RM2761/2	S4P523/46	RM3509/9
2509	8	18	78	C	3	S4S221/6	S4E195/16	RM2790/12	S4P543/21	RM3234/5
2514	8	18	78			NO S4S	TAPE			
2518	8	18	78	A	3	S4S215/1	S4E021/6	RM2909/7	S4P514/41	RM3070/9
2522	8	19	78			NO S4S	TAPE			
2527	8	19	78	C	2	S4S215/4	S4E186/21	RM2791/12	S4P544/21	RM3235/5
2532	8	19	78	A	3	S4S215/6	S4E022/6	RM2910/7	S4P514/46	RM3070/10
2535	8	19	78	A	3	S4S208/1	S4E097/6	RM2666/2	S4P513/31	RM3069/7
2539	8	20	78	A	3	S4S208/4	S4E098/6	RM2667/2	S4P513/36	RM3069/8
2544	8	20	78	C	3	S4S208/7	S4E187/21	RM2792/12	S4P535/26	RM3226/6
2548	8	20	78	A	3	S4S217/1	S4E023/6	RM2911/7	S4P515/6	RM3071/2
2552	8	20	78	A	3	S4S217/4	S4E007/15	RM2908/6	S4P570/36	RM2049/13
2556	8	21	78	A	2	S4S217/7	S4E127/6	RM2762/1	S4P523/41	RM3509/8
2561	8	21	78			NO S4S	TAPE			
2564	8	21	78	A	3	S4S209/1	S4E099/6	RM2668/2	S4P513/41	RM3069/9
2568	8	21	78	A	3	S4S209/4	S4E100/6	RM2669/2	S4P513/46	RM3069/10
2572	8	22	78	A	2	S4S209/7	S4E126/6	RM2761/1	S4P536/26	RM3227/6
2578	8	22	78	C	3	S4S214/1	S4E188/21	RM2938/12	S4P537/26	RM3228/6
2581	8	22	78	A	3	S4S214/4	S4E019/6	RM2914/4	S4P514/31	RM3070/7
2585	8	22	78	A	3	S4S214/7	S4E020/6	RM2912/4	S4P514/36	RM3070/8
2590	8	23	78	A	2	S4S218/1	S4E128/6	RM2759/2	S4P528/41	RM3514/8
2596	8	23	78	C	3	S4S218/3	S4E189/21	RM2939/12	S4P538/26	RM3229/6
2598	8	23	78	A	3	S4S218/6	S4E025/6	RM2912/7	S4P515/11	RM3071/3
2602	8	24	78	A	3	S4S205/1	S4E190/21	RM2940/12	S4P512/46	RM3068/10
2607	8	24	78			NO S4S	TAPE			
2613	8	24	78			NO S4S	TAPE			
2616	8	24	78	A	3	S4S205/4	S4E091/6	RM2760/5	S4P513/1	RM3069/1

2620	8	25	78	A	2	S4S205/7	S4E092/6	RM2667/1	S4P528/36	RM3069/2
2625	8	25	78	A	3	S4S213/1	S4E018/6	RM2911/4	S4P514/26	RM3070/6
2630	8	25	78	C	3	S4S213/4	S4E191/21	RM2786/13	S4P539/26	RM3230/5
2632	8	25	78	A	3	S4S213/7	S4E192/21	RM2787/13	S4P540/26	RM3231/6
2638	8	26	78	A	3	S4S210/1	S4E013/6	RM2908/4	S4P514/1	RM3070/1
2641	8	26	78	A	3	S4S210/4	S4E014/6	RM2909/4	S4P514/6	RM3070/2
2647	8	26	78	C	3	S4S210/7	S4E193/21	RM2788/13	S4P541/26	RM3232/6
2650	8	26	78	A	3	S4S216/1	S4E102/1	RM2664/3	S4P515/1	RM3071/1
2655	8	27	78	A	2	S4S216/4	S4E116/11	RM2666/7	S4P525/46	RM3511/9
2660	8	27	78			NO S4S	TAPE			
2665	8	27	78			NO S4S	TAPE			
2668	8	28	78	A	3	S4S211/1	S4E103/1	RM2910/4	S4P514/11	RM3070/3
2672	8	28	78	A	3	S4S211/4	S4E020/1	RM2894/1	S4P514/16	RM3070/4
2677	8	28	78	A	3	S4S211/7	S4E107/11	RM2894/2	S4P514/21	RM3070/5
2682	8	28	78	C	3	S4S259/2	S4E194/21	RM2789/13	S4P542/26	RM3233/6
2686	8	29	78	A	3	S4S259/5	S4E083/11	RM2663/3	S4P519/26	RM3075/6
2690	8	29	78	A	3	S4S258/1	S4E104/1	RM2668/3	S4P519/21	RM3075/5
2694	8	29	78	A	3	S4S116/1	S4E105/1	RM2669/3	S4P501/1	RM2784/2
2699	8	29	78	C	3	S4S258/4	S4E195/21	RM2790/13	S4P543/26	RM3234/6
2702	8	30	78	A	2	S4S258/7	S4E112/11	RM2670/6	S4P525/41	RM3511/8
2706	8	30	78	A	3	S4S275/1	S4E108/11	RM2667/6	S4P519/46	RM3075/10
1		S3-4				SPECT.	SPECT.	VAX COMP.	PHOT.	VAX COMP.
						TAPE	P.P.TAPE	TAPE	P.P.TAPE	TAPE
REV	MTH	DAY	YR	FT/F		-----	-----	-----	-----	-----
2711	8	30	78	A	3	S4S275/4	S4E106/1	RM2670/3	S4P520/1	RM3076/1
2716	8	30	78			NO S4S	TAPE			
2717	NO	B+L		C	3	S4S275/7				
2720	8	31	78	A	2	S4S256/1	S4E012/16	RM2908/7	S4P526/41	RM3512/8
2725	8	31	78	A	3	S4S256/3	S4E186/26	RM2791/13	S4P544/26	RM3235/6
2730	8	31	78	A	1	S4S256/6	S4E187/26	RM2792/13	S4P535/31	RM3226/7
2731	8	31	78	A	1	S4S274/1	S4E188/26	RM2938/13	S4P536/31	RM3227/7
2732	9	1	78	A	1	S4S274/2	S4E151/1	RM2626/7	S4P565/6	RM2076/13
2733	9	1	78	A	1	S4S274/3	S4E152/1	RM2627/5	S4P566/1	RM3898/12
2734	9	1	78	A	1	S4S269/1	S4E153/1	RM2628/4	S4P567/1	RM3899/12
2735	9	1	78	A	1	S4S269/2	S4E154/1	RM2629/5	S4P568/1	RM3901/12
2736	9	1	78	A	1	S4S269/3	S4E155/1	RM2630/5	S4P569/1	RM3902/12
2737	9	1	78	A	1	S4S268/1	S4E151/6	RM2621/8	S4P570/6	RM3899/13
2738	9	1	78	A	1	S4S268/2	S4E152/6	RM2622/8	S4P565/11	RM3900/13
2739	9	1	78	A	1	S4S268/3	S4E153/6	RM2623/8	S4P566/6	RM2077/13
2741	9	1	78	A	1	S4S266/1	S4E154/6	RM2624/8	S4P567/6	RM2078/13
2742	9	1	78	A	1	S4S266/2	S4E155/6	RM2625/8	S4P568/6	RM2079/13
2743	9	1	78	A	1	S4S266/3	S4E151/11	RM2621/9	S4P569/6	RM3898/13
2744	9	1	78	A	1	S4S273/1	S4E152/11	RM2622/9	S4P570/11	RM2077/14
2745	9	1	78	A	1	S4S273/2	S4E153/11	RM2623/9	S4P565/16	RM2078/14
2746	9	1	78	A	1	S4S273/3	S4E154/11	RM2624/9	S4P566/11	RM3901/13
2747	9	1	78	A	1	S4S255/1	S4E155/11	RM2625/9	S4P567/11	RM3902/13
2748	9	1	78	A	1	S4S255/2	S4E151/16	RM2627/6	S4P568/11	RM2075/14
2749	9	2	78	A	1	S4S255/3	S4E152/16	RM2628/5	S4P569/11	RM2076/14
2750	9	2	78	A	1	S4S270/1	S4E153/16	RM2629/6	S4P570/16	RM3901/14
2751	9	2	78	A	1	S4S270/2	S4E154/16	RM2630/6	S4P565/21	RM3902/14
2753	9	2	78	A	1	S4S270/3	S4E155/16	RM2622/10	S4P566/16	RM2079/14
2754	9	2	78	A	1	S4S267/1	S4E151/21	RM2623/10	S4P567/16	RM3898/14
2755	9	2	78	A	1	S4S267/2	S4E152/21	RM2624/10	S4P568/16	RM3899/14
2757	9	2	78	A	1	S4S267/3	S4E153/21	RM2625/10	S4P569/16	RM3900/14
2758	9	2	78	A	1	S4S272/1	S4E154/21	RM2627/7	S4P570/21	RM2079/15
2759	9	2	78	A	1	S4S272/2	S4E155/21	RM2628/6	S4P565/1	RM2077/12
2760	9	2	78	A	1	S4S272/3	S4E151/26	RM2629/7	S4P566/21	RM2075/15
2761	9	2	78	A	1	S4S264/1	S4E152/26	RM2630/7	S4P567/21	RM2076/15
2762	9	2	78	A	1	S4S264/2	S4E153/26	RM2621/10	S4P568/21	RM2077/15
2763	9	2	78	A	1	S4S264/3	S4E154/26	RM2622/11	S4P569/21	RM2078/15

2764	9	2	78	A	1	S4S265/1	S4E155/26	RM2623/11	S4P570/1	RM2075/13
2765	9	3	78	A	1	S4S265/2	S4E151/31	RM2624/11	S4P566/26	RM3899/15
2766	9	3	78	A	1	S4S265/3	S4E152/31	RM2625/11	S4P567/26	RM3900/15
2767	9	3	78	A	1	S4S261/1	S4E153/31	RM2626/8	S4P565/41	RM2049/13
2770	9	3	78	A	1	S4S261/2	S4E154/31	RM2627/8	S4P568/26	RM3901/15
2772	9	3	78	A	1	S4S261/3	S4E155/31	RM2628/7	S4P569/26	RM3902/15
2773	9	3	78	A	1	S4S262/1	S4E151/36	RM2629/8	S4P566/31	RM2052/12
2774	9	3	78	A	1	S4S262/2	S4E152/36	RM2630/8	S4P567/31	RM2053/12
2775	9	3	78	A	1	S4S262/3	S4E153/36	RM2621/11	S4P568/31	RM2044/13
2776	9	3	78	A	1	S4S263/1	S4E154/36	RM2622/12	S4P569/31	RM2045/13
2777	9	3	78	A	1	S4S263/2	S4E155/36	RM2623/12	S4P566/36	RM2051/13
2782	9	4	78	C	3	S4S263/3	S4E156/1	RM2624/12	S4P567/36	RM2083/13
2785	9	4	78			NO S4S	TAPE			
2792	NO	B+L	A	1		S4S260/1				
2793	9	4	78	A	3	S4S260/2	S4E107/1	RM2663/4	S4P519/31	RM3075/7
2799	9	5	78	C	3	S4S260/5	S4E157/1	RM2625/12	S4P568/36	RM2047/13
2804	9	5	78	A	3	S4S271/1	S4E108/1	RM2664/4	S4P519/36	RM3075/8
2808	9	5	78	A	3	S4S271/4	S4E131/11	RM2759/5	S4P520/31	RM3076/7
2811	9	5	78	A	3	S4S271/7	S4E109/1	RM2665/4	S4P519/41	RM3075/9
2816	9	6	78	A	1	S4S257/1	S4E158/1	RM2622/13	S4P569/36	RM2048/113
2817	NO	B+L	C	3		S4S257/2				
1		S3-4				SPECT.	SPECT	VAX COMP.	PHOT.	VAX COMP.
						TAPE	P.P. TAPE	TAPE	P.P. TAPE	TAPE
REV	MTH	DAY	YR	FT/F		-----	-----	-----	-----	-----
2820	9	6	78	A	3	S4S257/5	S4E110/1	RM2666/4	S4P519/16	RM3075/4
2825	9	6	78	A	3	S4S318/7	S4E003/6	RM2909/3	S4P524/1	RM3510/1
2829	9	6	78	A	3	S4S341/1	S4E034/11	RM2919/2	S4P529/1	RM3515/1
2834	9	7	78	C	2	S4S341/4	S4E159/1	RM2623/13	S4P565/26	RM3898/15
2839	9	7	78	A	2	S4S341/6	S4E113/11	RM2664/7	S4P524/46	RM3510/9
2841	9	7	78	A	1	S4S319/1	S4E160/1	RM2624/13	S4P570/26	RM2075/16
2842	9	7	78	A	3	S4S319/2	S4E004/6	RM2910/3	S4P525/1	RM3511/1
2845	9	7	78	A	3	S4S319/5	S4E005/6	RM2911/3	S4P526/1	RM3512/1
2851	9	8	78	C	3	S4S344/1	S4E146/11	RM2626/6	S4P565/31	RM2051/12
2856	9	8	78	A	3	S4S344/4	S4E037/11	RM2919/3	S4P530/1	RM3516/1
2860	9	8	78	A	3	S4S344/7	S4E038/11	RM2915/3	S4P531/1	RM3511/12
2864	9	9	78	A	3	S4S323/4	S4E011/11	RM2910/6	S4P527/1	RM3513/1
2868	9	9	78	C	3	S4S323/7	S4E156/6	RM2629/9	S4P570/31	RM2046/13
2883	9	10	78	A	3	S4S116/4	S4E115/11	RM2665/7	S4P502/1	RM2509/1

APPENDIX 2: Reprint of Paper Entitled "NO and O₂ Ultraviolet
Nightglow and Spacecraft Glow From the S3-4
Satellite"

NO AND O₂ ULTRAVIOLET NIGHTGLOW AND SPACECRAFT GLOW FROM THE S3-4 SATELLITE

R. W. EASTES and R. F. HUFFMAN

Phillips Laboratory/LIM, Hanscom AFB, MA 01731-5000, U.S.A.

and

F. J. LEBLANC

Northwest Research Associates, P.O. Box 3027, Bellevue, WA 98009, U.S.A.

(Received in final form 3 September 1991)

Abstract—Observations (1600–2950 Å) from the S3-4 satellite of the Earth's nightglow at ~6 Å resolution have been analyzed. These data indicate that the only significant emissions from NO are the δ and γ bands. The relative brightness of these bands was consistent with previous observations at lower resolution. The data support the presence of O₂ emissions in the Herzberg I, II, and III bands in ratios (~4.5:1:1.4), consistent with analyses of previous ground-based observations of these band systems. Spacecraft glow is seen from the N₂ Lyman-Birge-Hopfield bands, as previously reported; however, no spacecraft-related emissions were seen from NO or O₂.

INTRODUCTION

Atomic oxygen is a minor constituent in the Earth's lower thermosphere; however, it is an important constituent due to the numerous emissions and chemical reactions in which it is involved. Unfortunately, it is difficult to measure the density of atomic oxygen in this region. Atmospheric drag limits the spatial and temporal coverage of *in situ* measurements. These limitations make remote sensing attractive; however, a thorough understanding of any emissions used is necessary since contributions from unresolved and unexpected emissions can lead to errors in interpreting low-resolution observations. One emission, which is proportional to the square of the atomic oxygen density, is from the O₂ Herzberg I bands (Dufay, 1941; Bates, 1954). The three-body recombination of atomic oxygen produces this emission, which is most prominent at night. The Herzberg I band emission peaks near 95 km (Packer, 1961; Stecher, 1965; Reed, 1968; L. Thomas *et al.*, 1979; Llewellyn *et al.*, 1979; Dickinson, 1980; Thomas and Young, 1981; Thomas, 1981; Greer *et al.*, 1986; Murtagh *et al.*, 1986).

Similar problems exist for measurement of atomic nitrogen (a minor constituent throughout the Earth's atmosphere). Radiative recombination of atomic nitrogen with atomic oxygen produces nitric oxide emissions which peak near 150 km (McCoy, 1983a, b). Few existing data sets have either simultaneous NO and O₂ emissions or sufficient sensitivity for high-resolution observations at night. However, data from the S3-4 satellite (Huffman *et al.*, 1980) observed

emissions from both molecules at night with significantly higher resolution than most previous observations.

The nightglow spectra of NO and O₂ observed from the S3-4 satellite and an analysis of them are presented in this paper. As an initial step, we demonstrate that these measurements are not compromised by the spacecraft glow seen on this satellite. Given sufficient understanding of the excitation mechanisms, the nightglow emissions from NO and O₂ could be used for remote sensing of atomic oxygen and atomic nitrogen densities.

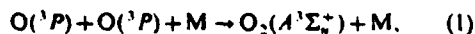
O₂ emissions

Most analyses of the O₂ Herzberg I band ($A^3\Sigma_u^+ - X^3\Sigma_g^-$) spectrum published (e.g. Slanger and Huestis, 1981) use ground-based observations (e.g. Broadfoot and Kendall (5.5 Å resolution) (1968); Chamberlain (~0.8 Å) (1955, 1961); Krassovsky *et al.*, (~5 Å) (1962); Ingham (0.6 Å) (1962)). These observations cover the 3100–5000 Å region at ~1 to ~6 Å resolution; however, the brightest bands from the higher vibrational levels ($v' = 7-10$) are below 3000 Å, wavelengths not observable from the ground.

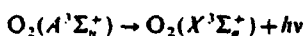
Observation of thermospheric emissions at wavelengths shorter than 3000 Å requires that the instrument be on a satellite, sounding rocket or balloon. Such observations of O₂ emissions are scarce (Hennes, 1966; Huffman *et al.*, 1980; Cebula and Feldman, 1982, 1984; Sharp and Siskind, 1989). The data which have received the most analysis were from Hennes

(1966), who observed the spectrum below 3000 Å at ~11 Å resolution. Degen (1969) used these data in determining the relative vibrational populations of the A state.

After nearly half a century of controversy, the excitation of the $O_2 A^1\Sigma_u^+$ state is now attributed to three-body recombination of atomic oxygen (Bates, 1954; Barth, 1961, 1964; Thomas, 1981):



which may be followed by



(Herzberg I bands). (2)

Quenching of the $A^1\Sigma_u^+$ state could change either the total amount of emission or the vibrational distribution of the emission. Such changes could adversely affect the oxygen density derived from low-resolution observations (McDade *et al.*, 1982).

As a test of theoretically predicted changes in the O_2 emission with altitude (McDade *et al.*, 1982), a series of rocket observations, *ETON* (Greer *et al.*, 1986; McDade *et al.*, 1986a, b; Murtagh *et al.*, 1986), designed to study the altitude dependence of the oxygen-dependent nightglow features, was launched. However, it was unable to conclusively determine the vibrational populations in these bands, or observe altitude variations in the Herzberg I vibrational populations. Higher-resolution observations may help in understanding these phenomena.

Emissions from O_2 other than Herzberg I have been identified at wavelengths longer than 3000 Å. Using the Broadfoot and Kendall (1968) data, Slanger and Huestis (1981) showed that there is a contribution to the nightglow from the $O_2 c^1\Sigma_u$ state through Herzberg II band emissions; this system also emits below 3000 Å. More recently, Herzberg II band emissions and possibly emissions from the Herzberg III bands were identified in some ultraviolet data (2650–3050 Å) by Sharp and Siskind (1989).

NO emissions

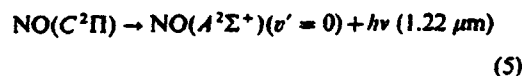
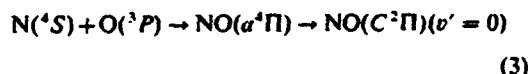
Nitric oxide emissions observed in the Earth's atmosphere are generally attributed to either resonance fluorescence of sunlight or radiative recombination. At solar zenith angles and viewing geometries which exclude resonance fluorescence, radiative recombination is the only source of excitation, leading to emissions from the $v' = 0$ levels of the $C^2\Pi$ and $A^2\Sigma^+$ states which produce the NO δ and γ bands respectively. Both band systems emit between 1600 and 2950 Å.

A number of daytime observations have been

reported since the first measurements by Barth (1964) (Barth, 1966; Pearce, 1969; Meira, 1971; Tisone, 1973; Tohmatsu and Iwagami, 1975, 1976; Thomas, 1978; Baker *et al.*, 1977; McCoy, 1981, 1983a) with Cleary (1986) giving the most recent observations. These sounding rocket experiments measured emissions attributed to resonance fluorescence.

The number of observations at solar zenith angles large enough to prevent resonance fluorescence is more limited due to the weakness of the NO emission from radiative recombination; however, rocket-borne observations of this emission have been reported by Feldman and Takacs (1974), Sharp and Rusch (1981) and McCoy (1981, 1983a) near evening twilight. The number of observations further into night is smaller. Detection of NO δ band emission in the nightglow was reported by Cohen-Sabban and Vuillemin (1973). Tennyson *et al.* (1986) reported more recent observations of NO emissions near local midnight.

The formation of the NO γ and δ bands has been discussed in the literature (Sharp and Rusch, 1981; McCoy, 1983a, b). The radiative recombination excitation scheme for NO is best explained by the equations:



Since the α -C energy level crossing is below the NO dissociation level for only the $v' = 0$ level of the C state, it is the only level energetically allowed. See McCoy (1981) for a detailed discussion of the allowed states.

MEASUREMENTS

The *S3-4* satellite carried two 0.25 m Ebert-Fastie spectrometers which scanned the 1100–1900 Å and 1600–2950 Å regions simultaneously (Huffman *et al.*, 1980) in ~22 s. They were mounted on the three-axis stabilized spacecraft with their line-of-sight toward the nadir. Three pairs of slits were mounted on each spectrometer, enabling them to observe at ~1, ~5 or ~25 Å resolution. Data were collected between March 30 and September 10, 1978. The elliptical, sun synchronous orbit had an inclination of 96.5° and took the satellite through the 160–270 km altitude region. The orbit crossed the Equator at approxi-

mately 10:30 and 22:30 local solar time. Apogee was in the southern hemisphere.

For these analyses, the data between 1600 and 2950 Å were summed. Although the nominal resolution of 5 Å full-width-half-maximum (FWHM) is confirmed by atomic emissions in the aurora, a coarser resolution was needed to fit the summed data. At least two effects contribute: first the resolution of the large number of scans summed will be degraded by any mechanical imperfections or wear over the time of the observations. The observations span ~3 months. Second, the coarseness of the binning (~1.3 Å) used for these data, relative to the 5 Å resolution, degrades the resolution in summed scans.

The wavelength calibration for the u.v. spectrometer was determined by using both the NO band emissions and the Rayleigh-scattered sunlight spectrum observed. The Rayleigh-scattered sunlight observations were compared with a high-resolution solar spectrum (Anderson and Hall, 1989) at wavelengths >2300 Å. The resulting wavelength calibration agrees with the observed wavelengths to within ± 0.75 Å.

DISCUSSION OF DATA

Spacecraft glow considerations

Ultraviolet spacecraft glow emission from the N₂ Lyman-Birge-Hopfield (LBH) bands was discovered on the S3-4 satellite (Huffman *et al.*, 1980), following analysis of data from the u.v. spectrometers and the multiband photometer. When this emission was initially observed at night it was thought to be airglow. It was subsequently observed during the day, where it was much weaker than the normal dayglow. With the emission peaking at the $v' = 0$ level of the upper state, it exhibited a different vibrational distribution than the normal LBH dayglow and auroral emissions.

This LBH band emission is now attributed to interaction of the spacecraft with the atmosphere (Conway *et al.*, 1987). Using data from night-time measurements, they found that spacecraft glow brightness depended on altitude, and no emission was detected when the satellite was above 230 km. The altitude variation of the signal was proportional to the cube of the N₂ density or the product of the square of the N₂ density and the O density. Conway *et al.* (1987) concluded that the ambient nitrogen molecules have enough kinetic energy, relative to the spacecraft, to excite the lowest vibrational levels of the $a^1\Pi$, electronic state. Excitation mechanisms involving O or O₂ were not excluded by the data, but no O I emissions were observed in the glow.

Additional suggestions regarding the production

mechanism of the spacecraft glow have come from Kofsky (1988), Swenson and Meyerott (1988), Cuthbertson and Langer (1989) and Meyerott and Swenson (1990). A heterogeneous reaction between two nitrogen atoms on a spacecraft surface is postulated, but the reactions producing the nitrogen atoms and many other details are in doubt. Controlled experiments rather than the current random observations would be valuable.

The data presented here are from the same time, but different orbits, as those analyzed by Conway *et al.* (1987). Therefore, the same spacecraft glow should be present. There is also the possibility of additional spacecraft glow at longer wavelengths where it would complicate analysis of the NO and O₂ emissions. Previously, the longer-wavelength data from S3-4 have not been examined as thoroughly as the shorter-wavelength data for the presence of additional spacecraft-related emissions. If there were enough energy available to produce the LBH band emissions, there would also be sufficient energy to produce NO and O₂ emissions at longer wavelengths. Therefore, these data were first examined for additional sources of spacecraft glow by comparing two separate sums of the data from different altitude ranges.

Shown in Fig. 1 is a u.v. nightglow spectrum (1600–2950 Å) measured from the S3-4 satellite. This sum of 1447 individual spectra corresponds to observing each of the 932 ~1.3 Å bins for 28.94 s. These data are smoothed over ~4 Å by taking running averages of 3 data bins. The $\pm 1\sigma$ statistical error is shown for the NO δ band (0, 2) peak at 2056 Å, and the NO δ and γ band heads ($v' = 0$) are marked. All the spectra summed were from solar zenith angles (SZAs) > 120°; had altitude > 230 km (average altitude = 251 km); and were outside the auroral regions.

Spectral scans containing auroral emissions were excluded by the following criteria. Whenever enhanced atomic oxygen emissions (1304 and 1356 Å) were observed by the far-u.v. spectrometer, which simultaneously observed shorter wavelengths, the data were excluded from the sums shown in this paper. These oxygen emissions are readily apparent whenever significant auroral emission occurs. The selection criteria is considered sufficient since N₂ Vegard-Kaplan and LBH band emissions, which are also produced in the aurora, are absent from the data shown in Fig. 1.

A second sum of 633 spectra observed when the satellite was at lower altitudes (<220 km (average altitude = 210 km)) is shown in Fig. 2. These observations, like those above, were from non-auroral conditions but with SZAs > 110°. The $\pm 1\sigma$ statistical error is shown for the emission peak at 2056 Å. The

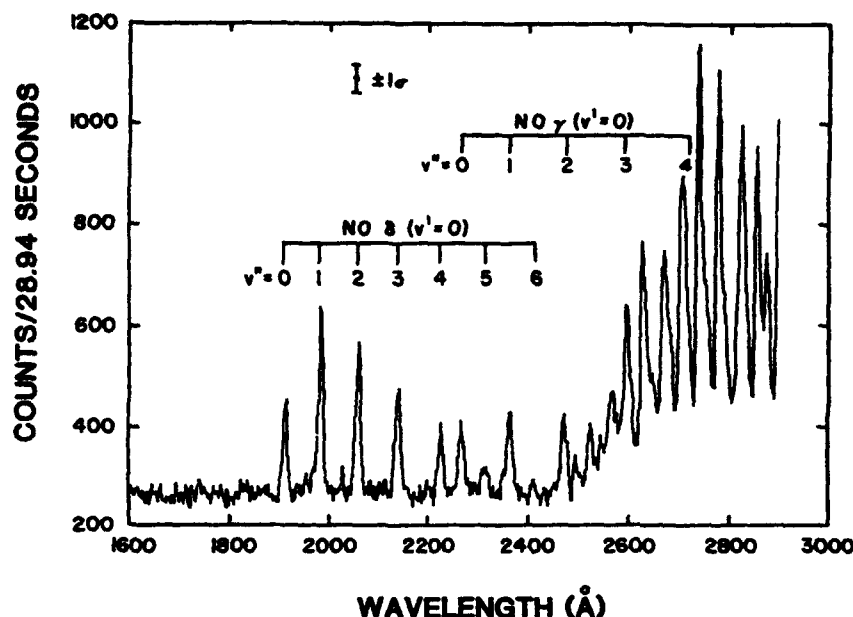


FIG. 1. ULTRAVIOLET NIGHTGLOW SPECTRUM MEASURED FROM S3-4 AT THE HIGHEST ALTITUDES. This sum of 1447 individual spectra, each taking ~ 22 s, corresponds to observing each of the $932 \sim 1.3$ Å bin for 28.94 s. All spectra summed were from solar zenith angles $> 120^\circ$; altitudes > 230 km (average altitude = 251 km); and outside the auroral regions. These data are smoothed over ≈ 4 Å by taking running averages over the 3 data bins. The $\pm 1\sigma$ statistical error is shown for the NO δ band (0, 2) peak at 2056 Å, and the NO δ and γ band heads ($v' = 0$) are marked.

dashed curve represents the response of the spectrometer to a 2 R emission line as a function of wavelength (after subtracting 100 counts per bin of background signal).

Weak emissions from the LBH spacecraft glow were seen at the shorter wavelengths of the lower-altitude spectrum (Fig. 2). This emission brightness is consistent with the N_2 LBH band emissions from spacecraft glow analyzed by Conway *et al.* (1987). Conway found that for an altitude of 210 km, 20–50 R were seen in the 1400–1700 Å region. Assuming the vibrational distribution derived by Conway *et al.* (1987), the data in Fig. 2 at 1650 Å indicate that the LBH band emissions in the 1400–1700 Å region are ≤ 160 R. Uncertainties in the background make a more precise brightness difficult to obtain. Figure 4 shows both the summed low-altitude data and the LBH spectrum which the instrument would record, assuming the vibrational population derived by Conway *et al.* (1987) ($v' = 0$ to 6 populations of 1.0, 0.76, 0.18, 0.16, 0.39, 0.20 and 0.00, respectively). As shown by Fig. 2, emissions from the LBH bands should be insignificant at the wavelengths of the NO δ and NO γ band emissions in Figs 1–3.

In Figs 1 and 2 the NO δ ($v' = 0$), NO γ ($v' = 0$),

and O_2 Herzberg I ($v' = 4-11$) bands are conspicuous. The presence of other O_2 bands will be discussed later. The NO bands dominate the spectrum at wavelengths < 2500 Å, while the O_2 Herzberg bands dominate at longer wavelengths. Within statistical error the brightness of the O_2 Herzberg bands was the same in both sums. This was expected. The three-body recombination of O, which produces the O_2 Herzberg band emission, peaks near 95 km and all significant emission comes from below 160 km, the typical perigee of the satellite. This indicates that no statistically significant emission comes from spacecraft glow at wavelengths $2500 \text{ Å} < \lambda < 2950 \text{ Å}$.

On the other hand, the brightness of the NO emission changes. A comparison of the higher altitude (Fig. 1) and lower altitude (Fig. 2) data shows that the NO emissions observed from higher altitudes are 1.6 times brighter than at lower altitudes. However, the NO emissions are expected to peak at ~ 150 km. Since the lower altitude data in Fig. 2 come from altitudes of 160–220 km, more of the emission is above the satellite and not in the field-of-view of the nadir-viewing instrument. The brightness of the NO bands decreases approximately as expected according to the model of McCoy (1983b). This agreement indicates

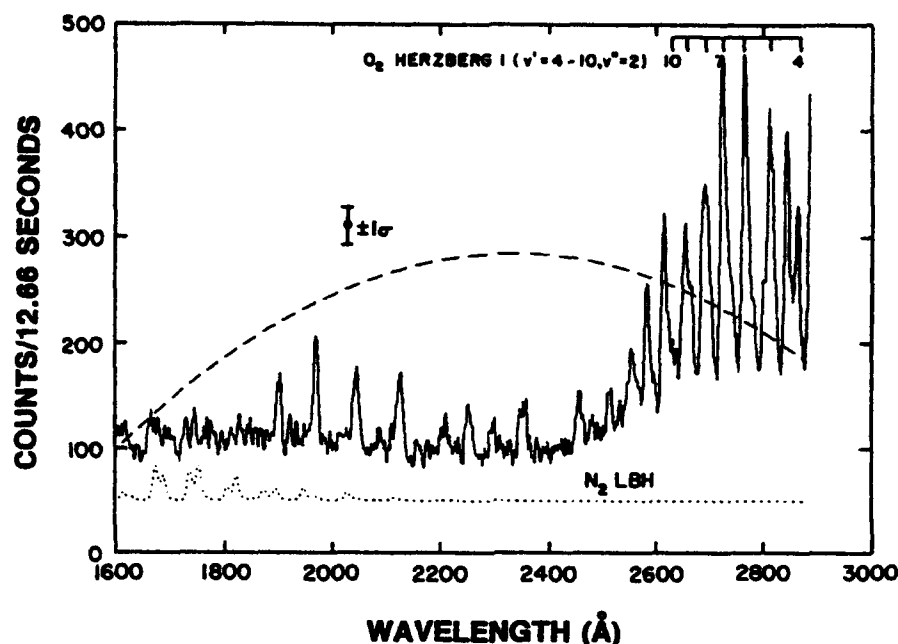


FIG. 2. ULTRAVIOLET NIGHTGLOW SPECTRUM MEASURED FROM S3-4 AT THE LOWEST ALTITUDES. Shown here is the sum of 633 spectra observed from lower altitudes (<220 km (average altitude = 210 km)) than the data in Fig. 1. These observations are from non-auroral conditions with solar zenith angles $>110^\circ$. These data are smoothed over ≈ 4 Å by taking running averages over the 3 data bins. The $\pm 1\sigma$ statistical error is shown for the emission peak at 2056 Å. The smooth, dashed curve represents the response of the spectrometer to a 2 R emission line as a function of wavelength (after subtracting 100 counts per bin of background signal). The dotted curve shows the N_2 Lyman-Birge-Hopfield band emissions calculated using the relative vibrational populations from Conway *et al.* (1987) ($v' = 0$ to 6 populations of 1.0, 0.76, 0.18, 0.16, 0.20, 0.00, respectively) and scaled to match the data near 1650 Å.

that there were probably no NO emissions produced by spacecraft glow. A more definitive conclusion is not justified from this comparison since the observations cover about 3 months, during which the NO production rate (and emission) may vary. However, spacecraft glow should not interfere with the analysis of the NO emissions.

Comparison of the data in Figs 1 and 2 indicates that there are no significant spacecraft-related emissions from NO or O_2 . Therefore, the two sums were combined to improve the counting statistics. Shown in Fig. 3 is the sum of all scans shown in Figs 1 and 2 plus scans at altitudes between 220 and 230 km. The resulting sum of 2385 scans will be used for the remaining analysis. The $\pm 1\sigma$ statistical error is shown for the emission peak at 2056 Å.

Analysis of NO band emissions

Before spectral analysis the background signal must be subtracted. To accomplish this the background between the NO δ and γ bands was first fit to a straight line. The emission observed from the N_2 LBH bands,

while insignificant, was avoided. At wavelengths where overlapping emissions from O_2 prohibited direct observation of the background, a constant background was used. This constant background level was determined during the fitting of the molecular emissions. The constant level was consistent with the fit to shorter wavelengths. In Fig. 4 the data shown in Fig. 3 has been plotted as brightness versus wavelength after subtraction of the background signal.

First, a synthetic NO δ band spectrum was fitted to the data (1877–2429 Å) in Fig. 4. The synthetic spectrum calculation for NO used Franck-Condon factors from Nicholls (1964) for the δ bands and from Spindler *et al.* (1970) for the γ bands. Molecular constants from Huber and Herzberg (1979) were used for the C and X states, and Engleman and Rouse (1971) were the source of constants for the A state. The synthetic spectrum calculations used only the P_1 , Q_1 , and R_1 branches. These are sufficient at ~ 5 Å resolution, given the noise in the data and the coarseness of the binning. The band origins calculated for both the δ and γ bands were in good agreement (± 0.2 Å)

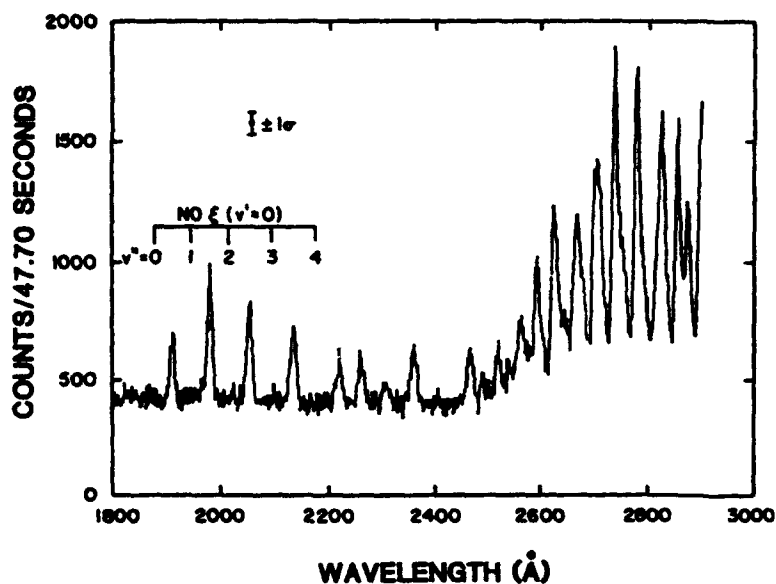


FIG. 3. ULTRAVIOLET NIGHTGLOW SPECTRUM MEASURED FROM S3-4 AT ALL ALTITUDES. This spectrum is the sum of all spectra shown in Figs 1 and 2 plus spectra at altitudes between 220 and 230 km. The resulting sum contains 2385 scans. These data have not been smoothed as were the data in Figs 1 and 2. The $\pm 1\sigma$ statistical error is shown for the emission peak at 2056 Å.

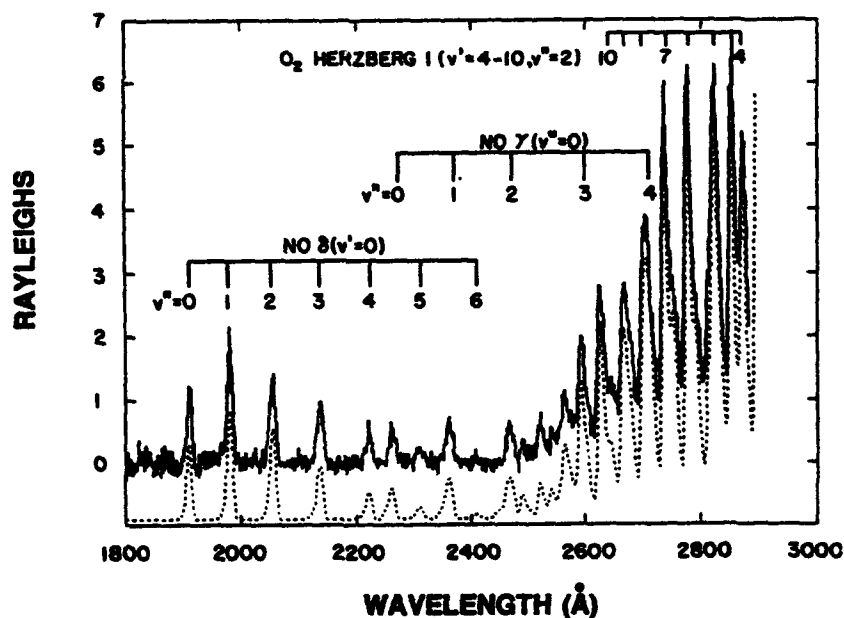


FIG. 4. ULTRAVIOLET NIGHTGLOW SPECTRUM IN RAYLEIGHs AS MEASURED FROM S3-4. After subtraction of the background from the data shown in Fig. 3, the relative sensitivity of the instrument was removed. The NO δ and γ bands are marked. The dotted curve is the best fit to the data when using the NO δ , NO γ , O₂ Herzberg I, and O₂ Herzberg II bands.

with published values by Wallace (1962) or Pearse and Gaydon (1963).

The synthetic spectrum included the rotational structure evident in the observed bands. The spectral resolution and rotational temperature (T_r) were varied iteratively to determine the least-squares fit. The singular value decomposition method (e.g. Press *et al.*, 1986) was used to solve for the least squares in all fitting to the data from the S3-4 satellite. The best fit (shown in Fig. 5) was obtained using 5.9 Å resolution (FWHM) and a rotational temperature (T_r) of ~700 K, approximately the ambient temperature (Hedin, 1987) at the altitude of the NO emission peak (McCoy, 1983b) of ~150 km.

Next, the NO γ bands were fitted using data (2234–2478 Å) from the (0, 0), (0, 1), and (0, 2) bands. Just as for the δ bands, the spectral resolution and rotational temperature of the γ bands were iterated until a best fit was obtained. A resolution of ~5.9 Å and T_r of ~700 K (same as for the δ bands) fitted the data best. The best fit is shown in Fig. 5.

The NO γ :NO δ brightness ratio of 1:1.4 (based on the best fit and Franck-Condon factors for the (0, 1) bands) indicates that the branching ratio from the $C^2\Pi$ to the $A^2\Sigma$ state is 0.41 ± 0.16 (see equations (4)–(7)). Within experimental error this agrees with previous observations (0.30 ± 0.06 by Tennyson *et al.*, 1986; 0.21 ± 0.06 by Sharp and Rusch, 1981; 0.23 ± 0.05 by McCoy, 1983a).

The emission from the NO ϵ bands was <0.25 R ($\Sigma_r - I(v' = 0, v'')$). The NO ϵ ($v' = 0$) band heads are shown in Fig. 3. This limit would be lower but for the LBH glow from the spacecraft.

Analysis of O_2 band emissions

After fitting the NO emissions, the longer-wavelength data were fit to synthetic molecular spectra of the O_2 Herzberg I ($A^3\Sigma_u^+ - X^3\Sigma_g^-$) and O_2 Herzberg II ($c^1\Sigma_u^- - X^3\Sigma_g^-$) bands. Possible contributions by the O_2 Herzberg III ($A'^1\Delta_u - X^3\Sigma_g^-$) bands will be discussed later since they have never been observed conclusively in the nightglow. The relative vibrational population of each level of the A state was fitted to the data independently, but the relative vibrational populations of the c state were fixed. It was necessary to assume relative populations for the c state due to the large number of parameters being fitted, resolution of the spectrum, statistical uncertainty, and the brightness of the Herzberg II bands relative to the Herzberg I bands.

To generate the synthetic O_2 Herzberg spectra, molecular constants suggested by Krupenie (1972) for the X state were used with constants from Ramsay (1986), Borrell *et al.* (1986), and Coquart and Ramsay (1986) for the c , A , and A' states. Transition probabilities from Bates (1989) were used for the Herzberg I, Herzberg II, and Herzberg III bands. Rotational formulae from Degen (1969) (for the Herzberg I

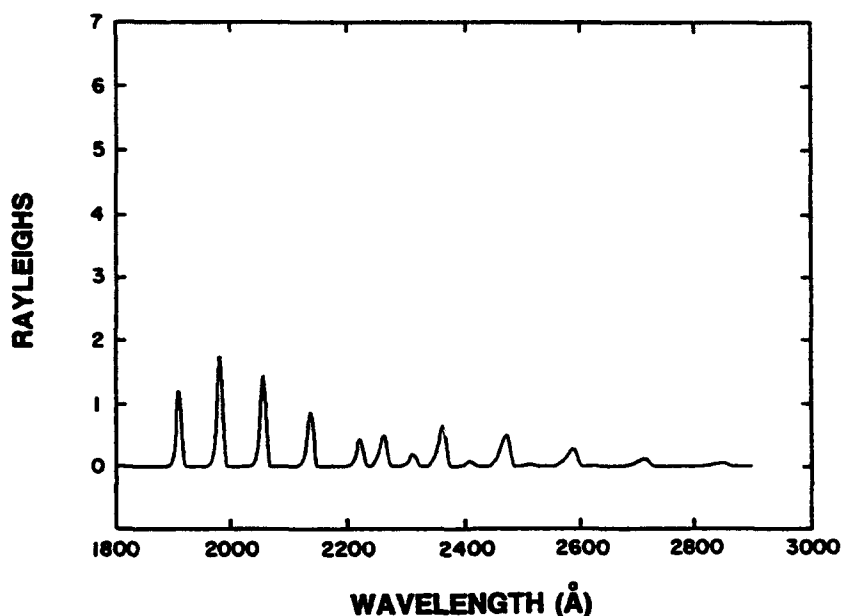


FIG. 5. BEST FIT TO THE NO δ AND γ BANDS IN THE SUMMED NIGHTGLOW DATA SHOWN IN FIG. 4. Shown in this plot is the best fit of the NO bands to the summed nightglow data shown in Fig. 4.

bands) and Kovacs (1969) (for Herzberg I and Herzberg II bands) were used. The rotational temperature of 200 K was based on the temperature of the *MSIS* neutral atmosphere (Hedin, 1987) at ~ 95 km. The resolution should be consistent with the shorter wavelength NO emissions; therefore, the O_2 spectra were calculated at 5.9 Å resolution.

The fitting was done iteratively using the last vibrational populations for the *A* state to determine those for the *c* state until the populations ceased to vary. The relative vibrational populations for the *c* state were derived from the populations of the *A* state by the relationship:

$$\text{population}(v'_c) = \text{population}(v'_A + 2),$$

an approach used by Slanger and Huestis (1981). Since vibrational populations for $v' \leq 3$ of the *A* state were not derived from this data, the populations for $v' \leq 5$ of the *c* state were taken from Slanger and Huestis (1981). The resulting fit, using the NO δ , NO γ , O_2 Herzberg I, and O_2 Herzberg II bands, is shown in Figs 4 and 6. In Fig. 4 the synthetic spectrum is plotted as a dashed line beneath the data. Shown in Fig. 5 is the contribution of the NO δ and γ bands. The total fit and the individual contributions from the O_2 Herzberg I and Herzberg II bands are shown in Fig. 6. The Herzberg I is plotted as a dashed line,

offset beneath the total fit. The Herzberg II spectrum is shown by the solid line offset beneath the total fit.

Although they were not clearly resolved, the Herzberg II bands have previously been observed in the nightglow. Using the Broadfoot and Kendall (1968) data Slanger and Huestis (1981) showed there is a contribution to the nightglow from the $O_2 c^1\Sigma^-$ state through Herzberg II band emissions. They found a Herzberg I: Herzberg II brightness ratio of 4:1 (when integrated over all emission, including wavelengths longer than 3000 Å), and showed that the Herzberg II bands appear as shoulders on many of the Herzberg I bands in the 3000–4000 Å range. More recently Sharp and Siskind (1989) reported observations at wavelengths < 3050 Å where the brightness ratio was 9:1. The Herzberg I: Herzberg II brightness ratio from the observations shown here is $3.7 \pm 0.1 : 1.0 \pm 0.3$ for Herzberg I emissions from the $v' = 4$ to 10 levels, over the entire range of emission. This ratio would be larger if the lower vibrational level emissions ($v' < 4$) from the Herzberg I system were included. However, the populations for levels from $v' < 4$ were uncertain, or not determinable. Assuming that the vibrational levels with $v' < 4$ were populated, relative to $v' = 4$, according to the populations found by Degen (1989) or Slanger and Huestis (1981), the brightness ratio would be $\sim 4.8 : 1$.

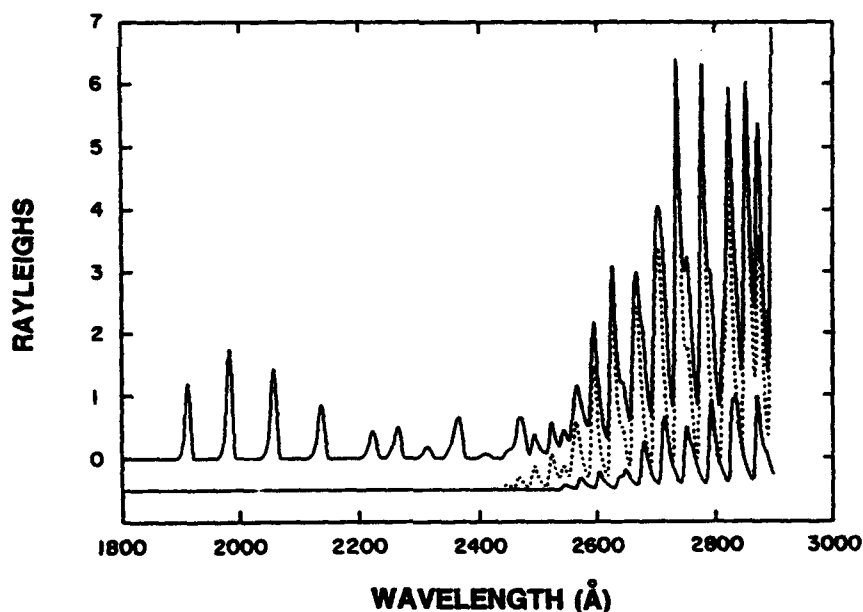


FIG. 6. BEST FIT TO THE NIGHTGLOW DATA SHOWN IN FIG. 4 (UPPER SOLID HISTOGRAM). This fit uses the NO δ and γ bands as well as the O_2 Herzberg I ($v' = 4$ to 10 only) and II bands. The dotted line shows the contribution of the Herzberg I bands and the bottom solid line shows the contribution of the Herzberg II bands. For this spectrum T_r is 200 K and the resolution is 5.9 Å.

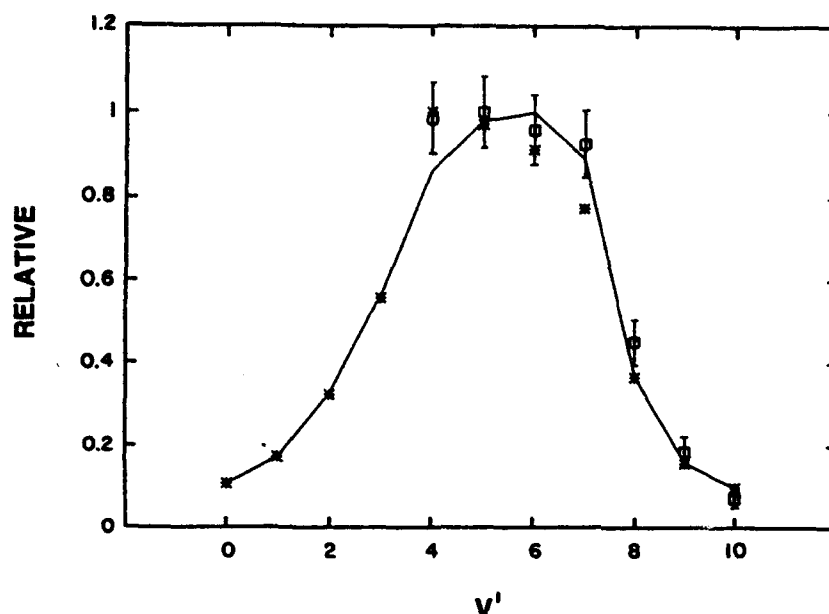


FIG. 7. RELATIVE VIBRATIONAL LEVEL POPULATIONS FOR THE $O_2 A^3\Sigma_u^+$ STATE, AS DERIVED FROM THE HERZBERG I EMISSIONS, ARE PLOTTED AS SQUARES WITH ERROR BARS. The populations derived by Degen (1969) are plotted as *, and the populations derived by Slanger and Huestis (1981) are represented by the solid line.

Shown in Fig. 7 as squares with $\pm 1 \sigma$ error bars are the relative vibrational populations for the $O_2 A^3\Sigma_u^+$ state as determined from the Herzberg I emissions. The populations given for these data are based on the assumption of equal emission probability from all levels. For equal populations the total emission from each level would be equal, under this assumption.

Vibrational levels with $v' \leq 3$ have such a small contribution to the wavelength range scanned that they could not be determined. Emissions from the Herzberg I $v' = 11$ level could not be fit since the emission has no distinct peaks at the wavelengths scanned. Populations for the $A^3\Sigma_u^+$ derived by Slanger and Huestis (1981) and Degen (1969) from analysis of the data of Broadfoot and Kendall (1968) and Hennes (1966) are shown for comparison as a solid line and asterisks, respectively. When fitting the Herzberg I and Herzberg II emissions in the data, the Herzberg I relative vibrational populations which gave the best fit were 0.99 ± 0.08 , 1.00 ± 0.08 , 0.96 ± 0.08 , 0.93 ± 0.08 , 0.45 ± 0.06 , 0.19 ± 0.04 , and 0.07 ± 0.02 for $v' = 4$ to 10 , respectively.

The populations for the $v' = 4$ to 9 vibrational levels agree well with previous observations. The $v' = 10$ contribution found may be subject to sig-

nificant systematic errors. This level was sensitive to the molecular constants. It was also more sensitive to the background subtraction than the other levels. The relative population of 0.07 ± 0.02 shown in Fig. 7 approximately doubles if the wavelength-dependent background subtraction used for the NO emission region is extrapolated to longer wavelengths. This suggests that the $v' = 10$ population derived here is best considered as a lower limit. The contributions from individual vibrational levels ($v' = 4$ to $v' = 10$) is shown in Fig. 8.

The recent publication of transition probabilities for the O_2 Herzberg III band emission ($A'-X$) (Bates, 1989) aids calculation of the spectrum of this band system. This band system has never been conclusively observed in the upper atmosphere. Sharp and Siskind (1989) have reported the possible presence of it in some observations at wavelengths $< 3050 \text{ \AA}$. Observation of this band system is difficult since the wavelengths of emission closely match those of the Herzberg I system from the A state and the emissions are weak.

Inclusion of Herzberg III emissions in the fitting of these data does not significantly affect the relative populations derived for the A state (relative populations are 0.95 ± 0.08 , 1.00 ± 0.8 , 0.87 ± 0.08 ,

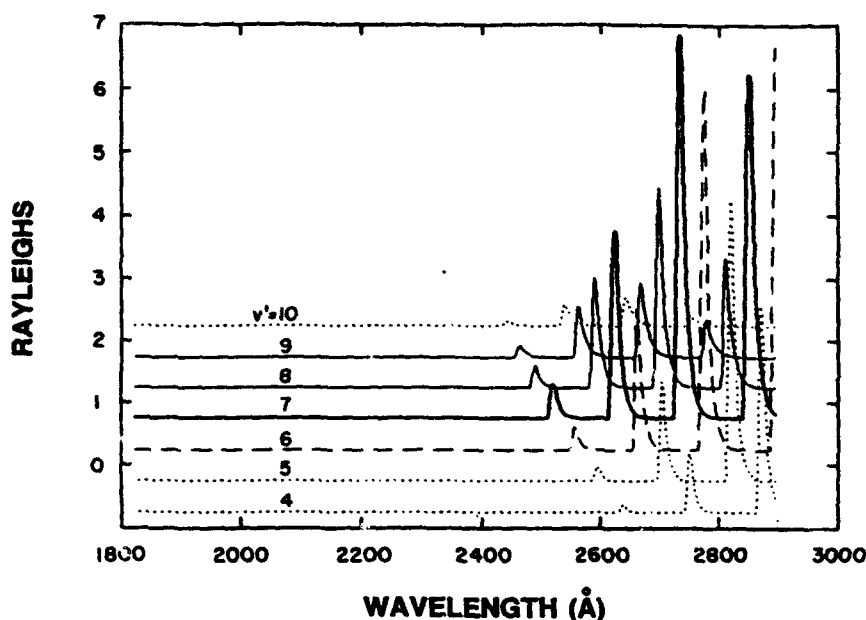


FIG. 8. BEST FIT OF THE $v' = 4$ TO 10 O_2 HERZBERG I BANDS TO THE DATA IN FIG. 4 WHEN USING ONLY THE O_2 HERZBERG I AND II BANDS IN THE FITTING (IN ADDITION TO THE NO BANDS). Shown here are the contributions from each v' to the total shown in Fig. 6.

0.86 ± 0.08 , 0.38 ± 0.05 , 0.20 ± 0.04 , and 0.06 ± 0.02 for $v' = 4$ to 10, respectively). It does slightly decrease the derived brightness (by ~ 0.9). The goodness of fit improves significantly also. The reduced χ^2 decreased from 5.8 to 4.7 when fitting to the data in bins 600–958 (2419–2896 Å). The populations for the $c^1\Sigma$ state (Herzberg II) were handled in the same way as when fitting Herzberg I and Herzberg II without Herzberg III. The relative populations used for the $A'^3\Delta$ state (Herzberg III) were from Slanger and Huestis (1981). The fit to the data is shown in Fig. 9. The Herzberg I (dotted), Herzberg II (solid), and Herzberg III (dashed) components of the fit are shown separately as the offset plots beneath the total fit. The brightness ratio for Herzberg I: Herzberg II: Herzberg III emissions in these data was $3.4 \pm 0.1: 1.0 \pm 0.1: 1.4 \pm 0.5$ for Herzberg I $v' = 4$ to 10. Assuming that the vibrational levels with $v' < 4$ are populated, relative to $v' = 4$, according to the populations found by Degen (1968) or Slanger and Huestis (1981), the brightness ratio would be $\sim 4.5: 1: 1.4$, which agrees with previous observations at longer wavelengths but is significantly lower than other observations (Sharp and Siskind, 1989) in this wavelength range (< 2950 Å).

The identification of Herzberg III emissions in these data must also be considered tentative as was Sharp and Siskind's (1989) identification. Any errors in cal-

culating the Herzberg I band emission, which is blended with the Herzberg III emission, could significantly affect the conclusions. Errors are possible due to the accuracy of the Dunham coefficients used and the approximations assumed when using them in calculating the spectra (see Slanger and Cosby, 1988). A significant portion of the emission in this wavelength region involves higher vibrational levels for which the molecular constants are less well known than for the lower levels.

CONCLUSIONS

The nightglow in the 1600–2950 Å region has been analyzed to aid in developing remote-sensing methods for atomic oxygen and atomic nitrogen. The NO δ and γ band emissions from radiative recombination have been observed at sufficient resolution (5.9 Å) to derive a rotational temperature of ~ 700 K. The $C^2\Pi$ to $A^2\Sigma$ branching ratio observed was 0.41 ± 0.16 , which is in agreement with previous observations. Emission from the NO ϵ bands was < 0.25 R.

Vibrational populations for the O_2 A state (0.95, 1.00, 0.87, 0.86, 0.38, 0.20, 0.06 for $v' = 4$ to 10, respectively) derived from these Herzberg I band observations are in agreement with previous observations. Emissions from the Herzberg II and III bands were

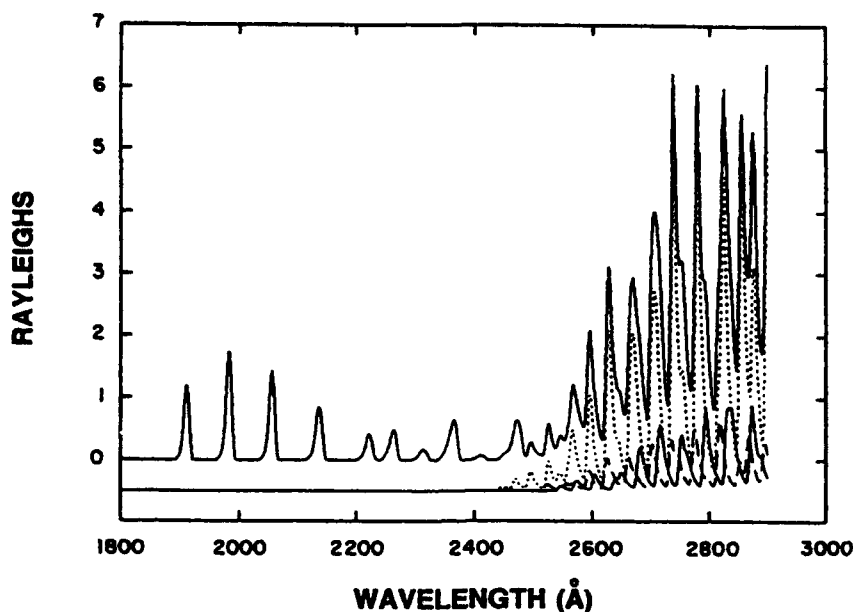


FIG. 9. THE UPPER HISTOGRAM SHOWS THE SUMMED NO AND O₂ EMISSIONS (HERZBERG I, II, AND III) WHICH BEST FIT THE DATA IN FIG. 4.

THE HERZBERG I, II, AND III EMISSIONS ARE SHOWN SEPARATELY BELOW THE TOTAL AS DOTTED, SOLID AND DASHED LINES, RESPECTIVELY.

also suggested by the data. The brightness ratio for Herzberg I:Herzberg II:Herzberg III emissions in these data was $\sim 4.5:1:1.4$, which agrees with previous observations at longer wavelengths but is significantly lower than other observations in this wavelength range (< 2950 Å).

No spacecraft-related emissions were detectable from the NO or O₂ band emissions observed. Weak emissions from the N₂ LBH bands were seen. These are attributed to spacecraft interactions, as previously reported. The lack of spacecraft-related emissions from O₂ and NO may constrain the excitation mechanisms for LBH emission from spacecraft.

Acknowledgements—We would like to thank Dr J. Thomas for enlightening discussions on calculations involving the NO γ bands and Dr J. Retterer for his suggestions on more robust fitting methods. We are also indebted to the reviewer for helpful and clarifying suggestions.

REFERENCES

- Anderson, G. P. and Hall, L. A. (1989) Solar irradiance between 2000 and 3100 Angstroms with spectral band pass of 1.0 Angstroms, *J. geophys. Res.* **94**, 6435.
- Baker, K. D., Nagy, A. F., Olsen, R. O., Oran, E. S., Randhawa, J., Strobel, D. F. and Tohmatsu, T. (1977) Measurement of the nitric oxide altitude distribution in the mid-latitude mesosphere, *J. geophys. Res.* **82**, 3281.
- Barth, C. A. (1961) The 5577-Angstrom airglow, *Science* **134**, 1426.
- Barth, C. A. (1964) Rocket measurement of the nitric oxide dayglow, *J. geophys. Res.* **69**, 3301.
- Barth, C. A. (1966) Nitric oxide in the upper atmosphere, *Ann. Geophys.* **22**, 198.
- Bates, D. R. (1954) The physics of the upper atmosphere, in *The Earth as a Planet* (Edited by Kuiper, G. P.), p. 576. University of Chicago Press, Chicago.
- Bates, D. R. (1989) Oxygen band system transitions arrays, *Planet. Space Sci.* **37**, 881.
- Borrell, P. M., Borrell, P. and Ramsay, D. A. (1986) High-resolution studies of the near-ultraviolet bands of oxygen: III: the $A^3\Sigma_u^+ - X^3\Sigma_g^-$ system, *Can. J. Phys.* **64**, 721.
- Broadfoot, A. L. and Kendall, K. R. (1968) The airglow spectrum, 3100–10,000 Å, *J. geophys. Res.* **73**, 426.
- Cebula, R. P. and Feldman, P. D. (1982) Ultraviolet spectroscopy of the zodiacal light, *Astrophys. J.* **263**, 987.
- Cebula, R. P. and Feldman, P. D. (1984) Rocket observations of the ultraviolet airglow during morning twilight, *J. geophys. Res.* **89**, 9080.
- Chamberlain, J. W. (1955) The ultraviolet airglow spectrum, *Astrophys. J.* **121**, 277.
- Chamberlain, J. W. (1961) *Physics of the Aurora and Airglow*, 704 pp. Academic Press, New York.
- Cleary, D. D. (1986) Daytime high-latitude rocket observations of the NO γ , δ , and ϵ bands, *J. geophys. Res.* **91**, 11,337.
- Cohen-Sabban, J. and Vuillemin, A. (1973) Ultra-violet nightglow spectrum from 1900 Å to 3400 Å, *Astrophys. Space Sci.* **24**, 127.
- Conway, R. R., Meier, R. R., Strobel, D. F. and Huffman,

- R. E. (1987) The far ultraviolet vehicle glow of the S3-4 satellite. *Geophys. Res. Lett.* 14, 628.
- Coquart, B. and Ramsay, D. A. (1986) High-resolution studies of the near-ultraviolet bands of oxygen: III: the $A^1\Delta_u - Y^1\Sigma_g^-$ system. *Can. J. Phys.* 64, 726.
- Cuthbertson, J. W. and Langer, W. D. (1989) A surface chemistry model for the altitude dependence of the N_2 Lyman Birge-Hopfield glow on spacecraft. *J. geophys. Res.* 94, 9149.
- Degen, V. (1969) Vibrational population of O^2 ($A^1\Sigma_g^+$) and synthetic spectra of the Herzberg bands in the night airglow. *J. geophys. Res.* 74, 5145.
- Degen, V. (1977) Nightglow emission rates in the O_2 Herzberg bands. *J. geophys. Res.* 82, 2437.
- Dickinson, P. H. G., Bain, W. C., Thomas, L., Williams, E. R., Jenkins, D. B. and Twiddy, N. D. (1980) The determination of the atomic oxygen concentration and associated parameters in the lower ionosphere. *Proc. R. Soc. Lond. A* 369, 379.
- Dufay, J. (1941) Une interpretation possible de certaines radiations intenses du ciel nocturne dans la region ultraviolette. *Comptes rendus* 213, 284.
- Engleman, R. Jr. and Rouse, P. E. (1971) The β and γ bands of nitric oxide observed during the flash photolysis of nitrosyl chloride. *J. Molec. Spectrosc.* 37, 240.
- Feldman, P. D. and Takacs, P. Z. (1974) Nitric oxide gamma and delta band emission at twilight. *Geophys. Res. Lett.* 1, 169.
- Greer, R. G. H., Murtagh, D. P., McDade, I. C., Dickinson, P. H. G., Thomas, L., Jenkins, B. D., Stegman, J., Llewellyn, E. J., Witt, G., Mackinnon, D. J. and Williams, E. R. (1986) *Eton 1*: a data base pertinent to the study of energy transfer in the oxygen nightglow. *Planet. Space Sci.* 34, 771.
- Hedin, A. (1987) MSIS-86 thermospheric model. *J. geophys. Res.* 92, 4649.
- Hennes, J. P. (1966) Measurement of the ultraviolet nightglow spectrum. *J. geophys. Res.* 71, 763.
- Huber, K. P. and Herzberg, G. (1979) *Molecular Spectra and Molecular Structure IV. Constants of Diatomic Molecules*, 716 pp. Van Nostrand, New York.
- Huffman, R. E., LeBlanc, F. J., Larrabee, J. C. and Paulsen, D. E. (1980) Satellite vacuum ultraviolet airglow and auroral observations. *J. geophys. Res.* 85, 2201.
- Ingham, M. F. (1962) The nightglow spectrum I. 223700-4650 Å. *Monthly Notices R.A.S.* 124, 505.
- Kofsky, I. L. (1988) Excitation of N_2 Lyman-Birge-Hopfield bands emission by low earth orbiting spacecraft. *Geophys. Res. Lett.* 15, 241.
- Kovacs, I. (1969) *Rotational Structure in the Spectra of Diatomic Molecules*, 320 pp. Elsevier, New York.
- Krassovsky, V. I., Shefov, N. N. and Yarin, V. I. (1962) Atlas of the airglow spectrum 3000-12,400 Å. *Planet. Space Sci.* 9, 883.
- Krupenie, P. H. (1972) The spectrum of molecular oxygen. *J. phys. Chem. Ref. Data* 1, 423.
- Llewellyn, E. J., Solheim, B. H., Stegman, J. and Witt, G. (1979) A measurement of the O_2 ultra-violet nightglow emission. *Planet. Space Sci.* 27, 1507.
- McCoy, R. P. (1981) Rocket measurements of thermospheric odd nitrogen and comparisons with a diffusive transport chemical model. Ph.D. thesis, Univ. of Colorado, Boulder.
- McCoy, R. P. (1983a) Thermospheric odd nitrogen 1. NO , $N(^4S)$, and $O(^1P)$ densities from rocket measurements of the NO δ and Δ bands and the O_2 Herzberg I bands. *J. geophys. Res.* 88, 3197.
- McCoy, R. P. (1983b) Thermospheric odd nitrogen 2. Comparison of rocket observations with a diffusive transport chemical model. *J. geophys. Res.* 88, 3206.
- McDade, I. C., Llewellyn, E. J., Greer, R. G. H. and Murtagh, D. P. (1982) The altitude dependence of the $O_2(A^1\Sigma_g^+)$ vibrational distribution in the terrestrial nightglow. *Planet. Space Sci.* 30, 1133.
- McDade, I. C., Murtagh, D. P., Greer, R. G. H., Dickinson, P. H. G., Witt, G., Stegman, J., Llewellyn, E. J., Thomas, L. and Jenkins, D. B. (1986a) ETON 2: quenching parameters for the proposed precursors of $O_2(b^1\Sigma_g^+)$ and $O(^1S)$ in the terrestrial nightglow. *Planet. Space Sci.* 34, 789.
- McDade, I. C., Llewellyn, E. J., Greer, R. G. H. and Murtagh, D. P. (1986b) Eton 3: altitude profiles of the nightglow continuum at green and near infrared wavelengths. *Planet. Space Sci.* 34, 801.
- Meira, L. G. Jr. (1971) Rocket measurements of upper atmospheric nitric oxide and their consequences to the lower ionosphere. *J. geophys. Res.* 76, 202.
- Meyerott, R. E. and Swenson, G. R. (1990) A surface chemistry model for the production of N_2 LBH spacecraft glow. *Planet. Space Sci.* 38, 555.
- Murtagh, D. P., McDade, I. C., Greer, R. G. H., Stegman, J., Witt, G. and Llewellyn, E. J. (1986) Eton 4: an experimental investigation of the altitude dependence of the $O_2(A^1\Sigma_g^+)$ vibrational population in the nightglow. *Planet. Space Sci.* 34, 811.
- Nicholls, R. W. (1964) Franck-Condon factors to high vibrational quantum numbers IV: NO band systems. *J. Res. Nat. Bur. Stand.* 68A, 535.
- Packer, D. M. (1961) Altitudes of the night airglow radiations. *Ann. Geophys.* 17, 67.
- Pearce, J. B. (1969) Rocket measurement of nitric oxide between 60 and 96 kilometers. *J. geophys. Res.* 74, 853.
- Pearse, R. W. B. and Gaydon, A. G. (1963) *The Identification of Molecular Spectra*, 347 pp. Wiley, New York.
- Press, W. H., Flannery, B. P., Teukolsky, S. A. and Vetterling, W. T. (1986) *Numerical Recipes: The Art of Scientific Computing*, 818 pp. Cambridge University Press, New York.
- Ramsay, D. A. (1986) High-resolution studies of the near-ultraviolet bands of oxygen: III: the $c^1\Sigma_u^- - X^3\Sigma_g^-$ system. *Can. J. Phys.* 64, 717.
- Reed, A. (1968) Night measurement of mesospheric ozone by observations of ultraviolet airglow. *J. geophys. Res.* 73, 2951.
- Sharp, W. E. and Rusch, D. W. (1981) Chemiluminescence of nitric oxide: The $NO(C^2\Sigma^- - A^2\Sigma^+)$ rate constant. *J. Quant. Spectrom. Rad. Trans.* 25, 413.
- Sharp, W. E. and Siskind, D. E. (1989) Atomic emission in the ultraviolet nightglow. *Geophys. Res. Lett.* 16, 1453.
- Slinger, T. G. and Cosby, P. C. (1988) O_2 spectroscopy below 5.1 eV. *J. phys. Chem.* 92, 267.
- Slinger, T. G. and Huestis, D. L. (1981) $O_2(c^1\Sigma_u^- - X^3\Sigma_g^-)$ emission in the terrestrial nightglow. *J. geophys. Res.* 86, 3551.
- Spindler, R. J. Jr., Isaacson, L. and Wentink, T. Jr. (1970) Franck-Condon factors and r -centroids for the gamma system of NO . *J. Quant. Spectrom. Rad. Trans.* 10, 621.
- Stecher, T. P. (1965) The spectral energy distribution of the earth's ultraviolet night airglow. *J. geophys. Res.* 70, 2209.
- Swenson, G. R. and Meyerott, R. E. (1988) Spacecraft ram cloud atom exchange and N_2 LBH glow. *Geophys. Res. Lett.* 15, 245.

- Tennyson, P. D., Feldman, P. D., Hartig, G. F. and Henry, R. C. (1986) Near-midnight observations of nitric oxide δ - and γ -band chemiluminescence. *J. geophys. Res.* 91, 10,141.
- Thomas, R. J. (1978) A high-altitude rocket measurement of nitric oxide. *J. geophys. Res.* 83, 513.
- Thomas, R. J. (1981) Analyses of atomic oxygen, the green line, and Herzberg bands in the lower thermosphere. *J. geophys. Res.* 86, 206.
- Thomas, R. J. and Young, R. A. (1981) Measurement of atomic oxygen and related airglows in the lower thermosphere. *J. geophys. Res.* 86, 7389.
- Thomas, L., Greer, R. G. H. and Dickinson, P. H. G. (1979) The excitation of the 557.7 nm line and Herzberg bands in the nightglow. *Planet. Space Sci.* 27, 925.
- Tisone, G. C. (1973) Measurements of NO densities during sunrise at Kauai. *J. geophys. Res.* 78, 746.
- Tohmatsu, T. and Iwagami, N. (1975) Measurement of nitric oxide distribution in the upper atmosphere. *Space Research XV*, Akademie-Verlag, Berlin.
- Tohmatsu, T. and Iwagami, N. (1976) Measurement of nitric oxide abundance in equatorial upper atmosphere. *J. Geomagnet. Geoelectr.* 28, 343.
- Wallace, L. (1962) Band-head wavelengths of C_2 , CH, CN, CO, NH, NO, O_2 , OH, and their ions. *Astrophys. J. Suppl. Ser.* 7, 165.

**APPENDIX 3: Reprint of Paper Entitled "Horizon UV Program (HUP)
Atmospheric Radiance Measurements," Describing HUP
Measurements**

PROCEEDINGS REPRINT

 SPIE—The International Society for Optical Engineering

Reprinted from

Ultraviolet Technology IV

**20–21 July 1992
San Diego, California**



Volume 1764

The U.S. Government is authorized to reproduce and sell this report.
Permission for further reproduction by others must be obtained from
the copyright owner.

©1993 by the Society of Photo-Optical Instrumentation Engineers
Box 10, Bellingham, Washington 98227 USA. Telephone 206/676-3290.

Horizon UV Program (HUP) Atmospheric Radiance Measurements

F. J. LeBlanc

NorthWest Research Associates, Inc.
P.O. Box 3027, Bellevue WA 98009

and

F. P. DelGreco, J. A. Welsh, R. E. Huffman

Geophysics Directorate
Phillips Laboratory, Hanscom AFB MA 01731

ABSTRACT

Spectrometric observations (1100 Å to 1800 Å) of the ultraviolet radiance of Earth's atmosphere have been obtained by the Horizon Ultraviolet Program (HUP) sensor from Space Shuttle altitude at two different points in the solar cycle. Most of the radiance measurements were made during horizon scans of the earthlimb or while the HUP field of view was directed toward nadir. The expected variation of dayglow radiance with solar zenith angle (SZA) in the several spectral bands was observed. These results compare favorably to the predictions of a preliminary version of the Atmospheric Ultraviolet Radiance Integrated Code (AURIC).

2. INTRODUCTION

A small but growing body of experimental measurements of atmospheric ultraviolet radiance is now extensive enough that it is reasonable to compare those data, obtained under a variety of geophysical conditions, with the predictions of atmospheric radiance models. This paper presents some results from just such a comparison. The range of conditions for which comparison is being reported here is purposely limited to simple cases of ultraviolet dayglow; at this level, issues of radiation transport and optically thick emission features are being avoided. We concentrate on the optically thin molecular nitrogen Lyman-Birge-Hopfield bands and the atomic oxygen line at 1356 Å. These provide an adequate set of initial test cases. In addition it is precisely those features of the dayglow which are candidates for use in the remote determination of the distribution of electrons and atmospheric species in the ionosphere. Spatial and temporal variability are important background characteristics for any surveillance systems but they are not addressed in this paper. There are other potential byproducts such as monitoring solar activity for its effect on communications and radar and as a horizon sensor to monitor spacecraft stability.

3. EXPERIMENTAL

Figure 1 is a diagram of the HUP instrument. It was an eighth meter Ebert-Fastie spectrometer fitted with a 230mm telescope. This was mounted on a platform which allowed the instrument to be pivoted through 20 degrees in 41 seconds. It could be operated as a photometer at a selected wavelength or as a spectrometer recording a spectrum every 5.8 seconds. The instrument was mounted in the shuttle bay so that it could be made to point perpendicularly out of the bay or scan 20 degrees between vertical and towards the shuttle nose so that when shuttle was in its gravity gradient mode (nose down) the horizon would be scanned. The diagram shows HUP oriented as it would be to view vertically out of the bay.

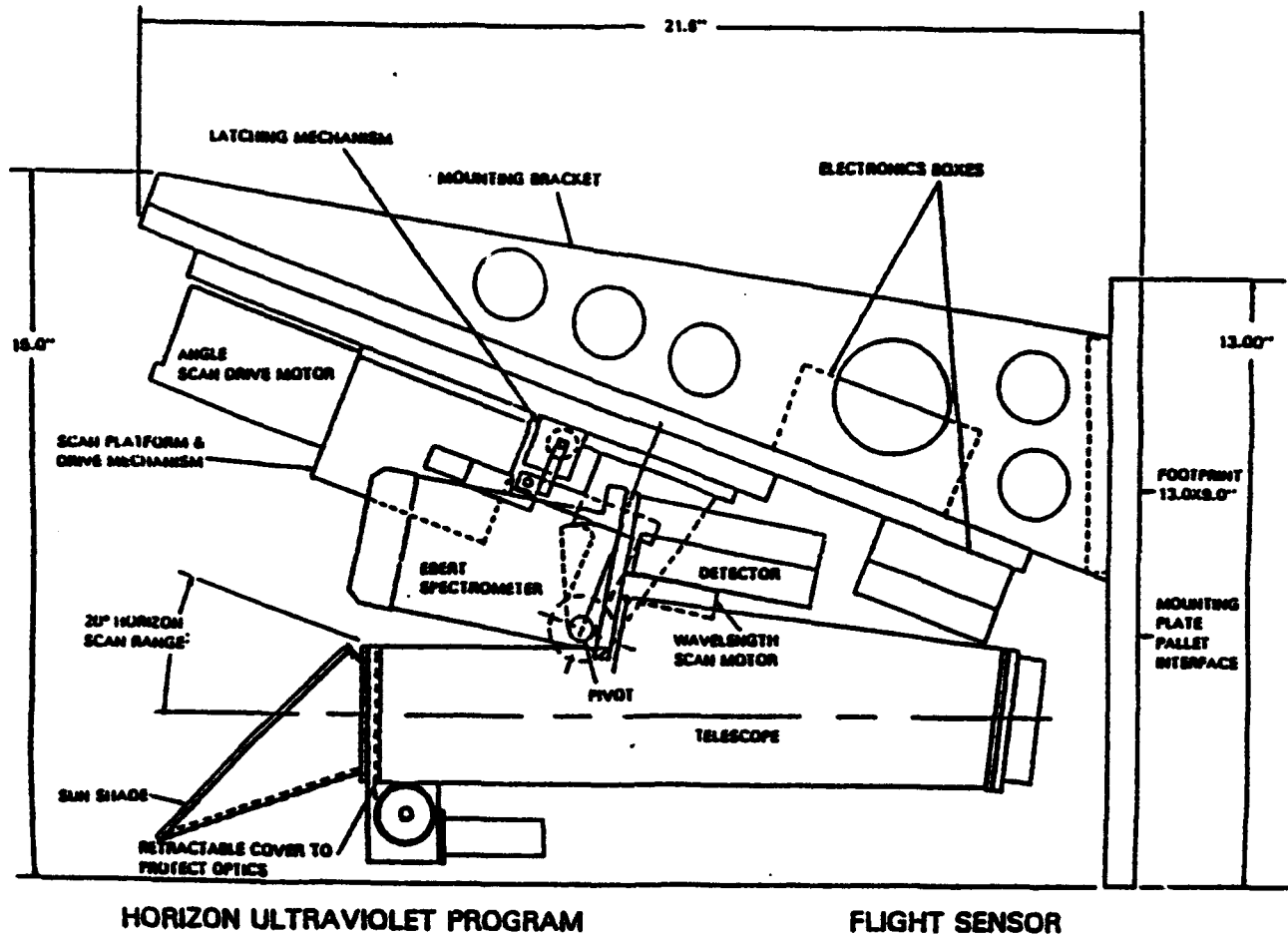


Fig. 1. Schematic of HUP instrument shown as mounted on Shuttle in launch position. The telescope, spectrometer and detector can be pivoted as a unit.

Fig. 2. shows the measured calibration curves for both flights for the wavelength range of 1150 Å to 1850 Å, shown in counts per Rayleigh-sec. The difference is due to the slit change, with a smaller contribution to loss of sensitivity after nine years of aging.

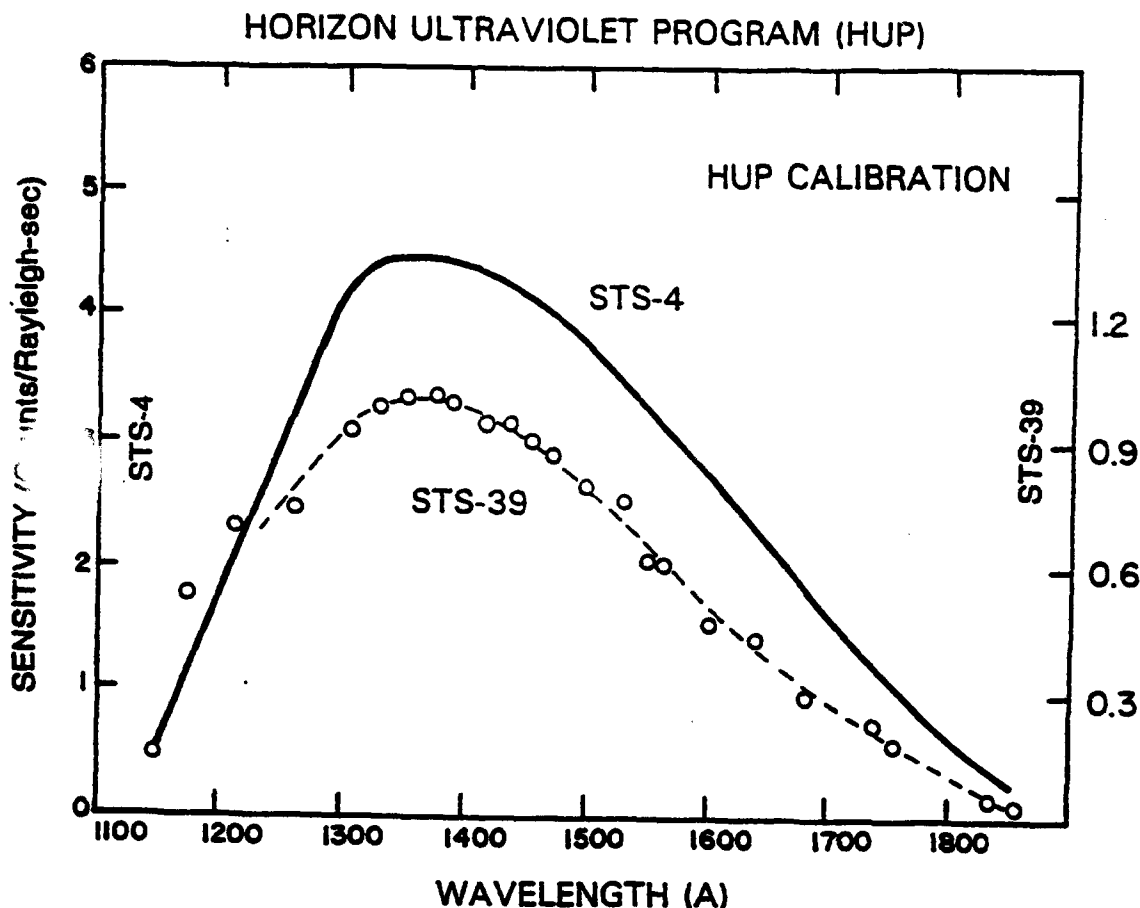


Fig. 2. HUP instrument sensitivity calibration for Shuttle flights.

For STS-39, the second flight, the slits, Table 1, of the spectrometer were narrowed to increase the spectral resolution. This also narrowed the FOV. In addition, the instrument was programmed to concentrate on oxygen 1356 Å and LBH radiation at 1384 Å to provide suitable data for comparison with ionospheric models such as AURIC.

The measured wavelength resolution for STS-4 was 20 Å and 8.3 Å for STS-39. STS-4 had a 0.2 x 1.5 deg field of view (FOV) with a footprint 3.8 x 28 km at a distance of 1100 km. For STS-39 the the FOV was 0.06 x 1.5 deg with a footprint of 1.2 x 28 km at 1100 km. STS-4 flew at 300 km altitude between latitudes of 28.6 degrees and STS-39 flew at 259 km between 57 degrees latitude.

4. Results

The observations presented here result from data collected on STS-4 June 28 and 29 1982 when the 10.7 cm solar index was about 112 and on May 5 1991 (STS-39) when the 10.7 cm solar index was about 183.

Fig. 3. displays a spectrum seen looking down from STS-39. The atomic lines are clearly resolved while the Lyman-Birge-Hopfield band system of Nitrogen (LBH) covers an extended wavelength range at lower

intensities. Fig. 4 is a spectrum from STS-4. The twenty Angstrom resolution is seen in the broader atomic line spectra.

Table 1. Features of the HUP instrument as flown.

	STS-4	STS-39
Slit Width:	0.80 mm	0.24 mm
Resolution:	20 Å	8.3 Å
Field of View:	0.188 x 1.45 deg.	0.058 x 1.45 deg.
Footprint; 1100 km:	3.8 x 28 km	1.2 x 28 km
Wavelengths:	1216 Å H 1304 Å O 1356 Å O, N ₂ LBH 1384 Å N ₂ LBH 1414 Å N ₂ LBH, N 1464 Å N ₂ LBH 1493 Å N ₂ LBH, N 1554 Å N ₂ LBH	1356 Å O 1384 Å N ₂ LBH
Maximum latitude:	28.6 deg	57 deg
Altitude:	300 km	268 km

The AURIC model, described by Strickland, et al else-where in this volume has been used to compare with our observations. We have overlaid our data with the AURIC predictions for the appropriate day, time of day, longitude, latitude, planetary index A_p and 10.7 cm solar activity index.

Figs. 5. to 9. display horizon scans of oxygen 1356 Å radiation obtained from STS-4 for a range of solar zenith angles with AURIC predictions superimposed (dotted line). The HUP traces are double, showing the upward and downward horizon scans. The offset seen between the upward and downward scans could be caused by a small amount of backlash in the cam groove driving the scan platform or by an offset of the zero angle position for the barrel cam rotation. Since both traces lie within the accuracy of our knowledge of shuttle pointing we have deferred fine tuning these results until it becomes advantageous to do so. With the exception of the night measurement, the agreement between tangent height (about 165 km) of the maximum radiance as well as the magnitude of the peak brightness (5 to 6kR) with the prediction of the model is very gratifying. It provides reassurance that, as expected, the model is fundamentally sound and that HUP, Polar BEAR and other good experimental data will be invaluable in validating AURIC for more problematic conditions.

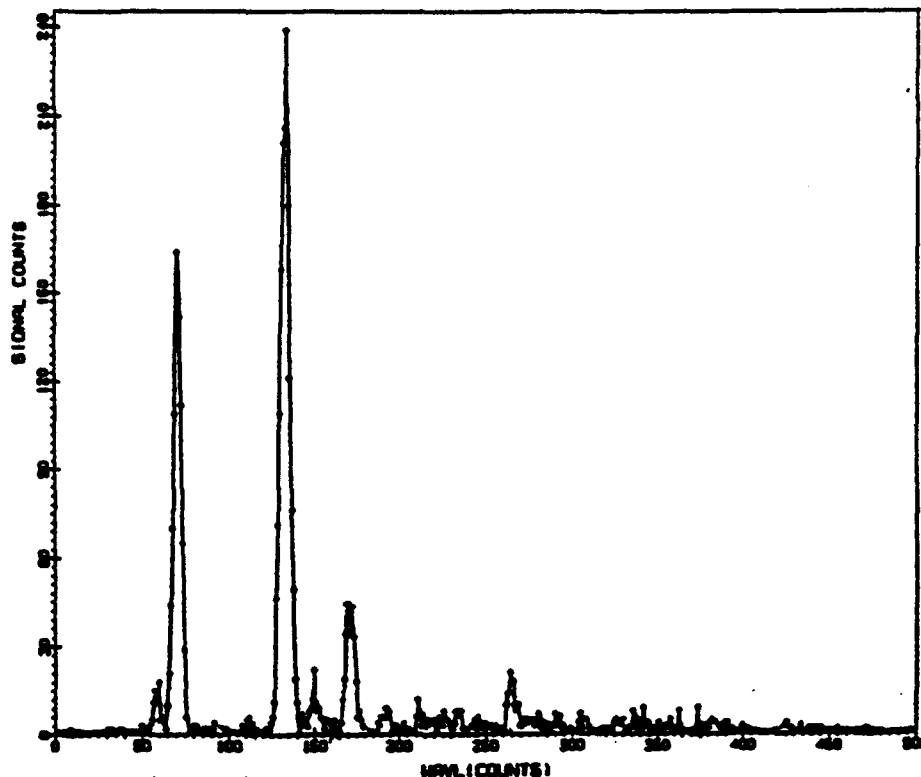


Fig. 3. HUP daytime spectra looking down from Space Shuttle STS-39 with 8.3Å resolution.

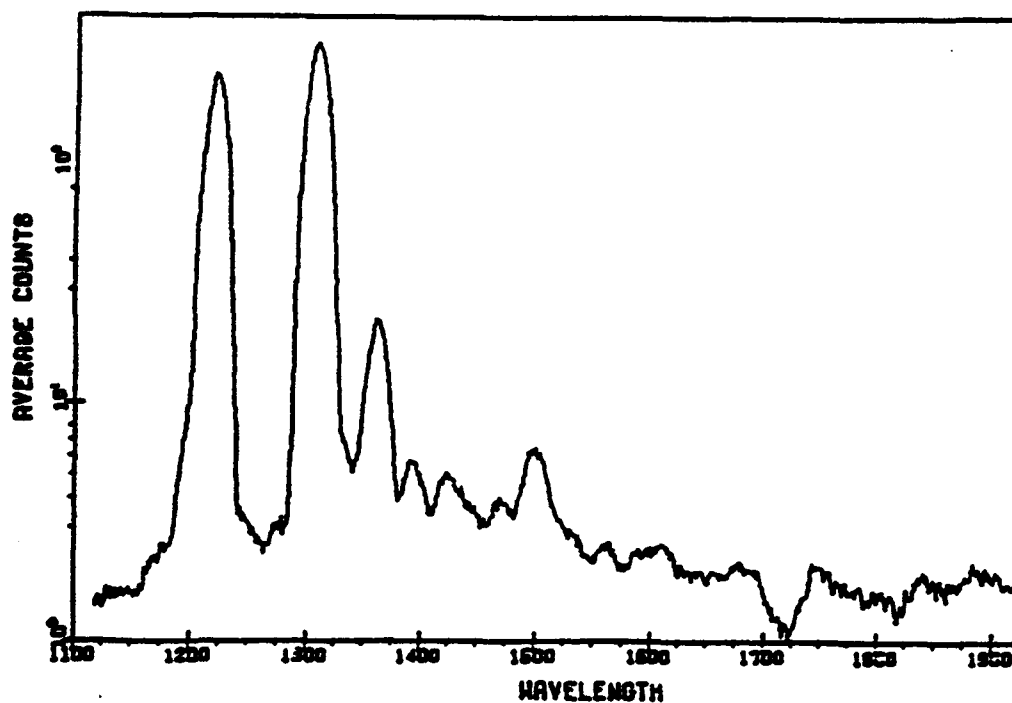


Fig. 4. HUP daytime spectra looking down from Space Shuttle STS-4 with 20Å resolution.

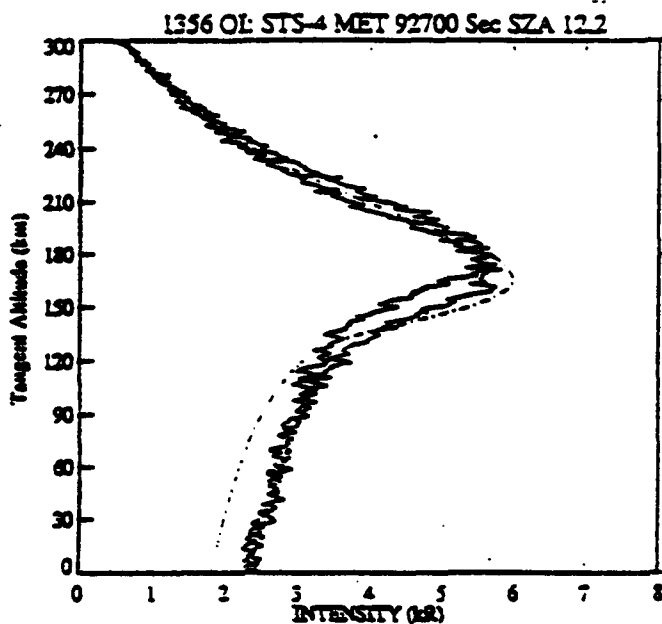


Figure 5.

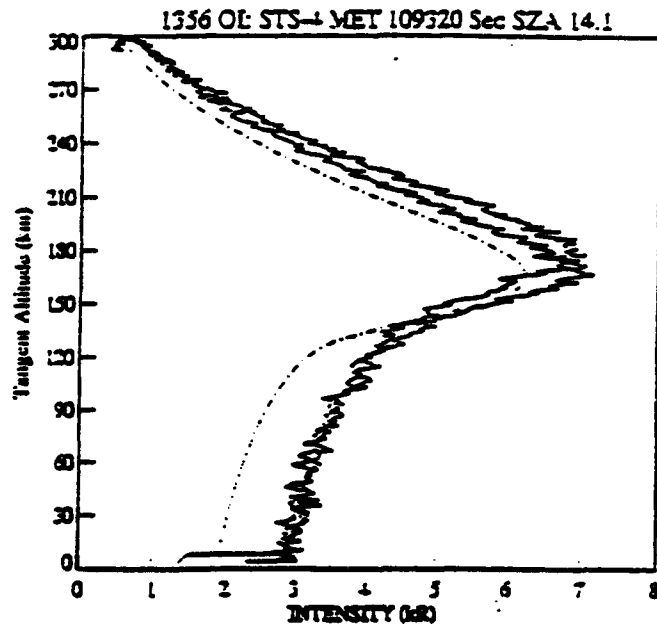


Figure 6.

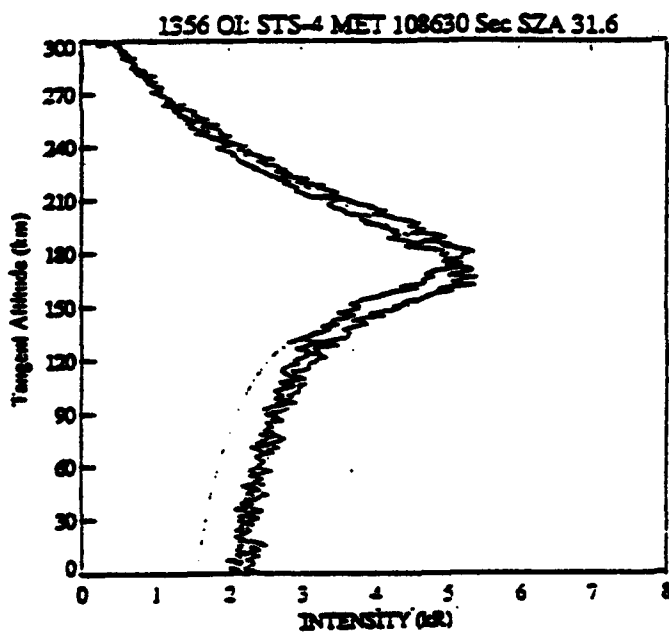


Figure 7.

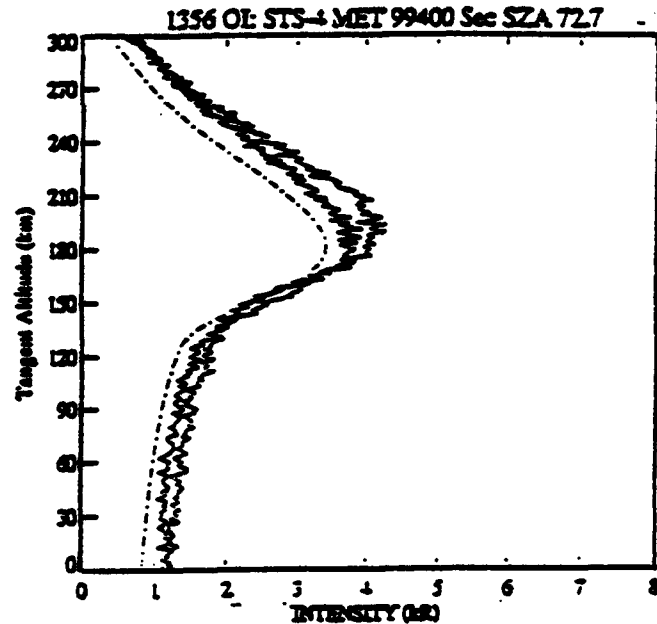


Figure 8.

Figs. 5 to 8. HUP horizon scans (up and downward) of 1356 Å Oxygen emission observed from Space Shuttle STS-4 for a range of solar zenith angles, overlaid with the AURIC prediction (broken line).

Fig. 10 is a plot of the peak 1356 Å oxygen line intensity as seen from STS-4 in the nadir direction. This was done for a range of SZAs (crosses) and is overlaid with AURIC predictions. The differences

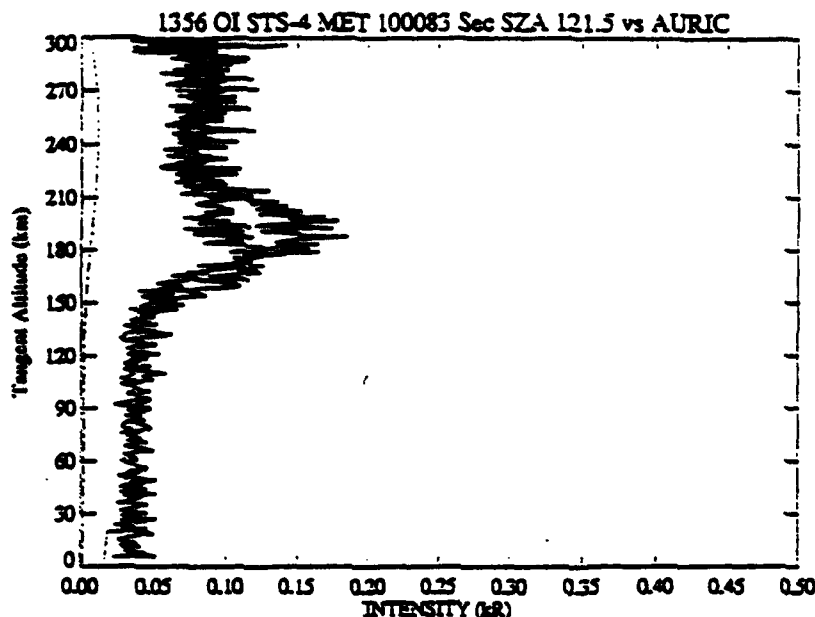


Fig. 9. HUP horizon scans (up and downward) of 1356 Å Oxygen emission observed from Space Shuttle STS-4 at a SZA of 121.5 deg. and overlaid with the AURIC prediction (broken line).

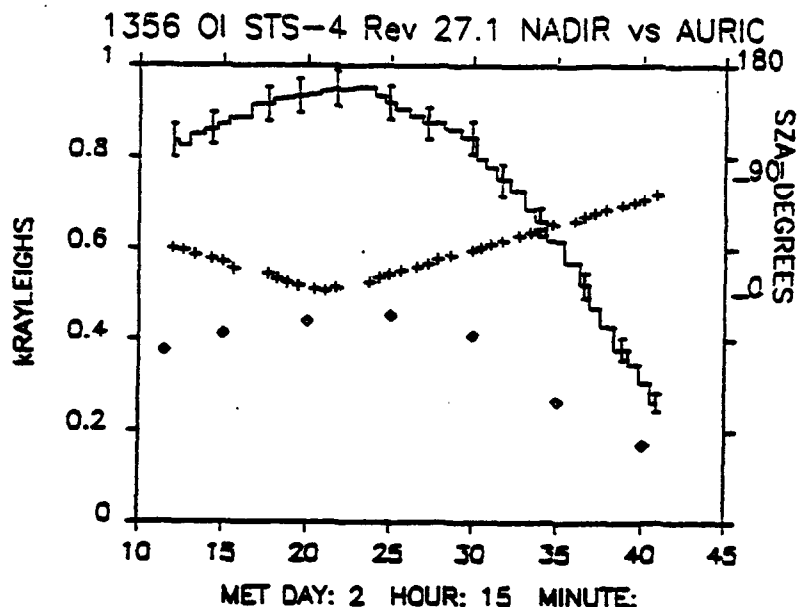


Fig. 10. Peak intensities of the 1356 Å oxygen line observed from Space Shuttle STS-4 looking in the nadir direction overlaid with SZA and AURIC predictions.

between the observed and the predicted are consistent with that observed in Figures 5 to 8 for the lower tangent altitudes.

Figures 11 and 12 shows the peak 1356 Å line intensities (circles) for the HUP instrument scan angles uncorrected for shuttle attitude while scanning in angle and wavelength on STS-39. The orbiter was in a nose down attitude. We are proceeding to analyze the data for true look angle and tangent height. Here the predicted and observed intensities are in agreement at about 11 kr. The increase in overall brightness compared with data from the earlier flight taken at similar solar zenith angles reflects the fact that these data were obtained at a more active part of the solar cycle, as indicated by the larger 10.7cm solar index value.

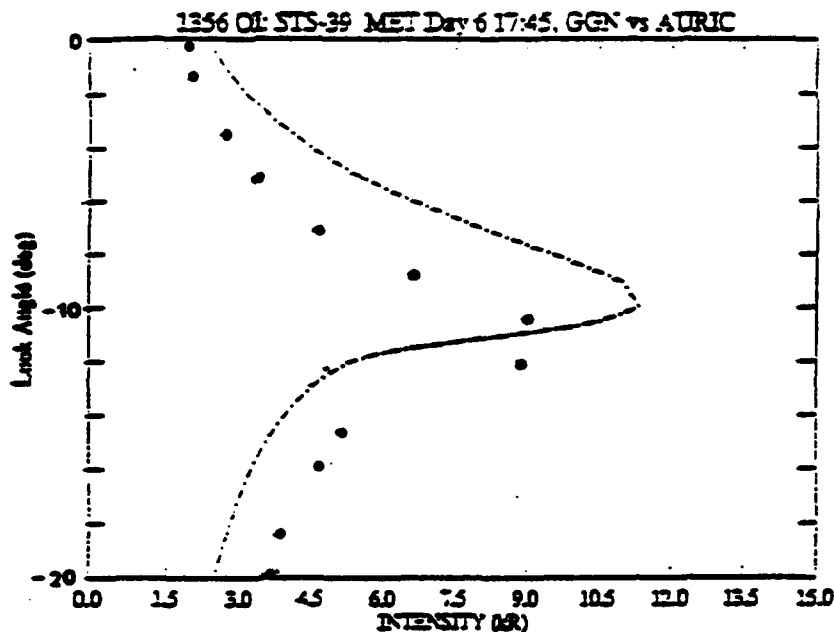


Fig. 11. Peak intensities of the Oxygen 1356 Å line emission (SZA = 23) vs uncorrected look angle observed from Space Shuttle STS-39 and overlaid with the AURIC prediction (broken line).

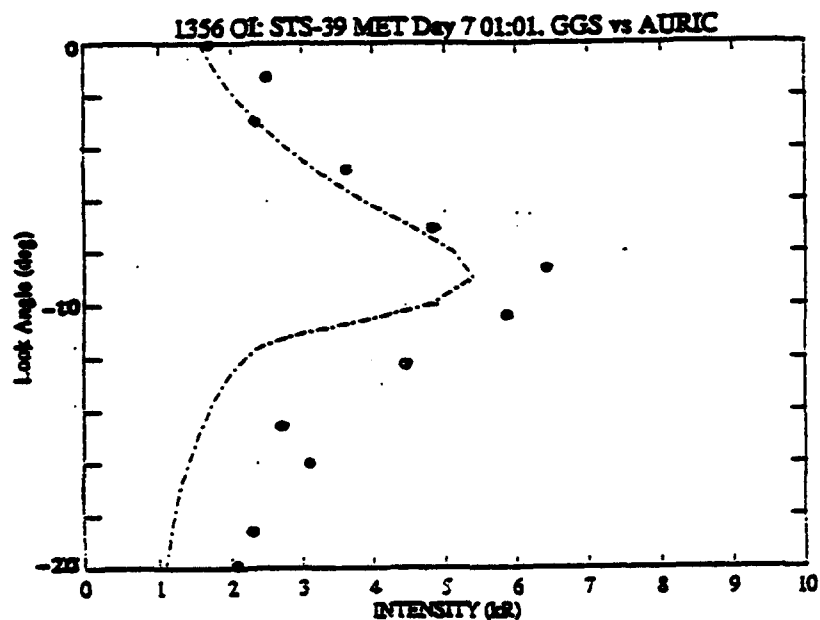


Fig. 12. Peak intensities of the Oxygen 1356 Å line emission (SZA = 61) vs uncorrected look angle observed from Space Shuttle STS-39 and overlaid with the AURIC prediction (broken line).

The deduced intensity of the total LBH band system as measured by HUP looking toward the earth from STS-39 is shown in Figure 13. That portion of the measured spectrum between 1376 Å and 1474 Å was integrated and used to represent the entire band system. The bands in that wavelength interval contain 18.6% of the total band strength of the system so the correction was straightforward. Also shown on the figure is an AURIC prediction of the total LBH intensity (small circular point at hour 2, minute 45) for the conditions at the time of the measurement.

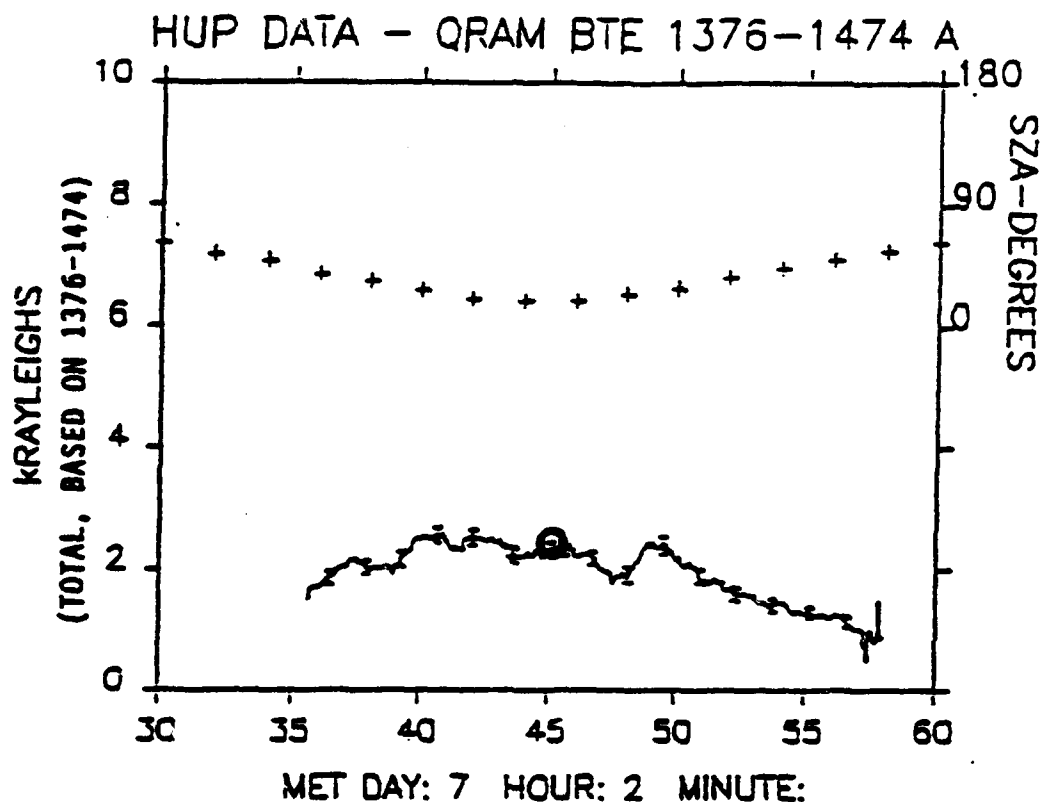


Figure 13. Radiance measured by HUP looking down from space shuttle STS-39 for LBH bands summed between 1376 Å and 1474 Å and corrected for the total LBH system. The AURIC prediction for one point is indicated by a small circle.

5. CONCLUSION

Even from this brief comparison it is evident that for well behaved daytime conditions in the ionosphere current state of the art ultraviolet radiance models are capable of providing excellent specification of atmospheric radiance. Future work will concentrate on extending the range of conditions for which experimental data can provide validation for the models.